ARKIV FÖR FYSIK Band 1 nr 9

Communicated 9 March 1949 by Manne Siegbahn and Bengt Edlén

# The arc spectrum of fluorine

By Kurt Lidén

With 10 plates and 6 figures in the text

***Summary.*** The arc spectrum of fluorine, F I, has been investigated in the infrared, visible, ultraviolet, and vacuum regions using suitable types of water-cooled hollow cathode discharge tubes as light sources. About 370 new lines have been identified and 67 new energy levels established. The n*s*- and n*d*-series can be unambiguously assigned to the components of the limit $^3P$ and they show almost perfect $J_1l$- or *pair*-coupling. Series of n*s*- and n*d*-levels are in excellent agreement in fixing the series limits within $\pm 0.1$ cm$^{-1}$, giving an ionization potential of 17.418 volts. The hyperfine structure has been studied with the Fabry-Perot interferometer and the strongest lines have been interferometrically measured against Ne I standards.

## Contents

Page
I. Introduction . . . . . . . . . . 229
II. Experimental arrangements . . . . . . . . . . 230
  1. The infrared, visible, and ultraviolet regions . . . . . . . . . . 230
  2. The vacuum ultraviolet . . . . . . . . . . 235
  3. Interferometric measurements . . . . . . . . . . 236
III. The determination of wave-lengths . . . . . . . . . . 237
  1. The region 12 000—2500 A . . . . . . . . . . 237
  2. The vacuum region . . . . . . . . . . 238
  3. The interferometer spectrograms . . . . . . . . . . 239
IV. Results . . . . . . . . . . 240
  1. The range 12 000—2500 A . . . . . . . . . . 240
  2. The vacuum range 1000—600 A . . . . . . . . . . 250
V. The structure of the arc spectrum . . . . . . . . . . 253
VI. Comparison with similar spectra . . . . . . . . . . 259
VII. Hyperfine structure . . . . . . . . . . 262
References . . . . . . . . . . 265

## I. Introduction

In an earlier investigation (33) the writer added some details to the knowledge of the arc spectrum of fluorine. A review of the actual state of the F I analysis was also given. In the isoelectronic series F I, Ne II, Na III etc., however, the spectra of several higher members were still much better analysed than F I (7, 56). Likewise, the first spectra of the elements chlorine and bromine in the halogen group were better known than that of fluorine (26, 27). The detailed discussion of the Stark effect in F I, observed by the writer (32), also required an improved knowledge of the energy level system of F I. Hence the need for a thorough investigation of F I in all available spectral ranges was apparent.

## II. Experimental arrangements

### 1. The infrared, visible, and ultraviolet regions

***Light source.*** The element fluorine was isolated in 1889 by H. MOISSON (38, 39), who also made an attempt to investigate its spectrum in the spark discharge at atmospheric pressure. Both this light source and a vacuum-tube discharge at low pressures were used in some later investigations by SMYTHE 1921 (53), GALE and MONK 1924 (21) and CARRAGAN 1926 (9). The chemical properties of fluorine caused difficulties and PORLEZZA (45) 1912 studied the vacuum-tube discharge at reduced pressure in silicon tetrafluoride, $SiF_4$. DINGLE (10) used the same light source 1926. CAMPBELL 1933 (8) was the first to use a Paschen hollow cathode, charged with potassiumfluoride, KF, as a light source for the arc spectrum of fluorine, which he obtained with good intensity and without troublesome chemical reactions in the apparatus. The same hollow cathode, charged with lithium fluoride, LiF, was then used by EDLÉN 1936 (14). MCNALLY, HARRISON and ROWE (42) 1947 developed a special Schüler-Gollnow hollow cathode light source for the purpose of spectro-chemical analysis. Further developments of light sources for research work on F I were published in 1948 (32) in connection with an investigation of the Stark effect of F I, which was made in this institute, using a Lo Surdo-Ryde glow discharge with sulphur hexafluoride, $SF_6$, as filling-gas. Further experiments were then made with a modified form of a Schüler-Gollnow hollow cathode discharge tube with helium and small amounts of $SF_6$ as filling-gas (33).

After several modifications of the hollow cathode source it was finally found possible to obtain a considerably improved intensity of the F I spectrum with the discharge tube shown in Fig. 1. The source contained a water-cooled anode, a brass-nickel cathode connected to a cooling-flange and partly heat-insulated from the water-cooled cathode support, and a Pyrex glass tube securely waxed to both the cathode support and the anode. A window of fused quartz, waxed to the anode, permitted light from the cathode to reach the spectrograph and the spectrometer used for visual testing of the discharge. A locally increased cooling of the open end of the cathode served to prevent dissociated fluorine from leaving the source chamber. The filling-gas, helium or a mixture of helium and neon, was purified by continuous circulation through a liquid-air-cooled charcoal trap (Fig. 2). In an electrically heated quartz tube, charged with CuO of analytical purity, traces of hydrogen could be removed.

Power was obtained from a 4000-volt, 1 amp. full wave rectifier, previously described (33), with current limiting resistors of 1000 ohms in series with the hollow cathode source. Operating conditions were 0.1—1.0 amp. at 450—250 volts across the tube.

The F I spectrum was excited very strongly when the filling-gas was continuously

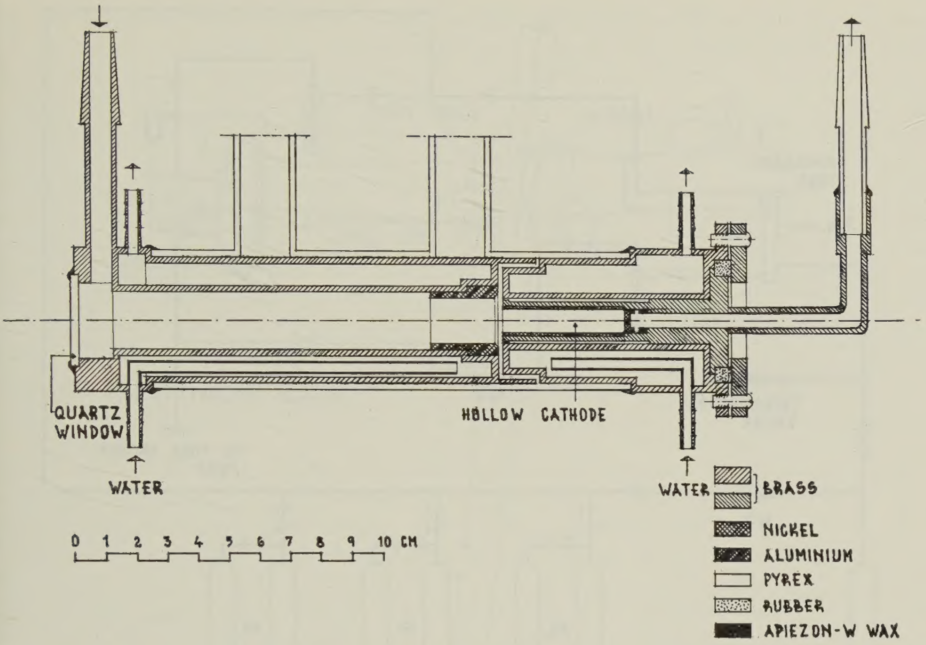

Fig. 1. A section through the hollow cathode light source used for excitation of F I.

supplied with small amounts of $SF_6$. The unavoidable excitation of a large number of lines from several other spectra, partly due to the chemical properties of fluorine, complicated the identification of the F I lines. A special investigation showed, however, that by a certain combination of cathode materials and discharge conditions a characteristic shape of the F I lines was obtained. After prolonged running of the hollow cathode source, charged with LiF, Li remained in the source chamber. If now the filling-gas was supplied with $SF_6$ in the usual way, the excitation of the F I lines showed a very special distribution in the hollow cathode as could be seen from the shape of the lines recorded by the stigmatic spectrograph. In this case the ends of the F I lines were most intense, due to strong excitation near the Li-covered walls of the chamber, if the current was smaller than 0.3 amp. and the filling-gas pressure about 3—5 mm (Plates IV—VI). Convenient and steady operating conditions could be maintained and a perfect line spectrum be recorded, free from disturbing molecular bands (Plates II—VI). At higher currents the special shape of the F I lines disappeared and the intensity of S II increased. Without lithium in the nickel-lined source chamber a large number of Ni I lines were very strong and shaped like the F I lines. Finally, it was found possible to improve the excitation of the F I electron transitions $3p - \mathrm{n}d$, using the filling-gas mixture 3 mm He + 3 mm Ne. F I and Ne I then showed the same line profile but the separation of Ne I caused no difficulties (43).

Spectrograms were also taken with LiF in the hollow cathode and no $SF_6$ in the filling-gas. The light source was in this case somewhat unstable and only after running for several hours did the molecular bands disappear. The samples of LiF might have contained small amounts of LiOH, causing a strong excitation of O I

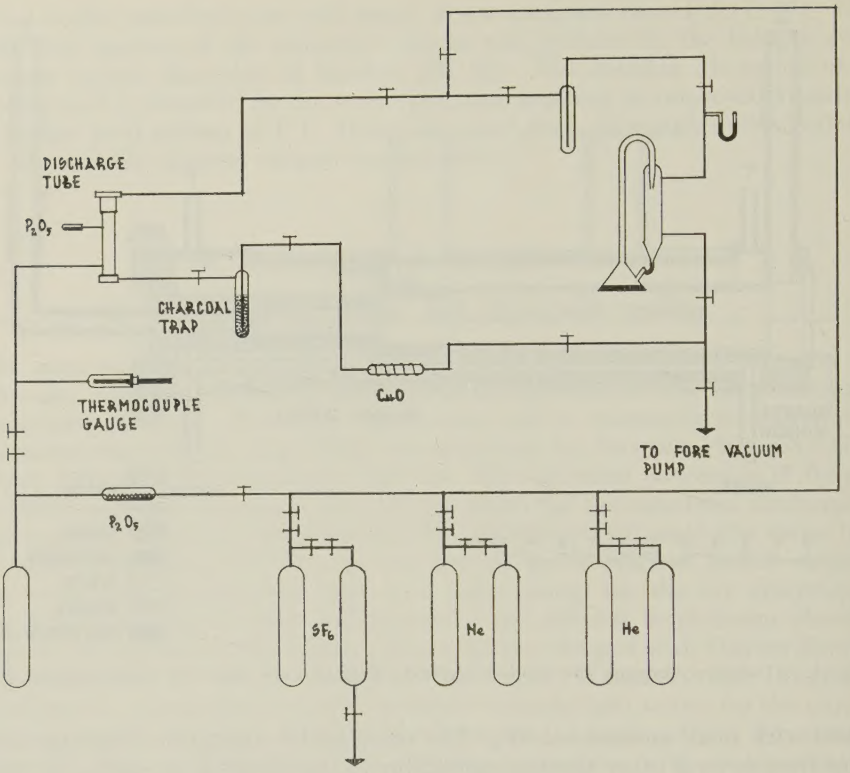

Fig. 2. The gas circulating system.

and H I; the intensity of the Balmer lines did not decrease in spite of strong heating of the CuO tube. It was possible, however, to make several excellent recordings in different spectral regions with exposure times up to 10 hours, but the special line shape of F I disappeared (Plate V).

***Spectrographs.*** The spectrograms were obtained with three different spectrographs. In the region 4000—2000 A some plates were taken with the quartz optical system of a large automatic spectrograph, Hilger E 478, with a dispersion of 4.8 A/mm at 3000 A. An older autocollimation glass prism spectrograph was also used (32), the Rutherfurd prism train of which was exchanged for a 60° glass prism of light flint, transmissible down to 3400 A, and an aluminized plane mirror. The objective lens was coated with an antireflecting layer of LiF. With this optical system the dispersion at 3700 A was 5.5 A/mm, but the lines were not perfect due to a slight inhomogeneity of the prism.

Most of the measured spectrograms were obtained with a 21-foot concave grating spectrograph in a stigmatic (Wadsworth) mounting. Fig. 3 is a schematic drawing of the instrument which was designed by the author and built in this laboratory for the present investigation. The grating, an original Rowland grating with 10 000 grooves per inch and a ruled surface of 2 × 6 inches, was the same used already by J. R. RYDBERG (49). The radius of the grating was 6.434 m and that of the alumin-

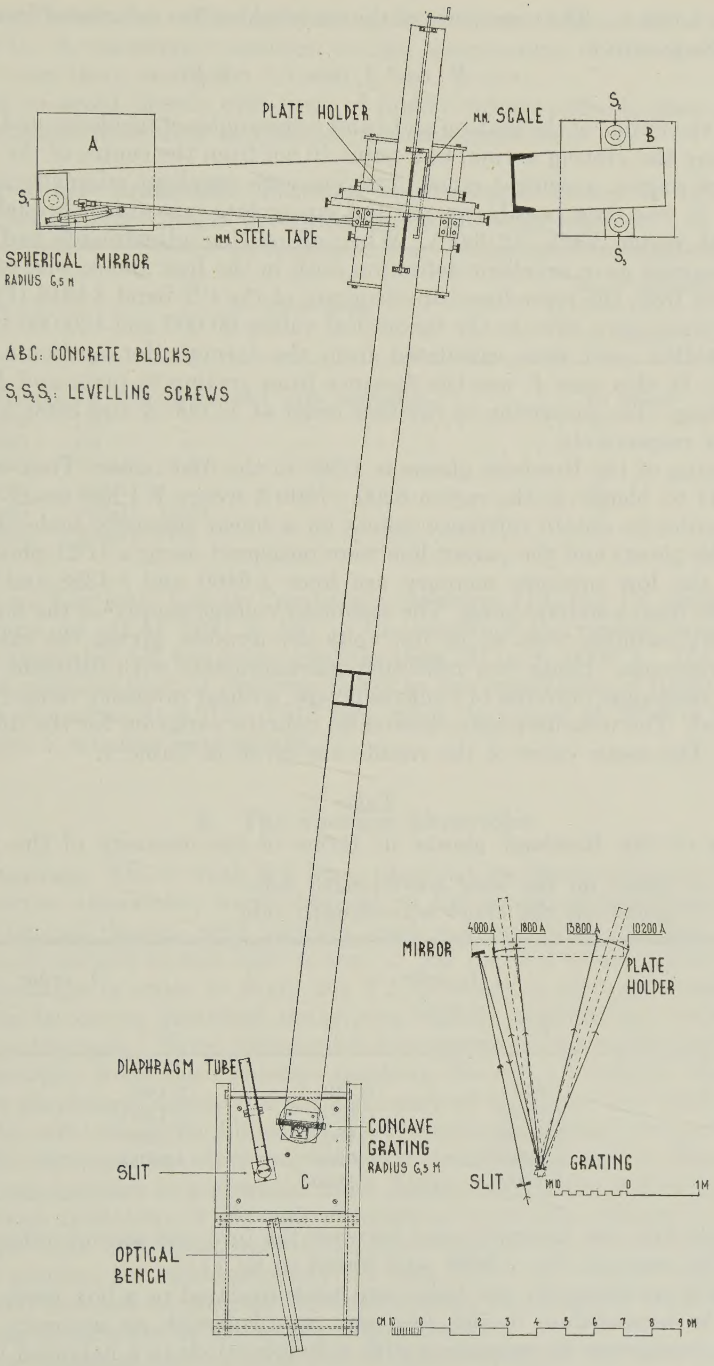

Fig. 3. The stigmatic grating spectrograph in Wadsworth mounting.

ized mirror 6.664 m. The curvature of the plateholder was calculated from a formula given by SHENSTONE:

$$r = R \cdot \cos^2 \beta / (\cos i + \cos \beta)$$

where $R$ is the radius of the grating and $i$ and $\beta$ the angles of incidence and diffraction. After setting the grating normal to a point 10 cm from the centre of the plateholder towards the mirror, a central range of 25 cm with excellent stigmatic imaging was obtained. It was then possible to use the same plate curvature through the whole wave-length region 3500—12 000 A. When all routine adjustments had been made the spectrograph gave excellent definition both in the first and second orders, which may be seen from the reproduced spectrogram of the CN band $\lambda$ 4216 (Plate I). The resolving power came close to the theoretical values 60 000 and 120 000 respectively. The slit widths used were calculated from the formula for optimum slit width, $s = \lambda$ F/D. In this case $F$ was the distance from grating to plate and $D$ the width of the grating. The dispersion in the first order at 11 000 A and 3800 A is 7.46 and 7.80 A/mm respectively.

The spacing of the Rowland ghosts is $\lambda/500$ in the first order. They caused some trouble due to blends in the region 6200—7800 A where F I has many very strong lines. In order to obtain reference points on a linear intensity scale the intensity ratios of the ghosts and the parent line were measured using a 1P21 photomultiplier tube and the low pressure mercury arc lines $\lambda$ 5460 and $\lambda$ 4358 and the $D$-lines $\lambda\lambda$ 5889—95 from a sodium lamp. The stabilized voltage supply[1] of the multiplier was continuously variable from 42 to 100 volts per dynode, giving the ratio 1:700 of intensity response. Using two reflecting galvanometers with different ranges and maximum multiplier currents of 1 microampere, a linear intensity range of 1:700 000 was covered. The measurements showed no definite variation for the different lines observed. The mean value of the results are given in Table 1.

*Table 1.*

Intensities of the Rowland ghosts in terms of the intensity of the parent line.

$I+$ = ghost on the long wave-length side.
$I-$ = ghost on the short wave-length side.

| Ghost no. | 1. order | | 2. order | |
|---|---|---|---|---|
| | $I+$ | $I-$ | $I+$ | $I-$ |
| 1 | 1/660 | 1/730 | 1/140 | 1/150 |
| 2 | 1/5100 | 1/5000 | 1/1300 | 1/1100 |
| 3 | 1/5000 | 1/4600 | 1/2200 | 1/980 |
| 4 | 1/8300 | 1/6900 | 1/3600 | 1/1500 |
| 5 | 1/18000 | 1/18000 | | |

At the same time the intensity ratio between the first and second orders was measured for the mercury line $\lambda$ 5460, and found to be 11:1.

The whole spectrograph was light- and heat-insulated in a box made of Treetex-plates. The temperature in this box was recorded with an accuracy of 0°.02 C. using two thermistors in connection with a double triode in a balanced bridge and a recording milliammeter. The room temperature was thermostatically controlled to ± 0°.3 C. A maximum variation in the temperature of the spectrograph of ± 0°.03 C was then recorded.

---

[1] Constructed at this institute by Fil. kand. L. Stigmark, electronic division.

In order to avoid blends with lines of higher orders, suitable glass filters from Chance Brothers were used in front of the condenser lens.

***Photographic material.*** Eastman Spectroscopic Plates of different types were used for different ranges according to the following scheme.

| Range | Plate type | Max. exposure time used | |
|---|---|---|---|
| | | 1. order | 2. order |
| 12000—9900 A | IZ hypersensitized with ammonia .......... | 15 hours | — |
| 10200—9000 | IM » » » .......... | 10 » | — |
| 9200—6900 | IN » » » .......... | 3 » | — |
| 7000—6300 | 103aF, IV F .......... | 2 » | 8 hours |
| 6500—5000 | 103aC .......... | 3 » | 8 » |
| 5800—4500 | 103aD, 103D .......... | 3 » | 8 » |
| 5000—2500 | 103aO, IVO .......... | 3 » | 3 » |

According to Eastman Kodak Company's catalogue (12) the IN emulsion should have a sharp cut off at 8700 A, but in the course of the present investigation it became evident that IN was more sensitive than IM up to 9200 A. The 103a-emulsions had a practical limit of resolving power at line separations of 0.020—0.025 mm and the IV-emulsions at 0.012—0.015 mm, when developed at 20° C in Kodak D19 for 4—5 and 2 minutes respectively.

## 2. The vacuum ultraviolet

***Light source.*** The 6 weak F I lines, observed by Bowen (5) and Edlén (13) in the vacuum ultraviolet, were obtained in the course of investigations of the spectra of ionized fluorine with vacuum spark sources. Since the first spectra are rather weakly excited in this light source, it was decided to use a suitable hollow cathode discharge in order to study the F I spectrum in the vacuum region. The hollow cathode source, described above, was slightly modified and connected to a vacuum spectrograph. Three rectangular diaphragms in the anode tube served to prevent particles from the discharge reaching the slit. A shutter was mounted close to the diaphragm nearest the slit and operated by means of a sylphon bellows. Through the exit tube of the filling-gas and a small hole at the bottom of the source chamber the discharge was observed visually in a small spectroscope. The circulating filling-gas was purified in a charcoal trap. After charging the hollow cathode with LiF, excellent excitation of F I was obtained at a helium pressure of 2—4 mm. Experiments with small amounts of $SF_6$ (less than 0.1 mm in the filling-gas) also gave good results, but simultaneously S I and S II were excited fairly strongly. The observed decrease of intensity towards shorter wave-lengths must be ascribed to increasing absorption in the sulphur hexafluoride.

Power was obtained from a 2000 volt, 2 amp. smoothed full wave rectifier, the output voltage of which was controlled by a variable transformer in the primary circuit. A resistance of 800 ohms was placed in series with the hollow cathode source. Usually 350—250 volts across the tube and a current of 0.3—0.6 amp. were the operating conditions for long exposures, but in order to make use of all fluorine from the LiF charge, sometimes currents up to 1.5 amp. were used for short periods. When running the discharge with $SF_6$, 0.4 amp. and 400 volts across the tube gave the best results.

In order to record Cu I and Cu II as reference spectra above 1000 A, the inside of the hollow cathode was lined with a copper foil. When the filling-gas was supplied with small amounts of $SF_6$ and the tube operated at 0.3 amp., 400 volts and helium pressure 4 mm, Cu I and Cu II were excited fairly strongly, and the foil was partly melted. The intensity ratio Cu I/Cu II was surprisingly higher with $SF_6$ in the discharge than with pure helium.

***Spectrograph.*** The work in the vacuum ultraviolet region was carried out with a 1.5 m grazing-incidence speculum grating spectrograph, formerly used at Uppsala and described by ARVIDSSON (1). The N.P.L.-grating had 567 grooves/mm and a ruled surface of 32 × 19 mm. The dispersion at 1000 A was 4.2 A/mm. The slit width was usually 0.003 mm and the resolving power came close to the theoretical value 18 000 (Plate VIII). No grating ghosts could be observed and the spectrograph gave intense spectra in the first order and fairly intense spectra in the second order. The spectrograph was continuously evacuated by an oil diffusion pump with a speed in the spectrograph of 10 l/sec at $10^{-3}$ mm. Small amounts of the filling-gas leaked through the slit into the spectrograph but here the pressure never exceeded $5 \cdot 10^{-3}$ mm. Constant operating pressure in the discharge tube was maintained by replacing the lost helium gas from the helium container through a needle valve.

***Photographic material.*** Various photographic emulsions were tested for sensitivity. Ilford Q2 plates had the greatest speed and were used for recording the fainter lines. For high precision measurements on selected lines the fine-grain Ilford Q1 plates were used. Q2 was developed for 1—2 min. in Ilford D2, and Q1 for 3—4 min. in Ilford D19 at 18° C. The only available glass plates with these emulsions had a thickness of 0.85—0.95 mm, which was really too thick for the curvature of the spectrograph and the plates often broke into several pieces. Hence only a few good spectrograms were obtained with exposure times up to 2 $^1/_2$ hours.

## 3. Interferometric measurements

***Light source.*** The hyperfine structure of the arc spectrum of fluorine was investigated by CAMPBELL 1933 (8), using a Paschen hollow cathode charged with KF. The high temperature in this discharge caused a considerable Doppler-broadening. In the present work experiments were made with a water-cooled hollow cathode, using the gaseous sulphur hexafluoride. It is estimated that the Doppler-broadening should be only about one third of that obtained by CAMPBELL. The hollow cathode discharge tube described above was slightly modified. The inner brass tube (diameter 15 mm, length 40 mm) of the water-cooled cathode support, was used as source chamber. The circulated filling-gas, 3 mm He + 1 mm Ne, was supplied with $SF_6$. In order to maintain a low temperature in the discharge, only 0.1—0.2 amp. was used, i. e. a current density of 5—10 milliamp/cm². The voltage across the tube was then 500—600 volts and increased with increasing partial pressure of $SF_6$.

Some spectrograms were recorded with exactly the same light source as in Fig. 1, in order to obtain the $3p-3d$ transitions of F I with sufficient intensity.

***Spectral apparatus.*** A Fabry-Perot interferometer was combined with the 21-foot stigmatic grating spectrograph, described above. A good achromat (Heliar, f = 24 cm, or Tessar, f = 60 cm) was placed at its focal distance from the slit and a condenser was used to obtain a parallel beam from the source. The interferometer was then inserted between the condenser lens and the achromat. No airtight chamber surrounded the interferometer but spectrograms were taken only when the prospects of constant temperature and barometric pressure were good. Constant conditions within 1 mm Hg and 0°.1 C were obtainable for exposures up to three hours.

The interferometer plates were made by the engineer H. A. HELM, Charlottenlund, Denmark from fused quartz and were silvered by evaporation in professor E. RASMUSSEN's Laboratory in Copenhagen. A test of the plates according to RASMUSSEN's method (48) showed that the combination was perfect to $\lambda/50$ with a single local deviation of $\lambda/20$. It was possible to separate the mercury isotope lines in $\lambda$ 5460 with a 15 mm spacing, indicating a resolving power of about 800 000. The spacers of invar available were 1, 2, 3, 5, 10, 15, and 25 mm.

The spectra were taken on Eastman Spectroscopic Plates, type 103aF for the visible region and type IN, hypersensitized with ammonia, for the infrared region.

## III. The determination of wave-lengths

### 1. The region 12 000—2500 A

A number of selected spectrograms were measured in a Hilger L 13 comparator. Its screw had a length of 15 cm and a pitch of 1 mm, the micrometer drum had 100 divisions and a vernier permitted convenient readings to 0.001 mm. Each spectrogram was measured at least twice, and before the second measurement the plate was displaced 0.5 mm in order to compensate for the periodic error of the drum, the maximum of which was 0.0015 mm.

Accurate and uniformly distributed reference lines were necessary if reliable wave-length values were to be obtained in all parts of the wide range recorded in the stigmatic grating spectrograph. It was decided to use only such lines as were excited simultaneously and in the same diffraction order as the F I lines to avoid any displacements between spectra from different light sources. Because the helium, used as filling-gas, contained 0.1% neon, a number of interferometric Ne I lines were always recorded, especially from the electron transitions $3s-3p$ and $3p-4s$ in the region 9700—5800 A. In the infrared region above 10 000 A, where spectrograms were taken with 50% neon in the filling-gas (Plate II), some Ne I lines could be accurately calculated (17) from term values, based on interferometric measurements (35). The other Ne I lines in this region measured by MEGGERS (34) were then corrected by an amount $+0.05$ cm$^{-1}$. In the region 5800—4900 A some F I and S II lines were measured in the second order on spectrograms taken with 50% neon in the filling-gas and then used as standards in the first order.

Below 5000 A the Ni I spectrum was excited with moderate intensity. Wave-lengths of Ni I are given in the "*M. I. T. Wavelength Tables*" (23) with an accuracy of about 0.005 A. The smooth correction curves obtained from the Ni I lines indicated an average error less than 0.005 A. Some Li I lines recently measured interferometrically by Meissner, Mundie and Stelson (37), were also used as standards (19). Finally, a few sensitive and interferometrically measured lines from Al I, Ca II, A I and Cu I in the range below 4000 A, were used as reference lines on spectrograms from all three spectrographs.

The Rowland ghosts of some tremendously overexposed He I lines, especially the ghosts nos. 2, 3, 4, 5, and 11, were first considered as good standards but were finally discarded since small deviations (0.01—0.02 A) from the calculated positions were discovered. However, the mean value of the wave-lengths for two ghosts with equal numbers and opposite sign seemed to give almost exactly the correct value of the parent line.

The measurements on the grating spectrograms were converted to wave-lengths by linear interpolation over appropriate ranges and the final wave-length values were obtained from a correction curve. The prism spectrograms were reduced with a Hartmann formula and a correction curve.

### 2. The vacuum region

The spectrograms obtained with the vacuum spectrograph were measured in the comparator described above. The plateholder [Arvidsson (1)] kept the plate in focus of the microscope throughout the whole range measured.

Reference lines were obtained from simultaneously excited spectra. When charging the hollow cathode with LiF, the O I spectrum was excited with moderate intensity in the region 800—1300 A, where accurate wave-lengths have been calculated by Edlén (16) ultimately based on More and Rieke's measurement of $\lambda\lambda$ 1302—06 (41). From 850 to 600 A some lines from C I, C II, O II and Ne II were used as standards but in this region the number of reference lines was rather too small. Probably the most accurate standards in the region investigated are the calculated wave-lengths of the Lyman series of hydrogen. It was possible to record simultaneously the strongest fluorine and hydrogen lines both in the first and in the second order with an intensity suitable for precision measurements (Plate VII). The hydrogen lines showed almost the same sharp definition as the fluorine lines. The wave-lengths of the Lyman lines were recalculated using Penney's formula (44), Birge's value of the Rydberg constant (4) and Bethe and Longmire's value of the fine structure constant (3). The values obtained are systematically 0.002 A greater than those calculated by Paschen (6). The recently discovered shift of the $^2S_{1/2}$ level in hydrogen-like atoms, however, calls for an additional correction. Lamb and Retherford (31) measured this shift accurately for $2s\ ^2S_{1/2}$ and Bethe (2) gave a theoretical calculation which agreed well with the measured shift, and showed that the shift should be proportional to $1/n^3$. No exact calculations were published for the ground state $1s\ ^2S_{1/2}$, but Bethe has kindly informed the author that on general grounds it was almost certain that the shift of $1s\ ^2S_{1/2}$ must be precisely 8 times the value of $2s\ ^2S_{1/2}$ and that it has now been accurately measured by Lamb and found to be 1062 Mc $\pm$ 1%. The shifts of $np\ ^2P_{1/2,\,3/2}$ should be quite negligible. The Bethe-correction, $-0.283$ cm$^{-1}$, was then applied to the Lyman lines giving a correction of $+0.004$ A to $\lambda$ 1215 etc. (Table 2).

*Table 2.*

Wave-lengths of the Lyman series in hydrogen.

$\nu = R_M(1-1/n^2)+R_M\alpha^2(1/4-2/3n^3+3/4n^4)$. $R_M = 109677.581$ cm$^{-1}$. $1/\alpha = 137.041$.
Bethe-correction of $1s\ ^2S_{1/2} = -0.283$ cm$^{-1}$.

| n | $\nu$ | $\lambda_{vac}$ | n | $\nu$ | $\lambda_{vac}$ |
|---|---|---|---|---|---|
| 2 | 82259.433 | 1215.6702 | 7 | 107440.731 | 930.7482 |
| 3 | 97492.565 | 1025.7222 | 8 | 107965.322 | 926.2258 |
| 4 | 102824.149 | 972.5369 | 9 | 108324.957 | 923.1507 |
| 5 | 105291.914 | 949.7431 | 10 | 108582.262 | 920.9631 |
| 6 | 106632.512 | 937.8028 | | | |

F I and H I lines in the second order were also measured together with SHENSTONE's calculated Cu II standards (51)[1] in the first order (Plate VII b). A small displacement of 0.020 A between lines in the first and the second order was observed, and its value could be measured precisely especially from the lines Cu II 1944.586 A and H I, 2 × 972.537 = 1945.074 A.

The wave-lengths were calculated with the aid of a dispersion table with the interval 1 mm [see for instance FERNER (20)]. The maximum error thus introduced was less than 0.001 A. The final correction was obtained in the usual way from a correction curve.

## 3. The interferometer spectrograms

The interferometric recordings were also measured with the Hilger comparator L 13, which was not quite convenient, however, for such purposes. When possible, at least 4 to 6 ring diameters were determined. The hyperfine structure separations were determined according to the rectangular array method [TOLANSKY (55)] on spectrograms taken with 10, 15, and 25 mm spacers. The accuracy of the measured intervals was sometimes influenced by unresolved weak components which broadened the strong components, especially in the case of transitions between levels with small $J$-values. In general, however, the uncertainty does not exceed 0.002—0.005 cm$^{-1}$.

The calculation of absolute wave-length values was made with the aid of Ne I[2] standards, excited simultaneously with the F I lines in the region 5700—8900 A. The method is described by several authors; see for instance MEISSNER (36). In this case several Ne I lines equally distributed in the whole range were measured, and the correction to be applied to the F I lines for phase change at reflection and for dispersion of air was then obtained from an ordinary correction curve. In general, spectrograms obtained with the 10 mm spacer were measured, supplemented by a few measurements on 25 mm spacer spectrograms. For F I lines showing separated *hfs* components the centre of gravity was calculated using the theoretical values of the relative intensities of the components (57) (Plate IX, X).

---

[1] The Cu II line $\lambda_{vac}$ 2000.339 is erroneously given as $\lambda_{air}$ 2000.348 in the *M. I. T. Tables.*

[2] In the draft report from the I. A. U. Zürich meeting 1948 Burns' unpublished values of Ne I lines above 7059 are given. They have been used in this investigation.

# IV. Results

## 1. The range 12 000—2500 A

The wave-lengths measured are given in the first column of Table 5. A total of 471 lines in the range 11 557—2967 A are listed as compared with the 85 lines from 9433—6047 A in EDLÉN's paper (14). The non-interferometric wave-lengths are weighted means from different plates. 44% of the lines are measured on three or more spectrograms, 39% on two and 17% on only one plate. 80% are measured on both LiF and $SF_6$ recordings. The 17% is made up of faint lines recorded only on the most intense and pure spectrograms. The estimated errors of the wave-lengths in different ranges and from different spectrographs are shown in Table 3.

*Table 3.*

Estimated uncertainty of wave-lengths in different spectral regions.

| Region | Grating spectrograph | | Prism spectrographs | |
|---|---|---|---|---|
| | 1. order | 2. order | glass | quartz |
| 12000—9700 A | ± (0.02−0.05) A | | | |
| 9700—7000 » | ± (0.01−0.03) » | | | |
| 7000—4000 » | » | ± (0.005−0.010) A | | |
| 4000—3500 » | » | » | ± (0.02−0.04) A | |
| 3500—2500 » | » | | | ± (0.01−0.02) A |

The interferometrically measured wave-lengths are marked with a star in Table 5. Most of them are determined from 2 to 3 spectrograms. Energy level differences indicate an uncertainty in these wave-lengths in general not exceeding 0.002 A. A few other lines obtained from several consistent determinations in the first and second orders of the grating spectrograph are also given to three decimal figures. Their uncertainty is probably less than 0.010 A.

In the second column of Table 5 the intensities are given on a linear scale ranging from 0.5 to 500 000. The differing sensitivities of the emulsions have been approxi-

*Table 4.*

Intensities of some He I and Ne I lines expressed on the same scale as used for the F I lines in Table 5.

| λ | Intensity | λ | Intensity |
|---|---|---|---|
| He I 10830 | 15 000 | He I 7281 | 70 000 |
| Ne I 9665 | 1 500 | He I 7065 | 150 000 |
| Ne I 8919 | 2 500 | He I 6678 | 900 000 |
| Ne I 8654 | 150 000 | He I 5875 | 1 000 000 |
| Ne I 8300 | 30 000 | He I 5015 | 60 000 |
| Ne I 7943 | 6 000 | He I 3888 | 70 000 |

*Table 5.*

Wave-lengths of F I lines in the region 11557—2967 A.

| $\lambda_{\text{air}}$ | Intensity | EDLÉN = E<br>LIDÉN = L | $\nu_{\text{vac.}}$ | Identification |
|---|---|---|---|---|
| 11557.17 | 50 | | 8650.26 | $3p\,^4D_{7/2}-4s\,^4P_{5/2}$ |
| 11544.65 | 20 | | 8659.65 | $3p\,^2D_{5/2}-4s\,^2P_{3/2}$ |
| 11480.22 | 12 | | 8708.25 | $3p\,^2D_{3/2}-4s\,^2P_{1/2}$ |
| 11473.70 | 30 | | 8713.19 | $3p\,^4D_{5/2}-4s\,^4P_{3/2}$ |
| 11414.20 | 15 | | 8758.61 | $3p\,^4D_{3/2}-4s\,^4P_{1/2}$ |
| 10940.37 | 40 | | 9137.95 | $3p\,^2P_{1/2}-3d\,^2D_{3/2}$ |
| 10924.81 | 25 | | 9150.97 | $3p\,^2P_{3/2}-3d\,^4D_{5/2}$ |
| 10883.28 | 25 | | 9185.89 | $3p\,^2P_{3/2}-3d\,^4D_{3/2}$ |
| 10862.31 | 200 | | 9203.62 | $3p\,^2P_{3/2}-3d\,^2D_{5/2}$ |
| 10769.43 | 40 | | 9283.00 | $3p\,^2P_{3/2}-3d\,^2D_{3/2}$ |
| 10592.28 | 18 | | 9438.25 | $3p\,^2P_{1/2}-3d\,^2P_{1/2}$ |
| 10588.71 | 45 | | 9441.43 | $3p\,^2P_{1/2}-3d\,^4P_{3/2}$ |
| 10490.21 | 10 | | 9530.08 | $3p\,^2P_{1/2}-3d\,^4F_{3/2}$ |
| 10431.92 | 12 | | 9583.34 | $3p\,^2P_{3/2}-3d\,^2P_{1/2}$ |
| 10426.29 | 60 | | 9588.51 | $3p\,^2P_{3/2}-3d\,^4F_{5/2}$ |
| 10417.29 | 70 | | 9596.80 | $3p\,^4P_{3/2}-4s\,^4P_{5/2}$ |
| 10380.84 | 70 | | 9630.49 | $3p\,^2P_{1/2}-3d\,^2P_{3/2}$ |
| 10332.95 | 25 | | 9675.13 | $3p\,^2P_{3/2}-3d\,^4F_{3/2}$ |
| 10293.01 | 35 | | 9712.67 | $3p\,^4S_{3/2}-3d\,^2D_{5/2}$ |
| 10287.96 | 15 | | 9717.44 | $3p\,^2S_{1/2}-3d\,^4D_{3/2}$ |
| 10285.45 | 150 | | 9719.81 | $3p\,^4P_{5/2}-4s\,^4P_{5/2}$ |
| 10270.75 | 40 | | 9733.72 | $3p\,^4P_{1/2}-4s\,^4P_{3/2}$ |
| 10241.98 | 35 | | 9761.06 | $3p\,^2P_{3/2}-3d\,^2F_{5/2}$ |
| 10226.82 | 30 | | 9775.53 | $3p\,^2P_{3/2}-3d\,^2P_{3/2}$ |
| 10222.50 | 20 | | 9779.66 | $3p\,^2S_{1/2}-3d\,^4D_{1/2}$ |
| 10209.57 | 40 | | 9792.05 | $3p\,^4S_{3/2}-3d\,^2D_{3/2}$ |
| 10186.15 | 50 | | 9814.56 | $3p\,^2S_{1/2}-3d\,^2D_{3/2}$ |
| 10163.50 | 30 | | 9836.44 | $3p\,^4P_{3/2}-4s\,^4P_{3/2}$ |
| 10087.13 | 60 | | 9910.91 | $3p\,^4S_{3/2}-3d\,^4P_{1/2}$ |
| 10074.17 | 10 | | 9923.65 | $3p\,^4P_{1/2}-4s\,^4P_{1/2}$ |
| 10064.25 | 40 | | 9933.45 | $3p\,^2S_{4/2}-3d\,^4P_{1/2}$ |
| 10038.03 | 35 | | 9959.39 | $3p\,^4P_{5/2}-4s\,^4P_{3/2}$ |
| 9970.92 | 40 | | 10026.41 | $3p\,^4P_{3/2}-4s\,^4P_{1/2}$ |
| 9905.65 | 15 | | 10092.48 | $3p\,^4S_{3/2}-3d\,^2P_{1/2}$ |
| 9902.65 | 125 | | 10095.54 | $3p\,^4S_{3/2}-3d\,^4P_{3/2}$ |
| 9883.58 | 80 | | 10115.02 | $3p\,^2S_{1/2}-3d\,^2P_{1/2}$ |
| 9822.11 | 150 | | 10178.32 | $3p\,^4S_{3/2}-3d\,^4P_{5/2}$ |
| 9794.80 | 60 | | 10206.70 | $3p\,^2S_{1/2}-3d\,^4F_{3/2}$ |
| 9753.57 | 15 | | 10249.85 | $3p\,^2D_{3/2}-3d\,^4D_{3/2}$ |
| 9736.70 | 90 | | 10267.60 | $3p\,^2D_{3/2}-3d\,^2D_{5/2}$ |
| 9734.34 | 250 | | 10270.09 | $3p\,^4S_{3/2}-3d\,^2F_{5/2}$ |
| 9720.57 | 12 | | 10284.64 | $3p\,^4S_{3/2}-3d\,^2P_{3/2}$ |
| 9699.40 | 70 | | 10307.09 | $3p\,^2S_{1/2}-3d\,^2P_{3/2}$ |
| 9662.04 | 125 | | 10346.95 | $3p\,^2D_{3/2}-3d\,^2D_{3/2}$ |
| 9574.80 | 30 | | 10441.22 | $3p\,^2D_{5/2}-3d\,^4D_{7/2}$ |

Table 5 (cont.).

| $\lambda_{\text{air}}$ | Intensity | Edlén = E<br>Lidén = L | $\nu_{\text{vac.}}$ | Identification |
|---|---|---|---|---|
| 9552.99 | 7 | | 10465.06 | $3p\,^2D_{5/2}-3d\,^4D_{5/2}$ |
| 9552.30 | 7 | | 10465.81 | $3p\,^2D_{3/2}-3d\,^4P_{1/2}$ |
| 9505.30 | 250 | | 10517.56 | $3p\,^2D_{5/2}-3d\,^2D_{5/2}$ |
| 9433.67 | 2000 | 3.63 E | 10597.42 | $3p\,^2D_{5/2}-3d\,^2F_{7/2}$ |
| 9389.47 | 8 | | 10647.31 | $3p\,^2D_{3/2}-3d\,^2P_{1/2}$ |
| 9386.75 | 25 | | 10650.39 | $3p\,^2D_{3/2}-3d\,^4P_{3/2}$ |
| 9384.96 | 400 | | 10652.42 | $3p\,^2D_{3/2}-3d\,^4F_{5/2}$ |
| 9314.34 | 600 | 4.40 E | 10733.19 | $3p\,^2D_{3/2}-3d\,^4P_{5/2}$ |
| 9262.69 | 80 | | 10793.04 | $3p\,^4D_{1/2}-3d\,^4D_{1/2}$ |
| 9244.57 | 150 | | 10814.20 | $3p\,^4D_{3/2}-3d\,^4D_{3/2}$ |
| 9235.38 | 500 | | 10824.96 | $3p\,^2D_{3/2}-3d\,^2F_{5/2}$ |
| 9232.85 | 60 | | 10827.93 | $3p\,^4D_{1/2}-3d\,^2D_{3/2}$ |
| 9229.40 | 250 | | 10831.97 | $3p\,^4D_{3/2}-3d\,^2D_{5/2}$ |
| 9223.05 | 60 | | 10839.43 | $3p\,^2D_{3/2}-3d\,^2P_{3/2}$ |
| 9191.65 | 100 | | 10876.46 | $3p\,^4D_{3/2}-3d\,^4D_{1/2}$ |
| 9178.68 | 3500 | 8.68 E | 10891.83 | $3p\,^2D_{5/2}-3d\,^4F_{7/2}$ |
| 9169.76 | 30 | | 10902.42 | $3p\,^2D_{5/2}-3d\,^4F_{5/2}$ |
| 9162.33 | 18 | | 10911.26 | $3p\,^4D_{3/2}-3d\,^2D_{3/2}$ |
| 9151.78 | 1800 | | 10923.84 | $3p\,^4D_{5/2}-3d\,^4D_{5/2}$ |
| 9132.53 | 14 | | 10946.86 | $3p\,^4D_{1/2}-3d\,^4P_{1/2}$ |
| 9122.63 | 400 | | 10958.74 | $3p\,^4D_{5/2}-3d\,^4D_{3/2}$ |
| 9107.87 | 100 | | 10976.51 | $3p\,^4D_{5/2}-3d\,^2D_{5/2}$ |
| 9102.33 | 500 | | 10983.18 | $3p\,^2D_{5/2}-3d\,^4P_{5/2}$ |
| 9097.49 | 35 | | 10989.03 | $3p\,^2D_{5/2}-3d\,^4F_{3/2}$ |
| 9042.10 | 4000 | 2.11 E | 11056.35 | $3p\,^4D_{5/2}-3d\,^2F_{7/2}$ |
| 9025.49 | 3500 | 5.49 E | 11076.69 | $3p\,^4D_{7/2}-3d\,^4D_{7/2}$ |
| 9015.19 | 7 | | 11089.35 | $3p\,^2D_{5/2}-3d\,^2P_{3/2}$ |
| 9006.19 | 500 | | 11100.43 | $3p\,^4D_{7/2}-3d\,^4D_{5/2}$ |
| 8983.65 | 35 | | 11128.28 | $3p\,^4D_{1/2}-3d\,^2P_{1/2}$ |
| 8981.18 | 125 | | 11131.34 | $3p\,^4D_{1/2}-3d\,^4P_{3/2}$ |
| 8963.66 | 40 | | 11153.10 | $3p\,^4D_{7/2}-3d\,^2D_{5/2}$ |
| 8936.61 | 7 | | 11186.86 | $3s\,^2P_{3/2}-3p\,^4P_{5/2}$ |
| 8916.89 | 20 | | 11211.60 | $3p\,^4D_{3/2}-3d\,^2P_{1/2}$ |
| 8914.43 | 70 | | 11214.69 | $3p\,^4D_{3/2}-3d\,^4P_{3/2}$ |
| 8912.78 | 3000 | 2.78 E | 11216.77 | $3p\,^4D_{3/2}-3d\,^4F_{5/2}$ |
| 8910.27 | 1400 | 0.24 E | 11219.93 | $3p\,^4D_{1/2}-3d\,^4F_{3/2}$ |
| 8900.92 | 10000 | 0.92 E | 11231.72 | $3p\,^4D_{7/2}-3d\,^4F_{9/2}$ |
| 8899.92 | 600 | | 11232.97 | $3p\,^4D_{7/2}-3d\,^2F_{7/2}$ |
| 8849.06 | 700 | 9.07 E | 11297.53 | $3p\,^4D_{3/2}-3d\,^4P_{5/2}$ |
| *8844.502 | 1200 | 4.50 E | 11303.358 | $3p\,^4D_{3/2}-3d\,^4F_{3/2}$ |
| *8831.232 | 1000 | 1.22 E | 11320.343 | $3p\,^4D_{1/2}-3d\,^2P_{3/2}$ |
| *8807.582 | 9000 | 7.59 E | 11350.740 | $3p\,^4D_{5/2}-3d\,^4F_{7/2}$ |
| 8799.36 | 700 | 9.37 E | 11361.35 | $3p\,^4D_{5/2}-3d\,^4F_{5/2}$ |
| 8792.50 | 350 | | 11370.21 | $(^1D)\,3p\,^2F_{7/2}-(^1D)\,3d\,^2G_{9/2}$ |
| 8785.63 | 140 | | 11379.10 | $(^1D)\,3p\,^2F_{5/2}-(^1D)\,3d\,^2G_{7/2}$ |
| 8777.73 | 1200 | 7.75 E | 11389.34 | $3p\,^4D_{3/2}-3d\,^2F_{5/2}$ |
| 8766.61 | 100 | | 11403.79 | $3p\,^4D_{3/2}-3d\,^2P_{3/2}$ |
| *8737.270 | 1400 | 7.28 E | 11442.083 | $3p\,^4D_{5/2}-3d\,^4P_{5/2}$ |
| 8732.80 | 60 | | 11447.94 | $3p\,^4D_{5/2}-3d\,^4F_{3/2}$ |
| 8672.62 | 350 | | 11527.38 | $3p\,^4D_{7/2}-3d\,^4F_{7/2}$ |

Table 5 (cont.).

| $\lambda_{\text{air}}$ | Intensity | EDLÉN = E<br>LIDÉN = L | $\nu_{\text{vac.}}$ | Identification |
|---|---|---|---|---|
| 8667.71 | 10 | | 11533.91 | $3p\,^4D_{5/2}-3d\,^2F_{5/2}$ |
| 8664.63 | 60 | | 11538.01 | $3p\,^4D_{7/2}-3d\,^4F_{5/2}$ |
| 8656.93 | 8 | | 11548.27 | $3p\,^4D_{5/2}-3d\,^2P_{3/2}$ |
| 8612.58 | 60 | | 11607.73 | |
| 8606.06 | 60 | | 11616.53 | |
| 8604.47 | 14 | | 11618.67 | $3p\,^4D_{7/2}-3d\,^4P_{5/2}$ |
| 8579.81 | 12 | | 11652.07 | |
| 8537.04 | 70 | | 11710.45 | $3p\,^4D_{7/2}-3d\,^2F_{5/2}$ |
| *8345.556 | 1200 | 5.57 E | 11979.137 | $3p\,^4P_{1/2}-3d\,^4D_{3/2}$ |
| 8302.40 | 6000 | 2.40 E | 12041.40 | $3p\,^4P_{1/2}-3d\,^4D_{1/2}$ |
| *8298.581 | 20000 | 8.59 E | 12046.946 | $3p\,^4P_{3/2}-3d\,^4D_{5/2}$ |
| 8278.44 | 20 | | 12076.25 | $3p\,^4P_{1/2}-3d\,^2D_{3/2}$ |
| *8274.615 | 15000 | 4.62 E | 12081.839 | $3p\,^4P_{3/2}-3d\,^4D_{3/2}$ |
| 8262.49 | 120 | 2.48 E | 12099.56 | $3p\,^4P_{3/2}-3d\,^2D_{5/2}$ |
| 8232.19 | 5000 | 2.18 E | 12144.10 | $3p\,^4P_{3/2}-3d\,^4D_{1/2}$ |
| *8230.773 | 30000 | 0.77 E | 12146.194 | $3p\,^4P_{5/2}-3d\,^4D_{7/2}$ |
| *8214.726 | 25000 | 4.72 E | 12169.919 | $3p\,^4P_{5/2}-3d\,^4D_{5/2}$ |
| *8208.634 | 3500 | 8.63 E | 12178.951 | $3p\,^4P_{3/2}-3d\,^2D_{3/2}$ |
| *8197.734 | 600 | 7.74 E | 12195.144 | $3p\,^4P_{1/2}-3d\,^4P_{1/2}$ |
| *8191.241 | 3000 | 1.24 E | 12204.811 | $3p\,^4P_{5/2}-3d\,^4D_{3/2}$ |
| *8179.339 | 6000 | 9.34 E | 12222.571 | $3p\,^4P_{5/2}-3d\,^2D_{5/2}$ |
| 8159.51 | 3000 | 9.52 E | 12252.27 | $3s\,^2P_{1/2}-3p\,^4D_{3/2}$ |
| 8129.26 | 6000 | 9.27 E | 12297.86 | $3p\,^4P_{3/2}-3d\,^4P_{1/2}$ |
| 8126.56 | 3500 | 6.56 E | 12301.95 | $3p\,^4P_{5/2}-3d\,^2D_{3/2}$ |
| *8077.521 | 3500 | 7.53 E | 12376.637 | $3p\,^4P_{1/2}-3d\,^2P_{1/2}$ |
| *8075.519 | 9000 | 5.52 E | 12379.706 | $3p\,^4P_{1/2}-3d\,^4P_{3/2}$ |
| *8040.931 | 10000 | 0.94 E | 12432.957 | $3s\,^2P_{3/2}-3p\,^4D_{5/2}$ |
| 8018.12 | 80 | 8.10 E | 12468.33 | $3p\,^4P_{1/2}-3d\,^4F_{3/2}$ |
| 8011.05 | 50 | | 12479.33 | $3p\,^4P_{3/2}-3d\,^2P_{1/2}$ |
| 8010.66 | 40 | | 12479.94 | |
| 8009.05 | 12 | | 12482.45 | $3p\,^4P_{3/2}-3d\,^4P_{3/2}$ |
| 8007.79 | 150 | 7.77 E | 12484.41 | $3p\,^4P_{3/2}-3d\,^4F_{5/2}$ |
| 7978.96 | 50 | | 12529.51 | |
| 7977.26 | 30 | | 12532.19 | |
| 7956.32 | 3000 | 6.31 E | 12565.17 | $3p\,^4P_{3/2}-3d\,^4P_{5/2}$ |
| 7954.09 | 600 | 4.08 E | 12568.70 | $3p\,^4P_{1/2}-3d\,^2P_{3/2}$ |
| 7952.66 | 18 | | 12570.96 | $3p\,^4P_{3/2}-3d\,^4F_{3/2}$ |
| 7948.52 | 400 | 8.52 E | 12577.50 | $3s\,^2P_{3/2}-3p\,^4D_{3/2}$ |
| *7936.314 | 3500 | 6.32 E | 12596.847 | $3p\,^4P_{5/2}-3d\,^4F_{7/2}$ |
| 7930.93 | 2200 | 0.94 E | 12605.40 | $3p\,^4P_{5/2}-3d\,^4P_{3/2}$ |
| 7929.65 | 40 | | 12607.44 | $3p\,^4P_{5/2}-3d\,^4F_{5/2}$ |
| *7898.588 | 5000 | 8.59 E | 12657.013 | $3p\,^4P_{3/2}-3d\,^2F_{5/2}$ |
| 7889.62 | 80 | | 12671.40 | $3p\,^4P_{3/2}-3d\,^2P_{3/2}$ |
| 7879.18 | 3000 | 9.19 E | 12688.19 | $3p\,^4P_{5/2}-3d\,^4P_{5/2}$ |
| 7875.56 | 80 | | 12694.02 | $3p\,^4P_{5/2}-3d\,^4F_{3/2}$ |
| 7822.59 | 800 | 2.61 E | 12779.98 | $3p\,^4P_{5/2}-3d\,^2F_{5/2}$ |
| 7820.79 | 60 | | 12782.92 | |
| 7813.76 | 100 | | 12794.42 | $3p\,^4P_{5/2}-3d\,^2P_{3/2}$ |
| *7800.212 | 150000 | 0.22 E | 12816.643 | $3s\,^2P_{1/2}-3p\,^2D_{3/2}$ |
| *7754.696 | 180000 | 4.70 E | 12891.869 | $3s\,^2P_{3/2}-3p\,^2D_{5/2}$ |

Table 5 (cont.).

| $\lambda_{\text{air}}$ | Intensity | Edlén = E<br>Lidén = L | $\nu_{\text{vac.}}$ | Identification |
|---|---|---|---|---|
| *7607.170 | 70000 | 7.17 E | 13141.881 | $3s\,^2P_{3/2}-3p\,^2D_{3/2}$ |
| *7573.384 | 50000 | 3.41 E | 13200.508 | $3s\,^4P_{1/2}-3p\,^4P_{3/2}$ |
| *7552.235 | 50000 | 2.24 E | 13237.475 | $3s\,^4P_{3/2}-3p\,^4P_{5/2}$ |
| *7514.919 | 9000 | 4.93 E | 13303.205 | $3s\,^4P_{1/2}-3p\,^4P_{1/2}$ |
| *7489.155 | 25000 | 9.14 E | 13348.971 | $3s\,^2P_{1/2}-3p\,^2S_{1/2}$ |
| *7482.723 | 22000 | 2.72 E | 13360.446 | $3s\,^4P_{3/2}-3p\,^4P_{3/2}$ |
| 7476.54 | 700 | 6.54 E | 13371.49 | $3s\,^2P_{1/2}-3p\,^4S_{3/2}$ |
| *7425.645 | 40000 | 5.64 E | 13463.141 | $3s\,^4P_{3/2}-3p\,^4P_{1/2}$ |
| *7398.688 | 100000 | 8.68 E | 13512.199 | $3s\,^4P_{5/2}-3p\,^4P_{5/2}$ |
| *7331.957 | 50000 | 1.95 E | 13635.173 | $3s\,^4P_{5/2}-3p\,^4P_{3/2}$ |
| 7319.33 | 60 | | 13658.70 | $3p\,^2P_{3/2}-5s\,^4P_{5/2}$ |
| *7314.303 | 7000 | 4.31 E | 13668.083 | $(^1D)\,3s\,^2D_{3/2}-(^1D)\,3p\,^2F_{5/2}$ |
| 7313.77 | 400 | 3.74 E | 13669.08 | $(^1D)\,3s\,^2D_{5/2}-(^1D)\,3p\,^2F_{5/2}$ |
| *7311.019 | 150000 | 1.02 E | 13674.223 | $3s\,^2P_{3/2}-3p\,^2S_{1/2}$ |
| *7309.033 | 10000 | 9.03 E | 13677.938 | $(^1D)\,3s\,^2D_{5/2}-(^1D)\,3p\,^2F_{7/2}$ |
| 7298.98 | 1500 | 9.00 E | 13696.78 | $3s\,^2P_{3/2}-3p\,^4S_{3/2}$ |
| 7240.12 | 20 | | 13808.13 | $3p\,^2P_{3/2}-5s\,^4P_{3/2}$ |
| *7202.360 | 150000 | 2.37 E | 13880.519 | $3s\,^2P_{1/2}-3p\,^2P_{3/2}$ |
| *7127.890 | 300000 | 7.88 E | 14025.537 | $3s\,^2P_{1/2}-3p\,^2P_{1/2}$ |
| 7109.61 | 30 | 9.63 L | 14061.59 | $3p\,^2P_{3/2}-5s\,^2P_{3/2}$ |
| *7037.469 | 450000 | 7.45 E | 14205.744 | $3s\,^2P_{3/2}-3p\,^2P_{3/2}$ |
| 6997.71 | 8 | 7.71 L | 14286.46 | $3p\,^2P_{3/2}-5s\,^2P_{1/2}$ |
| 6982.69 | 12 | | 14317.19 | $3p\,^4S_{3/2}-5s\,^4P_{3/2}$ |
| 6971.71 | 10 | | 14339.73 | $3p\,^2S_{1/2}-5s\,^4P_{3/2}$ |
| *6966.349 | 40000 | 6.35 E | 14350.770 | $3s\,^2P_{3/2}-3p\,^2P_{1/2}$ |
| *6909.816 | 60000 | 9.82 E | 14468.181 | $3s\,^4P_{1/2}-3p\,^4D_{3/2}$ |
| *6902.475 | 150000 | 2.46 E | 14483.569 | $3s\,^4P_{3/2}-3p\,^4D_{5/2}$ |
| *6870.215 | 80000 | 0.22 E | 14551.578 | $3s\,^4P_{1/2}-3p\,^4D_{1/2}$ |
| *6856.030 | 500000 | 6.02 E | 14581.684 | $3s\,^4P_{5/2}-3p\,^4D_{7/2}$ |
| 6837.74 | 50 | | 14620.69 | $3p\,^2P_{3/2}-4d\,^4D_{5/2}$ |
| *6834.264 | 90000 | 4.26 E | 14628.124 | $3s\,^4P_{3/2}-3p\,^4D_{3/2}$ |
| 6825.56 | 150 | | 14646.77 | $3p\,^2P_{3/2}-4d\,^2D_{5/2}$ |
| 6811.67 | 12 | | 14676.64 | $3p\,^2P_{3/2}-4d\,^4D_{1/2}$ |
| 6806.85 | 100 | | 14687.04 | $3p\,^2P_{3/2}-4d\,^2D_{3/2}$ |
| *6795.528 | 15000 | 5.52 E | 14711.507 | $3s\,^4P_{3/2}-3p\,^4D_{1/2}$ |
| *6773.984 | 70000 | 3.97 E | 14758.296 | $3s\,^4P_{5/2}-3p\,^4D_{5/2}$ |
| *6767.007 | 500 | 6.97 E | 14773.512 | $(^1D)\,3s\,^2D_{3/2}-(^1D)\,3p\,^2D_{3/2}$ |
| 6766.54 | 50 | | 14774.53 | $(^1D)\,3s\,^2D_{5/2}-(^1D)\,3p\,^2D_{3/2}$ |
| 6763.325 | 50 | | 14781.55 | $(^1D)\,3s\,^2D_{3/2}-(^1D)\,3p\,^2D_{5/2}$ |
| *6762.934 | 700 | 2.89 E | 14782.409 | $(^1D)\,3s\,^2D_{5/2}-(^1D)\,3p\,^2D_{5/2}$ |
| 6741.90 | 12 | | 14828.53 | $3p\,^2P_{1/2}-4d\,^2P_{1/2}$ |
| 6737.76 | 60 | | 14837.64 | $3p\,^2P_{1/2}-4d\,^4P_{3/2}$ |
| *6708.282 | 4000 | 8.27 E | 14902.840 | $3s\,^4P_{5/2}-3p\,^4D_{3/2}$ |
| *6690.481 | 18000 | 9.47 E | 14942.491 | $3s\,^4P_{3/2}-3p\,^2D_{5/2}$ |
| 6667.00 | 70 | | 14995.12 | $3p\,^2P_{3/2}-4d\,^4F_{5/2}$ |
| 6660.62 | 120 | | 15009.48 | $3p\,^2P_{1/2}-4d\,^2P_{3/2}$ |
| 6651.97 | 5 | | 15029.00 | $3p\,^2P_{3/2}-4d\,^4P_{5/2}$ |
| *6650.405 | 4000 | 0.39 E | 15032.535 | $3s\,^4P_{1/2}-3p\,^2D_{3/2}$ |
| 6649.51 | 60 | | 15034.56 | $3p\,^2P_{3/2}-4d\,^4F_{3/2}$ |
| 6611.04 | 50 | | 15122.04 | $3p\,^2D_{5/2}-5s\,^4P_{3/2}$ |

Table 5 (cont.).

| $\lambda_{\text{air}}$ | Intensity | EDLÉN = E<br>LIDÉN = L | $\nu_{\text{vac.}}$ | Identification |
|---|---|---|---|---|
| 6609.55 | 25 | | 15125.45 | $3p\,^2D_{3/2}-5s\,^2P_{3/2}$ |
| 6607.73 | 25 | | 15129.62 | $3p\,^4S_{3/2}-4d\,^4D_{5/2}$ |
| 6604.86 | 6 | | 15136.18 | $3p\,^2D_{3/2}-5s\,^4P_{1/2}$ |
| 6599.725 | 60 | | 15147.97 | $3p\,^2P_{3/2}-4d\,^2F_{5/2}$ |
| 6596.90 | 8 | | 15154.46 | $3p\,^2P_{3/2}-4d\,^2P_{3/2}$ |
| 6596.35 | 80 | | 15155.72 | $3p\,^4S_{3/2}-4d\,^2D_{5/2}$ |
| 6589.21 | 40 | | 15172.13 | $3p\,^2S_{1/2}-4d\,^4D_{3/2}$ |
| 6583.36 | 20 | | 15185.62 | $3p\,^4S_{3/2}-4d\,^4D_{1/2}$ |
| *6580.389 | 3000 | 0.38 E | 15192.482 | $3s\,^4P_{3/2}-3p\,^2D_{3/2}$ |
| 6578.871 | 120 | 8.85 L | 15195.99 | $3p\,^4S_{3/2}-4d\,^2D_{3/2}$ |
| 6573.61 | 50 | | 15208.15 | $3p\,^2S_{1/2}-4d\,^4D_{1/2}$ |
| *6569.694 | 4500 | 9.69 E | 15217.214 | $3s\,^4P_{5/2}-3p\,^2D_{5/2}$ |
| 6569.14 | 70 | | 15218.50 | $3p\,^2S_{1/2}-4d\,^2D_{3/2}$ |
| 6563.59 | 70 | | 15231.37 | $3p\,^4S_{3/2}-4d\,^4P_{1/2}$ |
| 6553.93 | 60 | | 15253.82 | $3p\,^2S_{1/2}-4d\,^4P_{1/2}$ |
| 6512.71 | 120 | 2.70 L | 15350.36 | $3p\,^2D_{3/2}-5s\,^2P_{1/2}$ |
| 6511.61 | 4 | | 15352.95 | $3p\,^4D_{1/2}-5s\,^4P_{3/2}$ |
| 6502.08 | 180 | 2.09 L | 15375.45 | $3p\,^2D_{5/2}-5s\,^2P_{3/2}$ |
| 6478.45 | 80 | 8.45 L | 15431.53 | $3p\,^4D_{5/2}-5s\,^4P_{5/2}$ |
| 6476.39 | 70 | 6.40 L | 15436.44 | $3p\,^4D_{3/2}-5s\,^4P_{3/2}$ |
| 6463.50 | 700 | 3.52 E | 15467.24 | $3s\,^4P_{5/2}-3p\,^2D_{3/2}$ |
| 6457.06 | 8 | | 15482.64 | $3p\,^4S_{3/2}-4d\,^2P_{1/2}$ |
| 6453.32 | 100 | 3.34 L | 15491.63 | $3p\,^4S_{3/2}-4d\,^4P_{3/2}$ |
| 6448.14 | 6 | | 15504.07 | $3p\,^4S_{3/2}-4d\,^4F_{5/2}$ |
| 6447.69 | 60 | 7.78 L | 15505.15 | $3p\,^2S_{1/2}-4d\,^2P_{1/2}$ |
| 6434.11 | 150 | 4.13 L | 15537.88 | $3p\,^4S_{3/2}-4d\,^4P_{5/2}$ |
| 6431.73 | 2 | | 15543.62 | $3p\,^4S_{3/2}-4d\,^4F_{3/2}$ |
| 6422.87 | 25 | | 15565.07 | $3s\,^4P_{1/2}-3p\,^2S_{1/2}$ |
| 6422.43 | 70 | | 15566.14 | $3p\,^2S_{1/2}-4d\,^4F_{3/2}$ |
| 6416.31 | 180 | 6.34 L | 15580.98 | $3p\,^4D_{5/2}-5s\,^4P_{3/2}$ |
| *6413.651 | 80000 | 3.66 E | 15587.444 | $3s\,^4P_{1/2}-3p\,^4S_{3/2}$ |
| 6405.171 | 600 | 5.17 L | 15608.08 | $3p\,^4D_{7/2}-5s\,^4P_{5/2}$ |
| 6385.17 | 100 | | 15656.97 | $3p\,^4S_{3/2}-4d\,^2F_{5/2}$ |
| 6373.33 | 20 | | 15686.06 | $3p\,^2S_{1/2}-4d\,^2P_{3/2}$ |
| 6371.77 | 20 | | 15689.90 | $3p\,^4D_{3/2}-5s\,^2P_{3/2}$ |
| 6367.43 | 100 | 7.43 L | 15700.59 | $3p\,^4D_{3/2}-5s\,^4P_{1/2}$ |
| 6365.84 | 8 | | 15704.52 | $3p\,^2D_{3/2}-4d\,^4D_{3/2}$ |
| 6363.34 | 80 | 3.33 L | 15710.68 | $3p\,^2D_{3/2}-4d\,^2D_{5/2}$ |
| *6348.508 | 100000 | 8.50 E | 15747.388 | $3s\,^4P_{3/2}-3p\,^4S_{3/2}$ |
| 6314.74 | 8 | | 15831.60 | $3p\,^4D_{1/2}-5s\,^2P_{1/2}$ |
| 6313.61 | 30 | | 15834.42 | $3p\,^4D_{5/2}-5s\,^2P_{3/2}$ |
| 6279.028 | 90 | 9.07 L | 15921.64 | $3p\,^2D_{5/2}-4d\,^4D_{7/2}$ |
| 6273.94 | 2 | | 15934.55 | $3p\,^2D_{5/2}-4d\,^4D_{5/2}$ |
| 6263.696 | 180 | 3.72 L | 15960.61 | $3p\,^2D_{5/2}-4d\,^2D_{5/2}$ |
| *6254.690 | 800 | 4.70 L | 15983.591 | $3p\,^2D_{5/2}-4d\,^2F_{7/2}$ |
| *6239.651 | 130000 | 9.64 E | 16022.115 | $3s\,^4P_{5/2}-3p\,^4S_{3/2}$ |
| 6230.11 | 30 | | 16046.64 | $3p\,^2D_{3/2}-4d\,^4P_{3/2}$ |
| 6225.356 | 180 | 5.39 L | 16058.90 | $3p\,^2D_{3/2}-4d\,^4F_{5/2}$ |
| 6212.249 | 180 | 2.28 L | 16092.78 | $3p\,^2D_{3/2}-4d\,^4P_{5/2}$ |
| 6210.87 | 4000 | 0.83 E | 16096.36 | $3s\,^4P_{1/2}-3p\,^2P_{3/2}$ |

Table 5 (cont.).

| $\lambda_{\text{air}}$ | Intensity | EDLÉN = E<br>LIDÉN = L | $\nu_{\text{vac.}}$ | Identification |
|---|---|---|---|---|
| 6166.628 | 250 | 6.66 L | 16211.84 | $3p\,^2D_{3/2}-4d\,^2F_{5/2}$ |
| 6164.136 | 15 | | 16218.40 | $3p\,^2D_{3/2}-4d\,^2P_{3/2}$ |
| 6155.359 | 9 | | 16241.52 | $3s\,^4P_{1/2}\quad 3p\,^2P_{1/2}$ |
| 6152.55 | 18 | | 16248.93 | $3p\,^4D_{3/2}-4d\,^4D_{5/2}$ |
| 6149.76 | 8000 | 9.73 E | 16256.32 | $3s\,^4P_{3/2}-3p\,^2P_{3/2}$ |
| 6145.029 | 80 | | 16268.82 | $3p\,^4D_{3/2}-4d\,^4D_{3/2}$ |
| 6134.52 | 2 | | 16296.68 | $3p\,^2D_{5/2}-4d\,^4P_{3/2}$ |
| *6133.220 | 700 | 3.24 L | 16300.148 | $3p\,^2D_{5/2}-4d\,^4F_{7/2}$ |
| 6131.43 | 12 | | 16304.89 | $3p\,^4D_{3/2}-4d\,^4D_{1/2}$ |
| 6129.93 | 10 | | 16308.89 | $3p\,^2D_{5/2}-4d\,^4F_{5/2}$ |
| 6127.49 | 6 | | 16315.38 | $3p\,^4D_{3/2}-4d\,^2D_{3/2}$ |
| 6117.222 | 100 | | 16342.77 | $3p\,^2D_{5/2}-4d\,^4P_{5/2}$ |
| 6115.08 | 3 | | 16348.49 | $3p\,^2D_{5/2}-4d\,^4F_{3/2}$ |
| 6098.34 | 250 | 8.37 L | 16393.37 | $3p\,^4D_{5/2}-4d\,^4D_{5/2}$ |
| 6090.902 | 60 | | 16413.40 | $3p\,^4D_{5/2}-4d\,^4D_{3/2}$ |
| 6088.61 | 25 | | 16419.57 | $3p\,^4D_{5/2}-4d\,^2D_{5/2}$ |
| *6080.113 | 1000 | 0.10 L | 16442.521 | $3p\,^4D_{5/2}-4d\,^2F_{7/2}$ |
| 6052.19 | 10 | | 16518.38 | $3p\,^4D_{1/2}-4d\,^2P_{1/2}$ |
| 6048.80 | 12 | | 16527.64 | $3p\,^4D_{1/2}-4d\,^4P_{3/2}$ |
| 6047.54 | 9000 | 7.53 E | 16531.09 | $3s\,^4P_{5/2}-3p\,^2P_{3/2}$ |
| 6038.944 | 180 | 8.97 L | 16554.61 | $3p\,^4P_{3/2}-5s\,^4P_{5/2}$ |
| 6038.04 | 800 | 8.04 L | 16557.10 | $3p\,^4D_{7/2}-4d\,^4D_{7/2}$ |
| 6033.34 | 80 | 3.36 L | 16569.99 | $3p\,^4D_{7/2}-4d\,^4D_{5/2}$ |
| 6029.95 | 200 | 9.97 L | 16579.32 | $3p\,^4D_{1/2}-4d\,^4F_{3/2}$ |
| 6021.91 | 100 | | 16601.43 | $3p\,^4P_{1/2}-5s\,^4P_{3/2}$ |
| 6018.47 | 12 | | 16610.93 | $3p\,^4D_{3/2}-4d\,^4P_{3/2}$ |
| *6015.828 | 1500 | 5.85 L | 16618.224 | $3p\,^4D_{7/2}-4d\,^4F_{9/2}$ |
| 6014.03 | 400 | 4.03 L | 16623.19 | $3p\,^4D_{3/2}-4d\,^4F_{5/2}$ |
| 6001.78 | 80 | 1.80 L | 16657.12 | $3p\,^4D_{3/2}-4d\,^4P_{5/2}$ |
| 5999.753 | 150 | 9.76 L | 16662.75 | $3p\,^4D_{3/2}-4d\,^4F_{3/2}$ |
| 5994.425 | 500 | 4.44 L | 16677.56 | $3p\,^4P_{5/2}-5s\,^4P_{5/2}$ |
| 5986.635 | 300 | 6.64 L | 16699.26 | $3p\,^4D_{1/2}-4d\,^2P_{3/2}$ |
| 5984.94 | 15 | 4.90 L | 16704.00 | $3p\,^4P_{3/2}-5s\,^4P_{3/2}$ |
| 5969.056 | 10 | | 16748.44 | $3p\,^2P_{3/2}-6s\,^4P_{3/2}$ |
| 5965.28 | 700 | 5.29 L | 16759.04 | $3p\,^4D_{5/2}-4d\,^4F_{7/2}$ |
| 5962.166 | 30 | | 16767.79 | $3p\,^4D_{5/2}-4d\,^4F_{5/2}$ |
| 5959.187 | 250 | 9.20 L | 16776.18 | $3p\,^4D_{3/2}-4d\,^2F_{5/2}$ |
| 5956.87 | 20 | | 16782.70 | $3p\,^4D_{3/2}-4d\,^2P_{3/2}$ |
| 5950.147 | 120 | 0.13 L | 16801.66 | $3p\,^4D_{5/2}-4d\,^4P_{5/2}$ |
| 5941.179 | 50 | | 16827.03 | $3p\,^4P_{5/2}-5s\,^4P_{3/2}$ |
| 5940.697 | 50 | | 16828.39 | $(^1D)\,3p\,^2F_{7/2}-(^1D)\,4d\,^2G_{9/2}$ |
| 5937.56 | 25 | | 16837.28 | $(^1D)\,3p\,^2F_{5/2}-(^1D)\,4d\,^2G_{7/2}$ |
| 5931.39 | 60 | | 16854.78 | $3p\,^4P_{1/2}-5s\,^2P_{3/2}$ |
| 5927.60 | 10 | | 16865.58 | $3p\,^4P_{1/2}-5s\,^4P_{1/2}$ |
| 5903.06 | 8 | | 16935.69 | $3p\,^4D_{7/2}-4d\,^4F_{7/2}$ |
| 5891.74 | 80 | | 16968.23 | $3p\,^4P_{3/2}-5s\,^4P_{1/2}$ |
| 5853.06 | 25 | | 17080.37 | $3p\,^4P_{5/2}-5s\,^2P_{3/2}$ |
| 5827.48 | 6 | | 17155.33 | $3p\,^2P_{3/2}-5d\,^2D_{5/2}$ |
| 5818.34 | 2 | | 17182.28 | $3p\,^4P_{3/2}-5s\,^2P_{1/2}$ |
| 5807.47 | 3 | | 17214.44 | $3p\,^2P_{3/2}-6s\,^2P_{1/2}$ |

Table 5 (cont.).

| $\lambda_{\text{air}}$ | Intensity | EDLÉN = E<br>LIDÉN = L | $\nu_{\text{vac.}}$ | Identification |
|---|---|---|---|---|
| 5793.05 | 1 | | 17257.29 | $3p\,^4S_{3/2}-6s\,^4P_{3/2}$ |
| 5785.45 | 5 | | 17279.97 | $3p\,^2S_{1/2}-6s\,^4P_{3/2}$ |
| 5754.37 | 2 | | 17373.30 | $3p\,^2P_{1/2}-5d\,^4F_{3/2}$ |
| 5734.39 | 30 | 4.40 L | 17433.82 | $3p\,^4P_{1/2}-4d\,^4D_{3/2}$ |
| 5722.59 | 60 | 2.59 L | 17469.76 | $3p\,^4P_{1/2}-4d\,^4D_{1/2}$ |
| 5719.16 | 15 | | 17480.25 | $3p\,^4P_{1/2}-4d\,^2D_{3/2}$ |
| 5713.34 | 4 | | 17498.06 | $3p\,^2P_{3/2}-5d\,^4F_{5/2}$ |
| 5710.69 | 3 | | 17506.18 | $3p\,^2P_{1/2}-5d\,^2P_{3/2}$ |
| 5707.62 | 20 | | 17515.59 | $3p\,^4P_{1/2}-4d\,^4P_{1/2}$ |
| 5707.31 | 250 | 7.33 L | 17516.55 | $3p\,^4P_{3/2}-4d\,^4D_{5/2}$ |
| 5700.82 | 250 | 0.84 L | 17536.47 | $3p\,^4P_{3/2}-4d\,^4D_{3/2}$ |
| 5692.81 | 1.5 | | 17561.15 | $3p\,^2S_{1/2}-6s\,^2P_{3/2}$ |
| 5690.81 | 2 | | 17567.32 | $3p\,^4S_{3/2}-6s\,^4P_{1/2}$ |
| 5689.14 | 180 | 9.18 L | 17572.47 | $3p\,^4P_{3/2}-4d\,^4D_{1/2}$ |
| 5685.74 | 80 | 5.77 L | 17582.99 | $3p\,^4P_{3/2}-4d\,^2D_{3/2}$ |
| 5674.39 | 80 | | 17618.17 | $3p\,^4P_{3/2}-4d\,^4P_{1/2}$ |
| 5671.668 | 900 | 1.69 L | 17626.62 | $3p\,^4P_{5/2}-4d\,^4D_{7/2}$ |
| 5667.532 | 400 | 7.55 L | 17639.48 | $3p\,^4P_{5/2}-4d\,^4D_{5/2}$ |
| 5664.00 | 2 | | 17650.49 | $3p\,^4S_{3/2}-5d\,^4D_{5/2}$ |
| 5661.106 | 70 | 1.12 L | 17659.50 | $3p\,^4P_{5/2}-4d\,^4D_{3/2}$ |
| 5659.15 | 150 | 9.15 L | 17665.61 | $3p\,^4P_{5/2}-4d\,^2D_{5/2}$ |
| 5653.052 | 1 | | 17684.66 | $3p\,^2S_{1/2}-5d\,^4D_{3/2}$ |
| 5652.601 | 5 | | 17686.07 | $3p\,^4S_{3/2}-5d\,^2D_{3/2}$ |
| 5649.26 | 2 | | 17696.55 | $3p\,^4S_{3/2}-5d\,^4P_{1/2}$ |
| 5646.254 | 80 | 6.27 L | 17705.96 | $3p\,^4P_{5/2}-4d\,^2D_{3/2}$ |
| 5645.44 | 2 | | 17708.50 | $3p\,^2S_{1/2}-5d\,^2D_{3/2}$ |
| 5642.11 | 4 | | 17718.96 | $3p\,^2S_{1/2}-5d\,^4P_{1/2}$ |
| 5626.93 | 120 | 6.94 L | 17766.76 | $3p\,^4P_{1/2}-4d\,^2P_{1/2}$ |
| 5624.06 | 200 | 4.06 L | 17775.84 | $3p\,^4P_{1/2}-4d\,^4P_{3/2}$ |
| 5612.55 | 1 | | 17812.30 | $3p\,^2D_{3/2}-6s\,^4P_{3/2}$ |
| 5607.66 | 5 | | 17827.82 | $3p\,^4P_{1/2}-4d\,^4F_{3/2}$ |
| 5591.734 | 10 | 1.76 L | 17878.59 | $3p\,^4P_{3/2}-4d\,^4P_{3/2}$ |
| 5587.888 | 12 | 7.90 L | 17890.89 | $3p\,^4P_{3/2}-4d\,^4F_{5/2}$ |
| 5577.33 | 100 | 7.33 L | 17924.77 | $3p\,^4P_{3/2}-4d\,^4P_{5/2}$ |
| 5570.216 | 25 | 0.21 L | 17947.65 | $3p\,^4P_{1/2}-4d\,^2P_{3/2}$ |
| 5554.33 | 2 | | 17998.99 | $3p\,^4S_{3/2}-5d\,^4P_{3/2}$ |
| 5553.53 | 7 | | 18001.57 | $3p\,^4P_{5/2}-4d\,^4P_{3/2}$ |
| 5552.43 | 120 | 2.43 L | 18005.14 | $3p\,^4P_{5/2}-4d\,^4F_{7/2}$ |
| 5549.70 | 1.5 | | 18014.00 | $3p\,^4P_{5/2}-4d\,^4F_{5/2}$ |
| 5549.449 | 1.5 | | 18014.82 | $3p\,^2S_{1/2}-5d\,^2P_{1/2}$ |
| 5546.74 | 7 | | 18023.61 | $3p\,^4S_{3/2}-5d\,^4P_{5/2}$ |
| 5540.52 | 180 | 0.52 L | 18043.83 | $3p\,^4P_{3/2}-4d\,^2F_{5/2}$ |
| 5539.33 | 60 | 9.30 L | 18047.74 | $3p\,^4P_{5/2}-4d\,^4P_{5/2}$ |
| 5538.61 | 5 | 8.53 L | 18050.07 | $\left\{\begin{array}{l}3p\,^2S_{1/2}-5d\,^4F_{3/2}\\3p\,^4P_{3/2}-4d\,^2P_{3/2}\end{array}\right.$ |
| 5537.57 | 1 | | 18053.45 | $3p\,^4P_{5/2}-4d\,^4F_{3/2}$ |
| 5534.862 | 18 | | 18062.29 | $3p\,^2D_{5/2}-6s\,^4P_{3/2}$ |
| 5525.37 | 0.5 | | 18093.32 | $3p\,^2D_{3/2}-6s\,^2P_{3/2}$ |
| 5516.55 | 1.5 | | 18122.25 | $3p\,^2D_{3/2}-6s\,^4P_{1/2}$ |
| 5506.15 | 2 | | 18156.47 | $3p\,^4S_{3/2}-5d\,^2F_{5/2}$ |
| 5503.02 | 4 | | 18166.81 | $3p\,^4P_{5/2}-4d\,^2F_{5/2}$ |

Table 5 (cont.).

| $\lambda_{\text{air}}$ | Intensity | EDLÉN = E<br>LIDÉN = L | $\nu_{\text{vac.}}$ | Identification |
|---|---|---|---|---|
| 5487.18 | 3 | | 18219.25 | $3p\,^2D_{3/2}-5d\,^2D_{5/2}$ |
| 5477.56 | 3 | | 18251.25 | $3p\,^2D_{3/2}-5d\,^4P_{1/2}$ |
| 5469.491 | 4 | | 18278.17 | $3p\,^2D_{3/2}-6s\,^2P_{1/2}$ |
| 5467.35 | 1 | | 18285.34 | $3p\,^2P_{3/2}-7s\,^4P_{3/2}$ |
| 5450.05 | 10 | | 18343.37 | $3p\,^2D_{5/2}-6s\,^2P_{3/2}$ |
| 5440.154 | 3 | | 18376.74 | $3p\,^4D_{3/2}-6s\,^4P_{3/2}$ |
| 5421.55 | 4 | | 18439.80 | $3p\,^4D_{5/2}-6s\,^4P_{5/2}$ |
| 5419.173 | 4 | | 18447.89 | $3p\,^2D_{5/2}-5d\,^4D_{7/2}$ |
| 5412.900 | 6 | | 18469.26 | $3p\,^2D_{5/2}-5d\,^2D_{5/2}$ |
| 5410.15 | 40 | | 18478.66 | $3p\,^2D_{5/2}-5d\,^2F_{7/2}$ |
| 5397.718 | 10 | | 18521.21 | $3p\,^4D_{5/2}-6s\,^4P_{3/2}$ |
| 5388.15 | 1 | | 18554.11 | $3p\,^2D_{3/2}-5d\,^4P_{3/2}$ |
| 5385.88 | 6 | | 18561.94 | $3p\,^2D_{3/2}-5d\,^4F_{5/2}$ |
| 5381.03 | 8 | | 18578.65 | $3p\,^2D_{3/2}-5d\,^4P_{5/2}$ |
| 5373.87 | 3 | | 18603.40 | $3p\,^4D_{1/2}-6s\,^4P_{1/2}$ |
| 5370.10 | 50 | | 18616.45 | $3p\,^4D_{7/2}-6s\,^4P_{5/2}$ |
| 5358.16 | 3 | | 18657.96 | $3p\,^4D_{3/2}-6s\,^2P_{3/2}$ |
| 5349.90 | 4 | | 18686.77 | $3p\,^4D_{3/2}-6s\,^4P_{1/2}$ |
| 5342.80 | 10 | | 18711.58 | $3p\,^2D_{3/2}-5d\,^2F_{5/2}$ |
| 5329.17 | 1 | | 18759.44 | $3p\,^4D_{1/2}-6s\,^2P_{1/2}$ |
| 5326.24 | 1.5 | | 18769.76 | $3p\,^4D_{3/2}-5d\,^4D_{5/2}$ |
| 5322.95 | 1.5 | | 18781.36 | $3p\,^4D_{3/2}-5d\,^4D_{3/2}$ |
| 5322.25 | 1.5 | | 18783.86 | $3p\,^4D_{3/2}-5d\,^2D_{5/2}$ |
| 5316.98 | 5 | | 18802.46 | $3p\,^4D_{5/2}-6s\,^2P_{3/2}$ |
| 5315.97 | 30 | | 18806.04 | $3p\,^2D_{5/2}-5d\,^4F_{7/2}$ |
| 5309.61 | 2 | | 18828.54 | $3p\,^2D_{5/2}-5d\,^4P_{5/2}$ |
| 5287.56 | 1 | | 18907.07 | $3p\,^4D_{5/2}-5d\,^4D_{7/2}$ |
| 5285.57 | 8 | | 18914.18 | $3p\,^4D_{5/2}-5d\,^4D_{5/2}$ |
| 5282.33 | 1.5 | | 18925.81 | $3p\,^4D_{5/2}-5d\,^4D_{3/2}$ |
| 5279.01 | 120 | | 18937.70 | $3p\,^4D_{5/2}-5d\,^2F_{7/2}$ |
| 5252.08 | 1 | | 19034.79 | $3p\,^4D_{1/2}-5d\,^4P_{3/2}$ |
| 5244.28 | 8 | | 19063.09 | $3p\,^4D_{1/2}-5d\,^4F_{3/2}$ |
| 5238.69 | 30 | | 19083.46 | $3p\,^4D_{7/2}-5d\,^4D_{7/2}$ |
| 5236.67 | 2 | | 19090.81 | $3p\,^4D_{7/2}-5d\,^4D_{5/2}$ |
| 5230.41 | 150 | | 19113.65 | $3p\,^4D_{7/2}-5d\,^4F_{9/2}$ |
| 5226.96 | 30 | | 19126.27 | $3p\,^4D_{3/2}-5d\,^4F_{5/2}$ |
| 5222.39 | 3 | | 19142.99 | $3p\,^4D_{3/2}-5d\,^4P_{5/2}$ |
| 5221.42 | 5 | | 19146.56 | $3p\,^4D_{3/2}-5d\,^4F_{3/2}$ |
| 5207.96 | 10 | | 19196.03 | $3p\,^4D_{1/2}-5d\,^2P_{3/2}$ |
| 5189.27 | 40 | | 19265.18 | $3p\,^4D_{5/2}-5d\,^4F_{7/2}$ |
| 5186.41 | 8 | | 19275.82 | $3p\,^4D_{3/2}-5d\,^2F_{5/2}$ |
| 5185.45 | 0.5 | | 19279.39 | $3p\,^4D_{3/2}-5d\,^2P_{3/2}$ |
| 5183.27 | 4 | | 19287.47 | $3p\,^4D_{5/2}-5d\,^4P_{5/2}$ |
| 5166.71 | 1 | | 19349.29 | $3p\,^2D_{3/2}-7s\,^4P_{3/2}$ |
| 5115.81 | 2 | | 19541.82 | $3p\,^4P_{1/2}-6s\,^4P_{3/2}$ |
| 5110.269 | 12 | | 19563.01 | $3p\,^4P_{3/2}-6s\,^4P_{5/2}$ |
| 5100.86 | 4 | | 19599.09 | $3p\,^2D_{5/2}-7s\,^4P_{3/2}$ |
| 5078.352 | 30 | | 19685.95 | $3p\,^4P_{5/2}-6s\,^4P_{5/2}$ |
| 5043.28 | 4 | | 19822.84 | $3p\,^4P_{1/2}-6s\,^2P_{3/2}$ |
| 5040.69 | 6 | | 19833.06 | $3p\,^2D_{5/2}-6d\,^2F_{7/2}$ |

Table 5 (cont.).

| $\lambda_{\text{air}}$ | Intensity | EDLÉN = E<br>LIDÉN = L | $\nu_{\text{vac.}}$ | Identification |
|---|---|---|---|---|
| 4989.31 | 18 | | 20037.29 | $3p\,^4P_{3/2}-5d\,^4D_{5/2}$ |
| 4986.43 | 25 | | 20048.86 | $3p\,^4P_{3/2}-5d\,^4D_{3/2}$ |
| 4981.54 | 15 | | 20068.55 | $\left\{\begin{array}{l}3p\,^2D_{3/2}-6d\,^2F_{5/2}\\3p\,^4P_{3/2}-5d\,^4D_{1/2}\end{array}\right.$ |
| 4980.45 | 8 | | 20072.92 | $3p\,^4P_{3/2}-5d\,^2D_{3/2}$ |
| 4977.85 | 2 | | 20083.41 | $3p\,^4P_{3/2}-5d\,^4P_{1/2}$ |
| 4960.65 | 60 | | 20153.04 | $3p\,^4P_{5/2}-5d\,^4D_{7/2}$ |
| 4958.85 | 30 | | 20160.33 | $3p\,^4P_{5/2}-5d\,^4D_{5/2}$ |
| 4957.41 | 3 | | 20166.20 | $3p\,^2D_{5/2}-6d\,^4F_{7/2}$ |
| 4956.01 | 10 | | 20171.91 | $3p\,^4P_{5/2}-5d\,^4D_{3/2}$ |
| 4955.41 | 15 | | 20174.37 | $3p\,^4P_{5/2}-5d\,^2D_{5/2}$ |
| 4952.20 | 25 | | 20187.43 | $3p\,^4D_{7/2}-7s\,^4P_{5/2}$ |
| 4950.16 | 12 | | 20195.73 | $3p\,^4P_{5/2}-5d\,^2D_{3/2}$ |
| 4930.45 | 12 | | 20276.46 | $3p\,^4P_{1/2}-5d\,^2P_{1/2}$ |
| 4929.77 | 1.5 | | 20279.28 | $3p\,^4D_{5/2}-6d\,^4D_{5/2}$ |
| 4928.83 | 18 | | 20283.15 | $3p\,^4P_{1/2}-5d\,^4P_{3/2}$ |
| 4926.67 | 8 | | 20292.04 | $3p\,^4D_{5/2}-6d\,^2F_{7/2}$ |
| 4904.02 | 1 | | 20385.76 | $3p\,^4P_{3/2}-5d\,^4P_{3/2}$ |
| 4898.06 | 12 | | 20410.56 | $3p\,^4P_{3/2}-5d\,^4P_{5/2}$ |
| 4889.95 | 2 | | 20444.42 | $3p\,^4P_{1/2}-5d\,^2P_{3/2}$ |
| 4888.37 | 8 | | 20451.03 | $3p\,^4D_{7/2}-6d\,^4D_{7/2}$ |
| 4884.25 | 25 | | 20468.27 | $3p\,^4D_{7/2}-6d\,^4F_{9/2}$ |
| 4880.46 | 6 | | 20484.16 | $3p\,^4D_{3/2}-6d\,^4F_{5/2}$ |
| 4874.02 | 15 | | 20511.25 | $3p\,^4P_{5/2}-5d\,^4F_{7/2}$ |
| 4868.69 | 5 | | 20533.69 | $3p\,^4P_{5/2}-5d\,^4P_{5/2}$ |
| 4866.33 | 20 | | 20543.67 | $3p\,^4P_{3/2}-5d\,^2F_{5/2}$ |
| 4847.13 | 5 | | 20625.00 | $3p\,^4D_{5/2}-6d\,^4F_{7/2}$ |
| 4845.28 | 1 | | 20632.89 | $3p\,^4D_{3/2}-6d\,^2F_{5/2}$ |
| 4736.23 | 1 | | 21107.96 | $3p\,^4D_{5/2}-7d\,^2F_{7/2}$ |
| 4735.70 | 2 | | 21110.33 | $3p\,^4D_{7/2}-8s\,^4P_{5/2}$ |
| 4730.40 | 4 | | 21133.97 | $3p\,^4P_{3/2}-7s\,^4P_{5/2}$ |
| 4703.06 | 10 | | 21256.80 | $3p\,^4P_{5/2}-7s\,^4P_{5/2}$ |
| 4697.00 | 6 | | 21284.23 | $3p\,^4D_{7/2}-7d\,^4F_{9/2}$ |
| 4671.13 | 4 | | 21402.13 | $3p\,^4P_{3/2}-6d\,^4D_{5/2}$ |
| 4645.42 | 20 | | 21520.59 | $3p\,^4P_{5/2}-6d\,^4D_{7/2}$ |
| 4644.43 | 10 | | 21525.16 | $3p\,^4P_{5/2}-6d\,^4D_{5/2}$ |
| 4642.94 | 2 | | 21532.05 | $3p\,^4P_{5/2}-6d\,^4D_{3/2}$ |
| 4642.65 | 3 | | 21533.43 | $3p\,^4P_{5/2}-6d\,^2D_{5/2}$ |
| 4640.20 | 2 | | 21544.80 | $3p\,^4P_{5/2}-6d\,^2D_{3/2}$ |
| 4618.90 | 4 | | 21644.13 | $3p\,^4P_{1/2}-6d\,^4P_{3/2}$ |
| 4594.05 | 3 | | 21761.23 | $3p\,^4P_{3/2}-6d\,^4P_{5/2}$ |
| 4583.03 | 2 | | 21813.54 | $3p\,^4D_{7/2}-8d\,^4F_{9/2}$ |
| 4564.83 | 6 | | 21900.50 | $3p\,^4P_{3/2}-6d\,^2F_{5/2}$ |
| 4018.812 | 4 | | 24875.97 | $3s\,^2P_{3/2}-4p\,^4P_{1/2}$ |
| 3992.210 | 20 | | 25041.73 | $3s\,^2P_{3/2}-4p\,^4D_{5/2}$ |
| 3966.14 | 15 | | 25206.31 | $3s\,^2P_{3/2}-4p\,^4D_{3/2}$ |
| 3953.799 | 20 | | 25285.00 | $3s\,^2P_{3/2}-4p\,^2D_{5/2}$ |
| 3948.563 | 50 | | 25318.53 | $3s\,^2P_{1/2}-4p\,^2P_{3/2}$ |
| 3934.262 | 50 | | 25410.56 | $3s\,^2P_{3/2}-4p\,^2D_{3/2}$ |
| 3933.11 | 30 | | 25418.03 | $3s\,^2P_{3/2}-4p\,^2S_{1/2}$ |
| 3930.689 | 80 | | 25433.66 | $3s\,^2P_{1/2}-4p\,^2P_{1/2}$ |

Table 5 (cont.).

| $\lambda_{air}$ | Intensity | EDLÉN = E<br>LIDÉN = L | $\nu_{vac.}$ | Identification |
|---|---|---|---|---|
| 3898.478 | 50 | | 25643.79 | $3s\,^2P_{3/2}-4p\,^2P_{3/2}$ |
| 3880.99 | 3 | | 25759.31 | $3s\,^2P_{3/2}-4p\,^2P_{1/2}$ |
| 3712.733 | 8 | | 26926.70 | $3s\,^4P_{3/2}-4p\,^4P_{1/2}$ |
| 3705.93 | 15 | | 26976.15 | $3s\,^4P_{5/2}-4p\,^4P_{5/2}$ |
| 3691.859 | 20 | | 27078.95 | $3s\,^4P_{5/2}-4p\,^4P_{3/2}$ |
| 3690.018 | 40 | | 27092.45 | $3s\,^4P_{3/2}-4p\,^4D_{5/2}$ |
| 3689.40 | 12 | | 27096.96 | $3s\,^4P_{1/2}-4p\,^4D_{3/2}$ |
| 3672.85 | 25 | | 27219.10 | $3s\,^4P_{1/2}-4p\,^4D_{1/2}$ |
| 3668.174 | 120 | | 27253.79 | $3s\,^4P_{5/2}-4p\,^4D_{7/2}$ |
| 3667.757 | 40 | | 27256.89 | $3s\,^4P_{3/2}-4p\,^4D_{3/2}$ |
| 3661.793 | 30 | | 27301.28 | $3s\,^4P_{1/2}-4p\,^2D_{3/2}$ |
| 3660.796 | 4 | | 27308.71 | $3s\,^4P_{1/2}-4p\,^2S_{1/2}$ |
| 3657.187 | 30 | | 27335.66 | $3s\,^4P_{3/2}-4p\,^2D_{5/2}$ |
| 3652.982 | 15 | | 27367.13 | $3s\,^4P_{5/2}-4p\,^4D_{5/2}$ |
| 3651.41 | 4 | | 27378.89 | $3s\,^4P_{3/2}-4p\,^4D_{1/2}$ |
| 3651.174 | 20 | | 27380.68 | $3s\,^4P_{1/2}-4p\,^4S_{3/2}$ |
| 3630.776 | 15 | | 27534.50 | $3s\,^4P_{1/2}-4p\,^2P_{3/2}$ |
| 3629.963 | 40 | | 27540.67 | $3s\,^4P_{3/2}-4p\,^4S_{3/2}$ |
| 3620.789 | 12 | | 27610.45 | $3s\,^4P_{5/2}-4p\,^2D_{5/2}$ |
| 3609.808 | 15 | | 27694.43 | $3s\,^4P_{3/2}-4p\,^2P_{3/2}$ |
| 3604.401 | 18 | | 27735.98 | $3s\,^4P_{5/2}-4p\,^2D_{3/2}$ |
| 3594.103 | 60 | | 27815.45 | $3s\,^4P_{5/2}-4p\,^4S_{3/2}$ |
| 3574.346 | 15 | | 27969.19 | $3s\,^4P_{5/2}-4p\,^2P_{3/2}$ |
| 3138.715 | 2 | | 31850.98 | $3s\,^4P_{5/2}-5p\,^4D_{7/2}$ |
| 2969.35 | 2 | | 33667.55 | |
| 2967.28 | 2 | | 33691.09 | |

mately compensated for, using the spectral sensitivity curves given in EASTMAN KODAK catalogue (12). All intensities have been reduced to the same brilliancy of the light source, viz. 0.3 amp. with 400 volts across the tube and the same He-pressure, and to the same exposure time of 3 hours. The measured intensity ratios of the Rowland ghosts and their parent line (see p. 234) combined with spectrograms of different exposure times have served as reference points for this intensity scale. A special intensity examination of some selected plates has been made, using a suitable illumination from a light box and a low power (×15) binocular microscope. For comparison the intensities of some lines from the He I and Ne I spectra are given in Table 4.

For comparison EDLÉN's (14) and the writer's (33) earlier measurements are given in the third column of Table 5. The wave-numbers in the fourth column have been calculated from KAYSER's "*Tabelle der Schwingungszahlen*" (25). As regards the identifications in the fifth column it should be noted that levels without limit indication belong to the $^3P$ limit.

## 2. The vacuum range 1000—600 A

The wave-lengths measured in the vacuum region are given in the first column of Table 6 (Plate VII, VIII). The majority of these wave-lengths represent mean values

*Table 6.*

Wave-lengths of F I lines in the vacuum region.

| $\lambda_{\text{obs.}}$ | Intensity | Identification | $\nu_{\text{calc.}}$ | $\lambda_{\text{calc.}}$ |
|---|---|---|---|---|
| 977.745 | 100 | $2p\,^2P_{1/2}-3s\,^4P_{3/2}$ | 102276.3 | 977.743 |
| 976.505 | 40 | $2p\,^2P_{3/2}-3s\,^4P_{5/2}$ | 102405.8 | 976.508 |
| 976.217 | 100 | $2p\,^2P_{1/2}-3s\,^4P_{1/2}$ | 102436.3 | 976.217 |
| 973.895 | 350 | $2p\,^2P_{3/2}-3s\,^4P_{5/2}$ | 102680.5 | 973.895 |
| 972.401 | 20 | $2p\,^2P_{3/2}-3s\,^4P_{1/2}$ | 102840.4 | 972.380 |
| 958.524 | 500 | $2p\,^2P_{1/2}-3s\,^2P_{3/2}$ | 104326.9 | 958.525 |
| 955.545 | 750 | $2p\,^2P_{1/2}-3s\,^2P_{1/2}$ | 104652.2 | 955.546 |
| 954.825 | 1000 | $2p\,^2P_{3/2}-3s\,^2P_{3/2}$ | 104731.1 | 954.826 |
| 951.871 | 500 | $2p\,^2P_{3/2}-3s\,^2P_{1/2}$ | 105056.3 | 951.870 |
| 809.599 | 125 | $2p\,^2P_{1/2}-(^1D)\,3s\,^2D_{3/2}$ | 123517.9 | |
| 806.964 | 150 | $2p\,^2P_{3/2}-(^1D)\,3s\,^2D_{5/2}$ | 123921.3 | |
| 796.982 | 3 | $2p\,^2P_{1/2}-4s\,^4P_{3/2}$ | 125473.2 | 796.983 |
| 795.774 | 2 | $2p\,^2P_{1/2}-4s\,^4P_{1/2}$ | 125663.1 | 795.778 |
| 794.417 | 10 | $\begin{cases}2p\,^2P_{1/2}-4s\,^2P_{3/2}\\2p\,^2P_{3/2}-4s\,^4P_{3/2}\end{cases}$ | 125878.5<br>125877.3 | 794.417<br>794.424 |
| 793.237 | 1 | $2p\,^2P_{3/2}-4s\,^4P_{1/2}$ | 126067.3 | 793.227 |
| 792.536 | 10 | $2p\,^2P_{1/2}-4s\,^2P_{1/2}$ | 126177.1 | 792.537 |
| 791.875 | 12 | $2p\,^2P_{3/2}-4s\,^2P_{3/2}$ | 126282.6 | 791.875 |
| 790.006 | 7 | $2p\,^2P_{3/2}-4s\,^2P_{1/2}$ | 126581.2 | 790.007 |
| 782.976 | 5 | $2p\,^2P_{1/2}-3d\,^4D_{3/2}$ | 127718.6 | 782.971 |
| 782.575 | 2 | $2p\,^2P_{1/2}-3d\,^4D_{1/2}$ | 127780.9 | 782.590 |
| 782.378 | 10 | $2p\,^2P_{1/2}-3d\,^2D_{3/2}$ | 127815.7 | 782.376 |
| 781.654 | 3 | $2p\,^2P_{1/2}-3d\,^4P_{1/2}$ | 127934.6 | 781.649 |
| 780.713 | 5 | $2p\,^2P_{3/2}-3d\,^4D_{5/2}$ | 128087.9 | 780.714 |
| 780.519 | 10 | $\begin{cases}2p\,^2P_{1/2}-3d\,^2P_{1/2}\\2p\,^2P_{1/2}-3d\,^4P_{3/2}\end{cases}$ | 128116.1<br>128119.2 | 780.542<br>780.523 |
| 780.390 | 15 | $2p\,^2P_{3/2}-3d\,^2D_{5/2}$ | 128140.5 | 780.393 |
| 780.134 | 1 | $2p\,^2P_{3/2}-3d\,^4D_{1/2}$ | 128185.0 | 780.122 |
| 779.972 | 2 | $2p\,^2P_{1/2}-3d\,^4F_{3/2}$ | 128207.8 | 779.984 |
| 779.910 | 5 | $2p\,^2P_{3/2}-3d\,^2D_{3/2}$ | 128219.9 | 779.910 |
| 779.365 | 6 | $2p\,^2P_{1/2}-3d\,^2P_{3/2}$ | 128308.2 | 779.373 |
| 779.192 | 2 | $2p\,^2P_{3/2}-3d\,^4P_{1/2}$ | 128338.8 | 779.188 |
| 778.059 | 6 | $\begin{cases}2p\,^2P_{3/2}-3d\,^2P_{1/2}\\2p\,^2P_{3/2}-3d\,^4P_{3/2}\end{cases}$ | 128520.3<br>128523.3 | 778.087<br>778.069 |
| 777.531 | 4 | $2p\,^2P_{3/2}-3d\,^4F_{3/2}$ | 128612.0 | 777.533 |
| 777.010 | 5 | $2p\,^2P_{3/2}-3d\,^2F_{5/2}$ | 128697.9 | 777.013 |
| 776.926 | 4 | $2p\,^2P_{3/2}-3d\,^2P_{3/2}$ | 128712.3 | 776.926 |
| 755.603 | 2 | $2p\,^2P_{1/2}-5s\,^4P_{3/2}$ | 132340.9 | 755.625 |
| 754.148 | 2 | $\begin{cases}2p\,^2P_{3/2}-5s\,^4P_{5/2}\\2p\,^2P_{1/2}-5s\,^2P_{3/2}\end{cases}$ | 132595.5<br>132594.3 | 754.173<br>754.180 |
| 753.303 | 4 | $2p\,^2P_{3/2}-5s\,^4P_{3/2}$ | 132745.0 | 753.324 |
| 752.884 | 4 | $2p\,^2P_{1/2}-5s\,^2P_{1/2}$ | 132819.1 | 752.904 |
| 751.861 | 4 | $2p\,^2P_{3/2}-5s\,^2P_{3/2}$ | 132998.4 | 751.889 |
| 750.885 | 1 | $2p\,^2P_{1/2}-4d\,^4D_{3/2}$ | 133173.3 | 750.901 |
| 750.610 | 3 | $2p\,^2P_{3/2}-5s\,^2P_{1/2}$ | 133223.3 | 750.620 |
| 750.418 | 1 | $2p\,^2P_{1/2}-4d\,^4P_{1/2}$ | 133255.0 | 750.441 |

Table 6 (cont.).

| $\lambda_{obs.}$ | Intensity | Identification | $\nu_{calc.}$ | $\lambda_{calc.}$ |
|---|---|---|---|---|
| 748.946 | 3 | $2p\,^2P_{1/2}-4d\,^4P_{3/2}$ | 133515.4 | 748.977 |
| 748.709 | 2 | $2p\,^2P_{1/2}-4d\,^4F_{3/2}$ | 133567.3 | 748.686 |
| 748.580 | 4 | $2p\,^2P_{3/2}-4d\,^2D_{5/2}$ | 133583.6 | 748.595 |
| 748.338 | 2 | $2p\,^2P_{3/2}-4d\,^2D_{3/2}$ | 133623.9 | 748.369 |
| 748.134 | 1 | $2p\,^2P_{3/2}-4d\,^4P_{1/2}$ | 133659.2 | 748.172 |
| 747.999 | 2 | $2p\,^2P_{1/2}-4d\,^2P_{3/2}$ | 133687.2 | 748.015 |
| 746.627 | 3 | $2p\,^2P_{3/2}-4d\,^4F_{5/2}$ | 133931.9 | 746.648 |
| 746.400 | 1 | $2p\,^2P_{3/2}-4d\,^4F_{3/2}$ | 133971.4 | 746.428 |
| 745.767 | 2 | $2p\,^2P_{3/2}-4d\,^2F_{5/2}$ | 134084.8 | 745.797 |
| 736.987 | 2 | $2p\,^2P_{3/2}-6s\,^4P_{3/2}$ | 135685.3 | 737.000 |
| 735.469 | 1 | $2p\,^2P_{3/2}-6s\,^2P_{3/2}$ | 135966.4 | 735.476 |
| 735.154 | 1 | $2p\,^2P_{1/2}-5d\,^4P_{3/2}$ | 136022.7 | 735.171 |
| 734.795 | 1 | $\left\{\begin{array}{l}2p\,^2P_{3/2}-5d\,^4D_{3/2}\\2p\,^2P_{3/2}-5d\,^2D_{5/2}\end{array}\right.$ | 136089.9<br>136092.3 | 734.808<br>734.796 |
| 734.642 | 1 | $\left\{\begin{array}{l}2p\,^2P_{3/2}-5d\,^4P_{1/2}\\2p\,^2P_{3/2}-5d\,^2D_{3/2}\end{array}\right.$ | 136124.4<br>136113.8 | 734.622<br>734.679 |
| 732.960 | 1 | $\left\{\begin{array}{l}2p\,^2P_{3/2}-5d\,^4F_{5/2}\\2p\,^2P_{3/2}-5d\,^4P_{3/2}\\2p\,^2P_{3/2}-5d\,^2P_{1/2}\end{array}\right.$ | 136434.9<br>136426.8<br>136420.1 | 732.950<br>732.994<br>733.030 |
| 682.581 | 2 | $2p\,^2P_{1/2}-(^1D)\,4s\,^2D_{3/2}$ | 146502.8 | |
| 680.709 | 2 | $2p\,^2P_{3/2}-(^1D)\,4s\,^2D_{5/2}$ | 146905.7 | |

## *Table 7.*

Precision measurements of some F I lines.

*A:* Measurements in the second order with H and Cu II standards.
*B:* Measurements in the first order with H and O I standards.

| Term combination | $\lambda$ | | Weighted mean value | EDLÉN | $\nu$ cm$^{-1}$ | Diff. $2p\,(^2P_{3/2}-{}^2P_{1/2})$ |
|---|---|---|---|---|---|---|
| | *A* | *B* | | | | |
| $2p\,^2P_{1/2}-3s\,^4P_{3/2}$ | 977.745 | .745 | .745 | | $102276.1_6$ | |
| $2p\,^2P_{1/2}-3s\,^4P_{1/2}$ | 976.219 | .214 | .217 | | $102436.2_4$ | $404.3_1$ |
| $2p\,^2P_{3/2}-3s\,^4P_{3/2}$ | 973.898 | .889 | .895 | | $102680.4_7$ | |
| $2p\,^2P_{1/2}-3s\,^2P_{3/2}$ | 958.525 | .522 | .524 | .528 | $104327.0_7$ | |
| $2p\,^2P_{1/2}-3s\,^2P_{1/2}$ | 955.545 | .545 | .545 | .535 | $104652.3_2$ | $404.1_6$ |
| $2p\,^2P_{3/2}-3s\,^2P_{3/2}$ | 954.826 | .823 | .825 | .817 | $104731.2_3$ | $403.9_3$ |
| $2p\,^2P_{3/2}-3s\,^2P_{1/2}$ | 951.870 | .873 | .871 | .857 | $105056.2_5$ | |

obtained from 2 to 4 spectrograms. The results of precision measurements of λλ 977—951 against H, O I and Cu II standards are given in Table 7 (Plate VII). The uncertainty of these wave-lengths probably does not exceed 0.003 A. λλ 809—806 were measured in the second order against the O II lines λλ 832—34 and some calculated F I wave-lengths and may be correct within ±0.005 A. The accuracy of the observed wave-lengths of the other lines is estimated to be within 0.005—0.015 A. The intensities in the second column of Table 6 are visual estimates from spectrograms of different exposure times. In the third column the limit notation is omitted for levels belonging to the ($^3P$) limit.

The wave-numbers, $\nu_{\text{calc}}$, in the fourth column of Table 6 are derived from the term values (see Table 12, p. 260) and the $\lambda_{\text{calc}}$ in the fifth column are the reciprocals of these calculated wave-numbers. These calculated values should have an uncertainty less than 0.3 cm$^{-1}$ or about 0.002 A, and may be recommended as standards in the vacuum region.

## V. The structure of the arc spectrum

***Theoretical structure.*** The energy levels of F I may be derived by adding an electron to the lowest states of F II, $2s^2\,2p^4\;^3P$, $^1D$, $^1S$. The F I levels in $LS$-symbols thus obtained are given in Table 8. The main features of F I are the single low-lying ground term $2s^2\,2p^5\;^2P$ and the higher term groups of $2s^2\,2p^4\,\mathrm{n}l$, $\mathrm{n} \geqq 3$, going to three different limits $^3P$, $^1D$, $^1S$. From a comparison with other F I-like spectra the term $2s\;2p^6\;^2S$ and most of the terms based on the limits $^1D$ and $^1S$ can be predicted to lie above the first ionization limit $^3P$.

*Table 8.*

Theoretical terms of F I.

| Electron configuration | Term symbols | | | |
|---|---|---|---|---|
| $2s^2\,2p^5$ | $^2P^0$ | | | |
| $2s\;\;2p^6$ | $^2S$ | | | |
| | Limits | | | |
| | $2s^2\,2p^4\,^3P$ | | $2s^2\,2p^4\,^1D$ | $2s^2\,2p^4\,^1S$ |
| $2s^2\,2p^4\,\mathrm{n}s\;(\mathrm{n} \geq 3)$ | $^4P$ | $^2P$ | $^2D$ | $^2S$ |
| $2s^2\,2p^4\,\mathrm{n}p\;(\mathrm{n} \geq 3)$ | $^4D^0\;^4P^0\;^4S^0$ | $^2D^0\;^2P^0\;^2S^0$ | $^2F^0\;^2D^0\;^2P^0$ | $^2P^0$ |
| $2s^2\,2p^4\,\mathrm{n}d\;(\mathrm{n} \geq 3)$ | $^4F\;\;^4D\;\;^4P$ | $^2F\;\;^2D\;\;^2P$ | $^2G\;\;^2F\;\;^2D\;\;^2P\;\;^2S$ | $^2D$ |
| $2s^2\,2p^4\,\mathrm{n}f\;(\mathrm{n} \geq 4)$ | $^4G^0\;^4F^0\;^4D^0$ | $^2G^0\;^2F^0\;^2D^0$ | $^2H^0\;^2G^0\;^2F^0\;^2D^0\;^2P^0\;^2S^0$ | $^2F^0$ |
| etc. | | | | |

***The ($^3P$) levels.*** From the electron configurations $p^4\,\mathrm{n}s$, $\mathrm{n}p$, $\mathrm{n}d$, and $\mathrm{n}f$ arise 5, 13, 17, and 18 energy level series respectively. The deviations from $LS$-coupling were evident already from the work of DINGLE on the $3s$ and $3p$-levels (10) and of EDLÉN on the $3d$-levels (14). In the latter case 16 $3d$-levels were observed but the combinations were not sufficient for an unambiguous determination of the $J$-values for all of them. In the present investigation it has been possible to identify many new $3p-3d$ lines, especially combinations with the $3p$-levels $^2S$, $^2P$, and $^4S$ which fall in the spectral range 9500—11 500 A not previously observed. The 17th level is obtained from several combinations and $J$-values have been uniquely assigned to all levels. The $4d$- and $5d$-groups have also been completely analysed and transitions from all the 17 levels observed. $^4F_{9/2}$ has been observed up to $8d$.

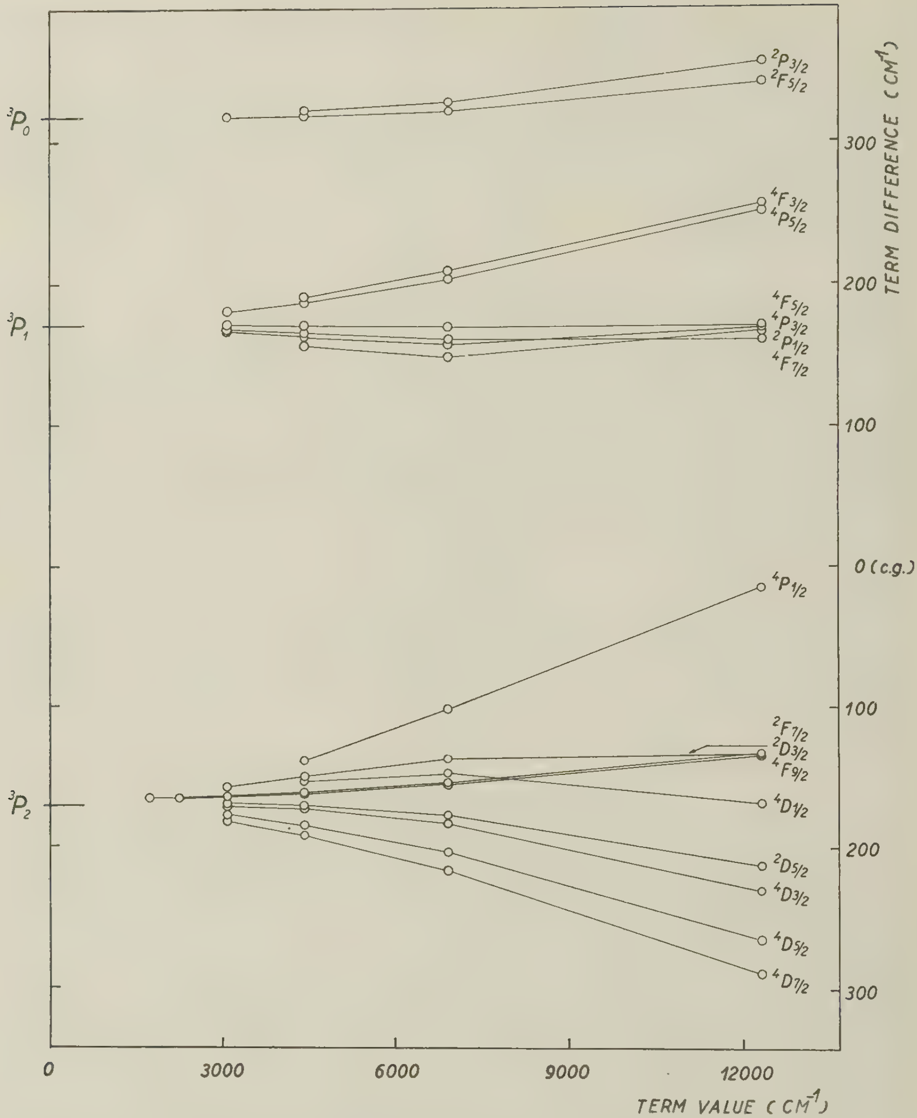

Fig. 4. Centroid diagram of the ($^3P$) n$d$ series of F I.

The n$d$-levels arrange themselves in three distinct subgroups associated with the three fine-structure components of the limit $^3P$ (Fig. 4). The coupling is therefore close to a type of $Jj$-coupling. Nevertheless it has seemed worth while to give the levels $LS$-symbols to indicate the chief constituent in their composition. This has been done chiefly on the basis of the intensities of the transitions $3p-3d$. There is a marked similarity between the combining properties of the higher n$d$-levels and those of the $3d$-levels.

*Table 9.*

The Ritz formulae for selected n$d$-series in F I.

| n | n $d\,^4F_{9/2}$ $\left\{\begin{array}{l}\alpha=0.022383\\ \beta=-7.002\times10^{-7}\end{array}\right.$ | | n $d\,^4F_{7/2}$ $\left\{\begin{array}{l}\alpha=0.031201\\ \beta=-9.590\times10^{-7}\end{array}\right.$ | | n $d\,^4F_{5/2}$ $\left\{\begin{array}{l}\alpha=0.027050\\ \beta=-7.272\times10^{-7}\end{array}\right.$ | |
|---|---|---|---|---|---|---|
| | Tn (calc) | Tobs−Tcalc | Tn (calc) | Tobs−Tcalc | Tn (calc) | Tobs−Tcalc |
| 3 | 12305.36 | +0.01 | 12009.75 | 0.00 | 11999.16 | 0.00 |
| 4 | 6918.93 | −0.04 | 6601.53 | −0.10 | 6592.68 | +0.01 |
| 5 | 4423.42 | +0.02 | 4095.26 | +0.11 | 4089.70 | −0.05 |
| 6 | 3068.83 | −0.01 | 2735.28 | +0.15 | 2731.74 | +0.04 |
| 7 | 2252.84 | +0.02 | | | | |
| 8 | 1723.71 | −0.16 | | | | |
| n | n $d\,^4D_{7/2}$ $\left\{\begin{array}{l}\alpha=0.038311\\ \beta=-4.741\times10^{-7}\end{array}\right.$ | | n $d\,^4D_{5/2}$ $\left\{\begin{array}{l}\alpha=0.033524\\ \beta=-3.176\times10^{-7}\end{array}\right.$ | | n $d\,^4D_{3/2}$ $\left\{\begin{array}{l}\alpha=0.025907\\ \beta=-0.410\times10^{-7}\end{array}\right.$ | |
| 3 | 12460.40 | 0.00 | 12436.68 | 0.00 | 12401.79 | 0.00 |
| 4 | 6980.01 | −0.05 | 6967.03 | +0.04 | 6947.10 | 0.00 |
| 5 | 4453.62 | 0.00 | 4446.30 | −0.04 | 4434.66 | −0.22 |
| 6 | 3086.03 | +0.07 | 3081.51 | −0.05 | 3074.53 | +0.01 |
| n | n $d\,^2F_{7/2}$ $\left\{\begin{array}{l}\alpha=0.021961\\ \beta=-6.780\times10^{-7}\end{array}\right.$ | | n $d\,^2F_{5/2}$ $\left\{\begin{array}{l}\alpha=0.028051\\ \beta=-10.430\times10^{-7}\end{array}\right.$ | | n $d\,^2D_{5/2}$ $\left\{\begin{array}{l}\alpha=0.024721\\ \beta=-1.175\times10^{-7}\end{array}\right.$ | |
| 3 | 12304.14 | 0.00 | 11826.61 | 0.00 | 12384.02 | 0.00 |
| 4 | 6917.99 | 0.00 | 6439.75 | 0.00 | 6941.10 | −0.17 |
| 5 | 4422.85 | 0.00 | 3940.05 | −0.14 | 4432.17 | +0.09 |
| 6 | 3068.47 | +0.01 | 2583.06 | +0.09 | 3073.07 | +0.09 |
| 7 | 2252.60 | −0.10 | | | | |

An examination of the fractional parts, n − n*, of the Rydberg denominators of the n$d$-levels shows that several series closely obey the Ritz formula, $n - n^* = \alpha + \beta T$, as may be seen from Table 9. This is specially true for levels with high $J$-values. Other levels, notably $^2D_{3/2}$, depart markedly from a Ritz formula. The fine structure intervals of the $^3P$ limit are taken from EDLÉN's measurements of the resonance lines of F II (13) with an experimental uncertainty of about 0.3—0.5 cm$^{-1}$. The series calculations just mentioned indicate that the interval $^3P_2$—$^3P_1$ might be 0.5 cm$^{-1}$ too large. Since, however, an accurate determination of the correction meets with difficulties, EDLÉN's values have been retained.

The constants $\alpha$ and $\beta$ in the Ritz formula have been calculated also for the levels not contained in Table 9, using the 3$d$- and 4$d$-levels only. The complete set of $\alpha$ and $\beta$ for the 17 series shows an interesting feature. The series may be unambiguously arranged in pairs, the two members in each pair having almost identical values of $\alpha$ and $\beta$ (Table 10). The $J$-values of each of the two members of a pair differ by one unit and the $\alpha$, $\beta$-set of the single level $^4P_{1/2}$ separates distinctly from the other sets. These facts prove that the coupling of the $d$-electron may be close to the $J_{\mathrm{I}}l$- or pair-coupling ($J_{\mathrm{I}}$ is the $J$-value of the ion), theoretically treated by RACAH (46) and used by EDLÉN for the rare gases (18). In the $J_{\mathrm{I}}l$-coupling scheme the total angular momentum $J_{\mathrm{I}}$ of the parent ion and the orbital moment $l$ of the external electron are coupled together and have a resultant $K$. $K$ is coupled with the spin

*Table 10.*

The constants $\alpha$ and $\beta$ of the Ritz formulae for the series $(^3P)\,nd$ in F I.

| *LS* symbol | $J_Il$ symbol | $\alpha$ | $\beta\times10^7$ | *LS* symbol | $J_Il$ symbol | $\alpha$ | $\beta\times10^7$ |
|---|---|---|---|---|---|---|---|
| $^4F_{9/2}$ | $(^3P_2)\,[4]_{9/2}$ | 0.0224 | −7.00 | $^4F_{7/2}$ | $(^3P_1)\,[3]_{7/2}$ | 0.0312 | − 9.59 |
| $^2F_{7/2}$ | $(^3P_2)\,[4]_{7/2}$ | 0.0220 | −6.78 | $^4F_{5/2}$ | $(^3P_1)\,[3]_{5/2}$ | 0.0271 | − 7.27 |
| $^4D_{7/2}$ | $(^3P_2)\,[3]_{7/2}$ | 0.0383 | −4.74 | $^4P_{5/2}$ | $(^3P_1)\,[2]_{5/2}$ | 0.0174 | − 7.44 |
| $^4D_{5/2}$ | $(^3P_2)\,[3]_{5/2}$ | 0.0335 | −3.18 | $^4F_{3/2}$ | $(^3P_1)\,[2]_{3/2}$ | 0.0145 | − 5.69 |
| $^2D_{5/2}$ | $(^3P_2)\,[2]_{5/2}$ | 0.0247 | −1.18 | $^4P_{3/2}$ | $(^3P_1)\,[1]_{3/2}$ | 0.0348 | −13.38 |
| $^4D_{3/2}$ | $(^3P_2)\,[2]_{3/2}$ | 0.0259 | −0.41 | $^2P_{1/2}$ | $(^3P_1)\,[1]_{1/2}$ | 0.0380 | −15.67 |
| $^2D_{3/2}$ | $(^3P_2)\,[1]_{3/2}$ | 0.0105 | +2.62 | $^2F_{5/2}$ | $(^3P_0)\,[2]_{5/2}$ | 0.0281 | −10.43 |
| $^4D_{1/2}$ | $(^3P_2)\,[1]_{1/2}$ | 0.0122 | +4.64 | $^2P_{3/2}$ | $(^3P_0)\,[2]_{3/2}$ | 0.0260 | −10.21 |
| $^4P_{1/2}$ | $(^3P_2)\,[0]_{1/2}$ | 0.0058 | −5.43 | | | | |

of this electron and their resultant is $J$. It is convenient to designate the levels in $J_Il$-coupling by giving the $K$-value of the pairs. For instance, the $J_Il$-symbol for $(^3P_2)\ 3d\ ^4F_{9/2}$ may be written $(^3P_2)\ 3d\ [4]_{9/2}$.

Each one of the different $d$-series can be unambiguously assigned to one of the three components of the $^3P$ limit (Fig. 4). SHENSTONE (52) observed an analogous behaviour in the $3d^9\,4s\,ns$ series of Cu I and claimed that this was the only complex series known at that time in which the individual series could be assigned to individual components of a limit with greater multiplicity than two.

Only the $3p$-group of the configuration $(^3P)\,np$ was known before. From combinations with $3s$ in the region 4000—3500 A the $4p$-group has now been completely analysed. The fairly good $LS$-coupling of $3p$ has partly disappeared in $4p$. Changes in the interval ratios and a decreasing total spread of the 13 levels make it possible to assign each one of these levels to a particular component of the limit. The lines of $3s\ ^4P$—$4p\ ^4P$ are surprisingly faint compared with the strong $3s\ ^4P$—$3p\ ^4P$ combinations. Of higher $p$-levels, only $5p\ ^4D_{7/2}$ has been observed.

In the $(^3P)\,ns$ group the $5s$-levels were previously analysed by the author (33). From combinations in the infrared region 9970—11 560 A and in the vacuum region, the $4s$-levels have now been determined. The $6s$-levels have also been obtained.

*Table 11.*

The Ritz formula for $(^3P)\ ns\ ^4P_{5/2}$ in F I.

| $ns\ ^4P_{5/2}\begin{cases}\alpha=1.27393\\ \beta=+7.438\times10^{-7}\end{cases}$ | | |
|---|---|---|
| n | Tn (calc) | Tobs − Tcalc |
| 3 | 38071.1 | +47.7 |
| 4 | 14886.90 | − 0.09 |
| 5 | 7928.97 | + 0.03 |
| 6 | 4920.57 | + 0.08 |
| 7 | 3349.71 | − 0.01 |
| 8 | 2426.90 | − 0.14 |

from transitions in the visible region. $^4P_{5/2}$ is observed up to $8s$. The $3s$-intervals indicate good $LS$-coupling but it may be pointed out that the intercombinations $2p\ ^2P-3s\ ^4P$ are fairly strong. The positions of higher $s$-levels agree well with the theory for intermediate coupling discussed in the previous paper (33). If the levels $^4P_{5/2}$, $^4P_{1/2}$, and $^2P_{3/2}$ of $4s$ and $^4P_{5/2}$, $^4P_{3/2}$, and $^2P_{1/2}$ of $6s$ are selected to fit the curves exactly, the coupling parameter $\chi$ becomes 0.909 for $4s$ and 4.95 ($1/\chi = 0.202$) for $6s$. $^4P_{5/2}$ follows a Ritz formula very closely, except for the lowest member, $3s$, which as usual shows a large deviation (Table 11). The mean values $1/2\ [^4P_{3/2} + {}^2P_{3/2}]$ and $1/2\ [^4P_{1/2} + {}^2P_{1/2}]$ also follow a Ritz formula while the individual components do not. The same relations were observed previously by EDLÉN in the analogous series of A II (15).

***The ($^1D$) and ($^1S$) term systems.*** EDLÉN's classification of some F I lines as combinations $3s-3p$ and $2p-3s$ of the ($^1D$) system indicated that only the $3s$- and $3p$-levels were situated below the first ionization limit $^3P_2$. Some levels above this limit have now been observed. $4s\ ^2D_{5/2,\,3/2}$ were obtained from a transition to $2p\ ^2P$ in the vacuum region. $3d$ and $4d\ ^2G_{9/2,\,7/2}$ have been determined from combinations with $3p\ ^2F$. With LiF only in the discharge tube these lines are weaker than with $SF_6$, contrary to other F I lines. The determination of the remaining ($^1D$) $3d$-levels is difficult. The two lines 8612—8606 A, showing the same separation as $3p\ ^2F$, may be tentatively classified as ($^1D$) $3p$—($^1D$) $3d$ transitions, but the interpretation of the high level is difficult.

The $^2P$ term of the ($^1D$) $3p$-group is still unknown. The transitions ($^1D$) $3s\ ^2D$ – ($^1D$) $3p\ ^2P$ which should fall around 6800—7000 A probably coincide with some of the very intense ($^3P$) $3s$ – ($^3P$) $3p$ lines in this region. The corresponding combinations in Ne II and Na III are fairly strong (7, 56).

In the spectra of Ne II, Na III, and Cl I (7, 56, 26) several transitions between the ($^3P$)- and the ($^1D$)-systems have been identified. In F I, however, only the lines $2p\ ^2P$—($^1D$) $3s\ ^2D$ are found, connecting the two systems with an uncertainty of about 1 $\mathrm{cm}^{-1}$. Two unidentified lines, 2967—2969 A, are observed in the region predicted for the transitions ($^3P$) $3s\ ^2P$—($^1D$) $3p\ ^2P$, but the ($^1D$) $3p\ ^2P$ levels thus obtained do not give any observable combinations with ($^1D$) $3s$.

In the hollow cathode light source the observed lines coming from levels above the ionization limit are perfectly sharp. The main conditions for autoionization into the $s$- and $d$-continuum above the $^3P$-limit are fulfilled and the non-appearance of this phenomenon must be explained from the different coupling conditions, viz. good $LS$-coupling for the ($^1D$)-levels in contrast to $J_1l$-coupling for the ($^3P$)-levels and their series continua.

All levels of the ($^1S$)-system must be situated above the ionization limit and none of them is observed. $3s\ ^2S_{1/2}$ has been extrapolated from the isoelectronic sequence Ne II, Na III, etc.

In the previously mentioned investigation of the Stark effect in F I (32) a displaced line was observed, the field-free part of which coincided with F I $3s-3p$ 6239 A. It was identified as $3p\ ^2D_{5/2}-4d\ Z_1$. In the present extensive investigation this identification has been disproved and it has not been possible to identify the line with any F I combination. The interferometric examination of $\lambda$ 6239 showed no components apart from the $h/s$ pattern (Plate X). The background, however, was surprisingly strong. The interpretation of the line as a forbidden combination $3p$—$4f$ or $3p-5p$, induced by the field, is possible but not very likely.

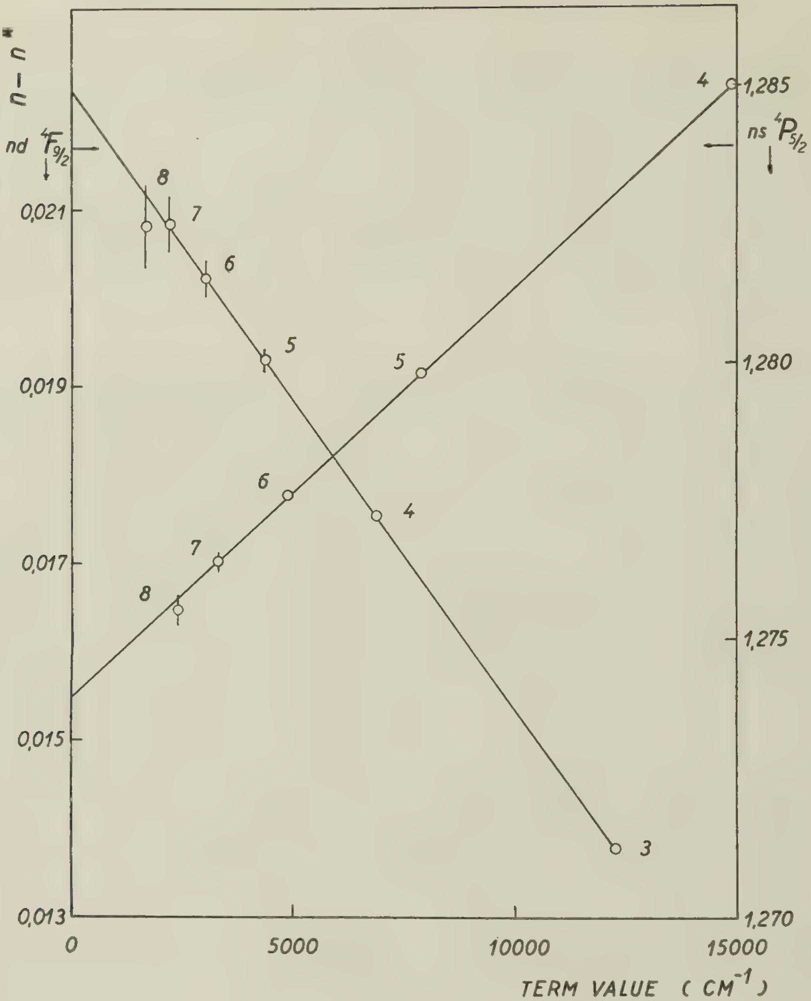

Fig. 5. The quantum defect, n − n*, of the levels n$d$ $^4F_{9/2}$ (n = 3—8) and n$s$ $^4P_{5/2}$ (n = 4—8) plotted against the level values. The vertical lines show the deviation of n − n* caused by a change of the limit by ±0.2 cm$^{-1}$.

***The series limit.*** The series limit of F I was previously known with an uncertainty of about 30 cm$^{-1}$ (33). It has now been much more accurately determined from an examination of several series which closely obey a Ritz formula. The effective quantum numbers $n^* = \sqrt{R/T_n}$ have been calculated using the Rydberg constant for fluorine, $R = 109734.16$ cm$^{-1}$, and the limit was graphically determined by successive approximations of the term values $T_n$. The series n$d$ $^4F_{9/2}$ with 6 members was selected to give the final value of the limit. As a result the previous value had to be corrected by —28.21 cm$^{-1}$. The estimated accuracy of the determination is ± 0.1 cm$^{-1}$ as shown in Fig. 5, where the values of n—n* of the series n$d$ $^4F_{9/2}$ and n$s$ $^4P_{5/2}$ are plotted against the term values.

A very accurate value for the ionization potential is now obtained from the previously described precision measurements on the resonance lines λλ 977—951 (p. 252). The value 140524.5 ± 0.4 cm$^{-1}$ results for the ground level $2p\ ^2P_{3/2}$. Using BIRGE's value of the conversion factor (12395 ± 2) × 10$^{-8}$ cm × absvolt (4) the ionization potential of F I in volts becomes 17.418 ± 0.003, the error entirely depending on the conversion factor.

The new wave-length material has been used for a recalculation of the entire term system of F I. The result is given in Table 12. Term values calculated from interferometric wave-lengths are given to 0.001 cm$^{-1}$. As mentioned above the uncertainty of the connection between the two systems built on ($^3P$) and ($^1D$) is about 1 cm$^{-1}$.

## VI. Comparison with similar spectra

***The isoelectronic sequence F I, Ne II, Na III, etc.*** The ($^3P$) $3p$-group of F I, Ne II (7), Na III (56), and Mg IV (partially) (54) has been analysed from the observed transitions $3s-3p$ and $3p-3d$. A representation of these levels is given in Fig. 6, where $\Delta T/(N+\delta)$ is plotted against the atomic number. $\Delta T$ is the difference between $^4D_{7/2}$ and the other levels, calculated from their limits. $N$ is the order of the spectrum and the constant $\delta$ is adapted to give parallel lines for the different levels. In this case $\delta = -0.42$ is chosen. This type of diagram, suggested by EDLÉN, is very convenient for extrapolations and studies of perturbations. Only the level $^2P_{3/2}$ of Na III differs markedly from the regularity of the scheme. The same deviation is observed for ($^1D$) $3p\ ^2P$ of Na III. It may be pointed out that the splitting of the ($^3P$) $^2P$ term decreases with increasing $N$ contrary to the regular-doublet law and the other term splittings.

The analogous diagram of $3d$ does not show the same regular features, partly because of the large deviations from $LS$-coupling and the change in coupling of the $3d$-electron in F I, Ne II, etc. which makes the assignments of $LS$-symbols uncertain.

***The first spectra of the halogens.*** The series ($^3P$) n$s$ and n$p$ of F I and Cl I (26) seem to obey the same coupling conditions, while the large deviations of $7s$ and $6p$ in Br I (28, 30) require special examination outside the scope of this work.

The n$d$-series of F I, Cl I, and Br I show a very different behaviour. The subgroups in F I due to the splitting of the $^3P$-limit can not be distinguished in Cl I and Br I, although the ($^3P$)-intervals are large, 299—697 (29) and 701—3139 cm$^{-1}$ (47) respectively. In Cl I, however, from an extensive study of the Zeeman effect, GREEN and LYNN (22) found that the $g$-values indicated $J_1l$-coupling. Very likely the main coupling conditions are the same in Br I but strong perturbations complicate the analysis.

The limit components of the ($^3P$) n$d$-series of Cl I were given by KIESS and DE BRUIN (27) using Hund's scheme. It has been known for a long time (50), that Hund's scheme for limit assignments is not reliable and has evidently led to wrong assignments in this case also. Thus, from the coupling between the $J$ of the parent ion and the $j$ of the $d$-electron it is clear that $^3P_0$ gives the $J$-values 5/2, 3/2, while KIESS and DE BRUIN give 3/2, 1/2. Moreover, they give three levels with $J = 5/2$ as based on $^3P_2$, while only two are possible.

## *Table 12.*

## The energy level system of F I.

| $2s^2\,2p^5\,{}^2P^0_{1/2}$ 140524.5<br>*404.1*<br>${}^2P^0_{3/2}$ 140120.4 | $2s\,2p^6\,{}^2S_{1/2}$ [− 29300] | Limits: $2s^2\,2p^4\,{}^3P_2 = 0$, ${}^3P_1 = -341.8$ ${}^3P_0 = -490.6$<br>$2s^2\,2p^4\,{}^1D_2 = -20876$<br>$2s^2\,2p^4\,{}^1S_0 = -44922$ |
|---|---|---|

| Term symbol | Limit | 3 *d* |  | 4 *d* |  | 5 *d* |  | 6 *d* |  | 7 *d* |  | 8 *d* |  |
|---|---|---|---|---|---|---|---|---|---|---|---|---|---|
|  |  | T | n* | T | n* | T | n* | T | n* | T | n* | T | n* |
| ${}^2P_{1/2}$ | ${}^3P_1$ | 12004.28 | 2.98130 | 6614.11 | 3.97186 | 4104.44 | 4.96792 |  |  |  |  |  |  |
|  |  | *192.08* |  | *180.89* |  | *167.93* |  |  |  |  |  |  |  |
| ${}^2P_{3/2}$ | ${}^3P_0$ | 11812.20 | 2.98654 | 6433.22 | 3.98105 | 3936.51 | 4.97864 |  |  |  |  |  |  |
| ${}^2D_{3/2}$ | ${}^3P_2$ | 12304.67 | 2.98632 | 6900.65 | 3.98773 | 4410.69 | 4.98790 | 3061.79 | 5.98664 |  |  |  |  |
|  |  | *−79.35* |  | *−40.28* |  | *−21.57* |  | *−11.37* |  |  |  |  |  |
| ${}^2D_{5/2}$ | ${}^3P_2$ | 12384.02 | 2.97673 | 6940.93 | 3.97614 | 4432.26 | 4.97575 | 3073.16 | 5.97556 |  |  |  |  |
| ${}^2F_{5/2}$ | ${}^3P_0$ | 11826.61 | 2.98480 | 6439.75 | 3.97918 | 3940.05 | 4.97665 | 2583.06 | 5.97507 |  |  |  |  |
|  |  | *−477.53* |  | *−478.24* |  | *−482.80* |  | *−485.42* |  |  |  |  |  |
| ${}^2F_{7/2}$ | ${}^3P_2$ | 12304.14 | 2.98638 | 6917.99 | 3.98273 | 4422.85 | 4.98104 | 3068.48 | 5.98011 | 2252.50 | 6.97973 |  |  |
| ${}^4P_{1/2}$ | ${}^3P_2$ | 12185.78 | 3.00085 | 6865.38 | 3.99796 | 4400.20 | 4.99384 |  |  |  |  |  |  |
|  |  | *184.56* |  | *260.37* |  | *302.50* |  |  |  |  |  |  |  |
| ${}^4P_{3/2}$ | ${}^3P_1$ | 12001.22 | 2.98167 | 6605.01 | 3.97446 | 4097.70 | 4.97169 | 2736.80 | 5.97027 |  |  |  |  |
|  |  | *82.81* |  | *46.19* |  | *24.69* |  | *14.40* |  |  |  |  |  |
| ${}^4P_{5/2}$ | ${}^3P_1$ | 11918.41 | 2.99173 | 6558.82 | 3.98774 | 4073.01 | 4.98557 | 2722.40 | 5.98429 |  |  |  |  |
| ${}^4D_{1/2}$ | ${}^3P_2$ | 12339.51 | 2.98210 | 6911.09 | 3.98472 | 4415.07 | 4.98542 |  |  |  |  |  |  |
|  |  | *−62.28* |  | *−36.01* |  | *−19.59* |  |  |  |  |  |  |  |
| ${}^4D_{3/2}$ | ${}^3P_2$ | 12401.781 | 2.97460 | 6947.10 | 3.97438 | 4434.66 | 4.97440 | 3074.54 | 5.97422 |  |  |  |  |
|  |  | *−34.890* |  | *−19.97* |  | *−11.60* |  | *−6.92* |  |  |  |  |  |
| ${}^4D_{5/2}$ | ${}^3P_2$ | 12436.671 | 2.97043 | 6967.07 | 3.96868 | 4446.26 | 4.96791 | 3081.46 | 5.96750 |  |  |  |  |
|  |  | *−23.726* |  | *−12.89* |  | *−7.36* |  | *−4.57* |  |  |  |  |  |
| ${}^4D_{7/2}$ | ${}^3P_2$ | 12460.397 | 2.96760 | 6979.96 | 3.96501 | 4453.62 | 4.96380 | 3086.03 | 5.96308 |  |  |  |  |
| ${}^4F_{3/2}$ | ${}^3P_1$ | 11912.58 | 2.99244 | 6553.12 | 3.98939 | 4069.42 | 4.98760 |  |  |  |  |  |  |
|  |  | *−86.57* |  | *−39.57* |  | *−20.23* |  |  |  |  |  |  |  |
| ${}^4F_{5/2}$ | ${}^3P_1$ | 11999.15 | 2.98192 | 6592.69 | 3.97799 | 4089.65 | 4.97620 | 2731.78 | 5.97515 |  |  |  |  |
|  |  | *−10.60* |  | *−8.74* |  | *−5.72* |  | *−3.65* |  |  |  |  |  |
| ${}^4F_{7/2}$ | ${}^3P_1$ | 12009.75 | 2.98064 | 6601.43 | 3.97549 | 4095.37 | 4.97299 | 2735.43 | 5.97160 |  |  |  |  |
|  |  | *−295.62* |  | *−317.46* |  | *−328.07* |  | *−333.39* |  |  |  |  |  |

| Term symbol | Limit | T | n* | T | n* | T | n* | T | n* | T | n* | T | n* |
|---|---|---|---|---|---|---|---|---|---|---|---|---|---|
| $^2P_{1/2}$ | $^3P_0$ | 35468.218 | 1.74690 | 13943.32 | 2.75727 | 7301.25 | 3.75276 | 4373.29 | 4.74984 | | | | |
| | | *−325.232* | | *−298.60* | | *−224.87* | | *−184.82* | | | | | |
| $^2P_{3/2}$ | $^3P_1$ | 35793.450 | 1.74263 | 14241.92 | 2.74307 | 7526.12 | 3.73457 | 4558.11 | 4.73235 | | | | |
| $^4P_{1/2}$ | $^3P_1$ | 37684.124 | 1.69876 | 14457.27 | 2.72304 | 7515.37 | 3.73713 | 4529.23 | 4.74636 | | | | |
| | | *−159.941* | | *−189.95* | | *−264.16* | | *−310.00* | | | | | |
| $^4P_{3/2}$ | $^3P_2$ | 37844.065 | 1.70283 | 14647.22 | 2.73712 | 7779.53 | 3.75573 | 4839.23 | 4.76193 | 3302.31 | 5.76450 | | |
| | | *−274.725* | | *−239.59* | | *−149.47* | | *−81.42* | | *−47.39* | | | |
| $^4P_{5/2}$ | $^3P_2$ | 38118.790 | 1.69646 | 14886.81 | 2.71500 | 7929.00 | 3.72016 | 4920.65 | 4.72237 | 3349.70 | 5.72358 | 2426.76 | 6.72446 |

| Term symbol | Limit | $3p$ | | $4p$ | | $5p$ | |
|---|---|---|---|---|---|---|---|
| | | T | n* | T | n* | T | n* |
| $^2S^0_{1/2}$ | $^3P_1$ | 22119.233 | 2.21032 | 10375.43 | 3.19985 | | |
| $^2P^0_{1/2}$ | $^3P_0$ | 21442.680 | 2.23676 | 10034.57 | 3.22891 | | |
| | | *−145.023* | | *−115.07* | | | |
| $^2P^0_{3/2}$ | $^3P_0$ | 21587.703 | 2.22940 | 10149.64 | 3.21140 | | |
| $^2D^0_{3/2}$ | $^3P_1$ | 22651.584 | 2.18459 | 10382.85 | 3.19874 | | |
| | | *−249.993* | | *−125.55* | | | |
| $^2D^0_{5/2}$ | $^3P_1$ | 22901.577 | 2.17281 | 10508.40 | 3.18018 | | |
| $^4S^0_{3/2}$ | $^3P_1$ | 22096.677 | 2.21144 | 10303.38 | 3.21066 | | |
| $^4P^0_{1/2}$ | $^3P_2$ | 24380.921 | 2.12151 | 10917.43 | 3.17038 | | |
| | | *−102.696* | | *−122.41* | | | |
| $^4P^0_{3/2}$ | $^3P_2$ | 24483.617 | 2.11706 | 11039.84 | 3.15275 | | |
| | | *−122.974* | | *−102.80* | | | |
| $^4P^0_{5/2}$ | $^3P_2$ | 24606.591 | 2.11176 | 11142.64 | 3.13817 | | |
| $^4D^0_{1/2}$ | $^3P_1$ | 23132.550 | 2.16209 | 10465.10 | 3.18655 | | |
| | | *−83.392* | | *−122.07* | | | |
| $^4D^0_{3/2}$ | $^3P_2$ | 23215.942 | 2.17409 | 10587.17 | 3.21944 | | |
| | | *−144.552* | | *−164.50* | | | |
| $^4D^0_{5/2}$ | $^3P_2$ | 23360.494 | 2.16735 | 10751.67 | 3.19472 | | |
| | | *−176.612* | | *- 113.33* | | | |
| $^4D^0_{7/2}$ | $^3P_2$ | 23537.106 | 2.15921 | 10865.00 | 3.17802 | 6267.81 | 4.18421 |

| Designation | Limit | T | n* |
|---|---|---|---|
| $3s\,^2D_{3/2}$ | $^1D_2$ | 16602.49 | 1.71112 |
| | | *− 0.96* | |
| $^2D_{5/2}$ | » | 16603.45 | 1.71109 |
| $4s\,^2D_{3/2}$ | » | −6382.4 | 2.75158 |
| $^2D_{5/2}$ | » | −6381.1 | |
| $3p\,^2D^0_{3/2}$ | » | 1828.94 | 2.19842 |
| | | *7.96* | |
| $^2D^0_{5/2}$ | » | 1820.98 | 2.19880 |
| $^2F^0_{5/2}$ | » | 2934.41 | 2.14678 |
| | | *8.90* | |
| $^2F^0_{7/2}$ | » | 2925.51 | 2.14718 |
| $3d\,^2G_{7/2}$ | » | −8444.69 | 2.97107 |
| $^2G_{9/2}$ | » | −8444.70 | |
| $4d\,^2G_{7/2}$ | » | −13902.87 | 3.96696 |
| $^2G_{9/2}$ | » | −13902.88 | |
| $3s\,^2S_{1/2}$ | $^1S_0$ | [− 8460] | |

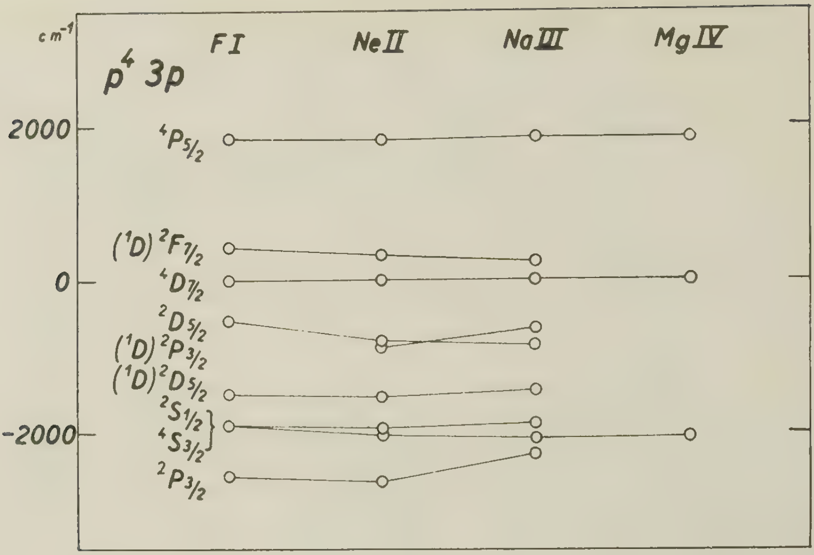

Fig. 6. The $3p$-terms of F I, Ne II, Na III and Mg IV. $\Delta T/(N-0.42)$ is plotted against th atomic number. $\Delta T = T - {}^4D_{7/2}$. $N$ is the order of the spectrum.

An intensity scheme for all observed transitions $3p$—n$d$ of F I, Cl I, and Br I has been arranged. The strong components of the combinations $3p$—n$d$ $^4F$, $^4D$ seem to show good mutual agreement between different elements and different $n$ In F I the leading components of the combinations of the other n$d$-levels have approximately the same relative intensities for different n, while in Cl I and Br I no such regularity exists. An extensive study of the n$d$-series of the heavier halogens will be necessary before a reliable correlation of levels can be established.

## VII. The hyperfine structure

As previously mentioned (p. 236) CAMPBELL 1933 (8) measured the hyperfine structure of some F I lines and found that $F^{19}$ had a nuclear spin of 1/2. With the water-cooled hollow cathode used in the present investigation it has been possible to reduce the line-width considerably and to measure the separated $h/s$-components of 26 F I lines as compared to 8 lines in CAMPBELL's paper. The decreased Doppler-broadening has permitted measurements of weak components in some $h/s$-patterns and the use of etalons up to 25 mm. In tab. 13 the measured line splittings are given together with CAMPBELL's values. Some incompletely resolved lines and their estimated structure are given in tab. 14. The completely unresolved F I lines, also included in tab. 14, have the same sharpness as the simultaneously excited Ne I lines (Plate IX).

The nuclear spin $I$ and the total angular momentum $J$ of the extranuclear electrons are combined to the resultant $F$, the total angular momentum of the whole atom. In F I with $I = 1/2$ each level is a narrow doublet. For all $3s$- and $3p$-levels these doublet intervals are computed from the line splittings in

## *Table 13.*

### Hyperfine structure of F I lines.

If a line pattern is given with more than one interval in the third column the intervals follow in the order of increasing wave-number of the components. The interval between the strongest components is underlined.

In the fifth column r and v denotes that the weaker component is situated on the red and violet side respectively.

| $\lambda$ | Combination | Structure, cm$^{-1}$ | | |
|---|---|---|---|---|
| | | | CAMPBELL | |
| 8737 | $3p\,^4D_{5/2}-3d\,^4P_{5/2}$ | 0.098 | | v |
| 8345 | $^4P_{1/2}-\ ^4D_{3/2}$ | 0.181 | | r |
| 7898 | $^4P_{3/2}-\ ^2P_{3/2}$ | 0.133 | | v |
| 7800 | $3s\,^2P_{1/2}-3p\,^2D_{3/2}$ | 0.090 | | r |
| 7607 | $^2P_{3/2}-\ ^2D_{3/2}$ | 0.068 | | v |
| 7573 | $^4P_{1/2}-\ ^4P_{3/2}$ | 0.127 | 0.125 | r |
| 7552 | $^4P_{3/2}-\ ^4P_{5/2}$ | 0.071 | 0.07* | r |
| 7482 | $^4P_{3/2}-\ ^4P_{3/2}$ | 0.089 | | r |
| 7425 | $^4P_{3/2}-\ ^4P_{1/2}$ | 0.067 | 0.06* | v |
| 7398 | $^4P_{5/2}-\ ^4P_{5/2}$ | 0.108 | | r |
| | | $\underline{0.154}$ | 0.161 | v |
| | | 0.101 | | v |
| 7331 | $^4P_{5/2}-\ ^4P_{3/2}$ | $\underline{0.138}$ | 0.144 | v |
| | | 0.124 | | v |
| 7311 | $^2P_{3/2}-\ ^2S_{1/2}$ | $\underline{0.105}$[1] | 0.135 | v |
| | | 0.128 | | |
| 7037 | $^2P_{3/2}-\ ^2P_{3/2}$ | 0.110 | ~0.2* | v |
| 6966 | $^2P_{3/2}-\ ^2P_{1/2}$ | 0.126 | | v |
| 6909 | $^4P_{1/2}-\ ^4D_{3/2}$ | 0.054 | 0.04* | r |
| 6902 | $3s\,^4P_{3/2}-3p\,^4D_{5/2}$ | 0.083 | 0.08* | r |
| 6856 | $^4P_{5/2}-\ ^4D_{7/2}$ | 0.233 | narrow | r |
| | | $\underline{0.051}$ | | v |
| 6773 | $^4P_{5/2}-\ ^4D_{5/2}$ | 0.106 | | r |
| | | $\underline{0.151}$ | 0.155 | v |
| | | 0.097 | | v |
| 6762 | $(^1D)3s\,^2D_{5/2}-(^1D)\,3p\,^2D_{5/2}$ | 0.127 | | v |
| 6708 | $3s\,^4P_{5/2}-3p\,^4D_{3/2}$ | 0.205 | 0.231 | v |
| 6690 | $^4P_{3/2}-\ ^2D_{5/2}$ | 0.136 | 0.153 | r |
| 6650 | $^4P_{1/2}-\ ^2D_{3/2}$ | 0.105 | 0.10* | r |
| 6569 | $^4P_{5/2}-\ ^2D_{5/2}$ | 0.084 | narrow | v |
| 6239 | $^4P_{5/2}-\ ^4S_{3/2}$ | 0.269 | 0.267 | v |
| 6133 | $3p\,^2D_{5/2}-4d\,^4F_{7/2}$ | 0.156 | | v |
| 5994 | $3p\,^4P_{5/2}-5s\,^4P_{5/2}$ | 0.097 | | r |

---

[1] The components of $\lambda$ 7311 have theoretically the relative intensities 5 : 2 : 1. The value 0.128 is measured for the separation between the component 5 and the centre of gravity of the components 2 and 1.

* CAMPBELL: not fully resolved.

*Table 14.*

F I lines with no observable *h/s* or with observed but not clearly resolved *h/s.*

| $\lambda$ | Combination | Estimated separation | see Table 13 |
|---|---|---|---|
| 8807 | $3p\,^4D_{5/2}-3d\,^4F_{7/2}$ | 0.07 | v |
| 8777 | $^4D_{3/2}-\ ^2F_{5/2}$ | 0.07 | v |
| 8040 | $3s\,^2P_{3/2}-3p\,^4D_{5/2}$ | 0.05 | v |
| 7754 | $^2P_{3/2}-\ ^2D_{5/2}$ | broad | ? |
| 7514 | $^4P_{1/2}-\ ^4P_{1/2}$ | none | |
| 7489 | $^2P_{1/2}-\ ^2S_{1/2}$ | none | |
| 7202 | $^2P_{1/2}-\ ^2P_{3/2}$ | small | r |
| 7127 | $^2P_{1/2}-\ ^2P_{1/2}$ | small | r? |
| 6870 | $^4P_{1/2}-\ ^4D_{1/2}$ | 0.03 | r |
| 6834 | $^4P_{3/2}-\ ^4D_{3/2}$ | none | |
| 6795 | $^4P_{3/2}-\ ^4D_{1/2}$ | none | |
| 6413 | $^4P_{1/2}-\ ^4S_{3/2}$ | none | |
| 6348 | $3s\,^4P_{3/2}-3p\,^4S_{3/2}$ | none | |

tab. 13. When necessary the centre of gravity of unresolved *h/s*-components has been calculated from the theoretical intensity ratios (57). CAMPBELL did not observe any complete hypermultiplet and based his calculations on the assumption that the splitting of $3p\,^4S_{3/2}$ was negligible. Now all components of the hypermultiplets $3s\,^4P_{5/2}-3p\,^4P_{5/2}$, $-^4P_{3/2}$, $-^4D_{7/2}$, and $-^4D_{5/2}$ have been measured and the doublet interval of $3s\,^4P_{5/2}$ found to be 0.259 cm $^{-1}$. The calculation of the intervals of the other levels in the ($^3P$)-system is then based on this value. CAMPBELL's values agree surprisingly well with those now obtained (Tab. 15).

*Table 15.*

The hyperfine structure of F I levels.

| Level | $\Delta\nu$ cm$^{-1}$ | CAMPBELL | Level | $\Delta\nu$ cm$^{-1}$ | CAMPBELL |
|---|---|---|---|---|---|
| $3s\,^2P_{1/2}$ | +0.006 | small | $3p\,^4S_{3/2}$ | −0.011 | small |
| $^2P_{3/2}$ | +0.153 | +0.14 | $^4P_{1/2}$ | +0.050 | small |
| $^4P_{1/2}$ | −0.005 | +0.02 | $^4P_{3/2}$ | +0.121 | +0.14 |
| $^4P_{3/2}$ | +0.034 | +0.05 | $^4P_{5/2}$ | +0.105 | +0.12 |
| $^4P_{5/2}$ | +0.259 | +0.27 | $^4D_{1/2}$ | +0.03 | +0.03 |
| $5s\,^4P_{5/2}$ | +0.202 | | $^4D_{3/2}$ | +0.054 | +0.04 |
| $3p\,^2S_{1/2}$ | +0.043 | small | $^4D_{5/2}$ | +0.108 | +0.13 |
| $^2P_{1/2}$ | +0.040 | | $^4D_{7/2}$ | +0.208 | +0.25 |
| $^2P_{3/2}$ | +0.052 | | $3d\,^2P_{3/2}$ | −0.016 | |
| $^2D_{3/2}$ | +0.102 | +0.11 | $^4P_{5/2}$ | +0.011 | |
| $^2D_{5/2}$ | +0.175 | +0.18 | $^4D_{3/2}$ | +0.147 | |
| | | | $4d\,^4F_{7/2}$ | +0.020 | |

In the $(^1D)$-system hyperfine structure has been observed only for the line $3s\,^2D_{5/2}-3p\,^2D_{5/2}$ (Plate X). From comparison with the splitting of $(^3P)\,3p\,^2D_{5/2}$ it is probable that this structure is mainly due to the level $(^1D)\,3p\,^2D_{5/2}$. The lines $3s\,^2D_{3/2}-3p\,^2D_{3/2}$, $^2F_{5/2}$ and $3s\,^2D_{5/2}-3p\,^2F_{7/2}$ show no observable structure.

The $hfs$ separation of some $3d$-, $4d$- and $5s$-levels is also measured. The large splitting of $3d\,^4D_{3/2}$ is remarkable as well as the considerable separation of $5s\,^4P_{5/2}$. These observations indicate that the coupling between the nuclear spin and the electron group $2p^4$ contributes more to the hyperfine structure separations than the n$s$ or n$p$ electrons with $\mathrm{n} \geqq 3$.

***Acknowledgments.*** The author wishes to acknowledge his indebtedness to Professor BENGT EDLÉN, under whose direction this research was carried on, for his continued interest and advice during the course of the work and for making available his unpublished material on atomic spectra.

To Fil. mag. STIG AVELLÉN the author is greatly indebted for invaluable and skilful experimental assistance throughout the vacuum spectroscopic work.

For silvering and testing the interferometer plates and for valuable discussions the author should like to express his thanks to Professor EBBE RASMUSSEN, Kongl. Veterinær- og Landbohöjskole, Copenhagen.

The great burden of numerical calculation and checking has rested on my wife, Fil. mag. MÄRTA LIDÉN, and on Mrs. SONJA AVELLÉN. Their conscientious work is hereby gratefully acknowledged.

The work described in this paper has been assisted by grants from the *Swedish Natural Science Research Council.* A grant from "*Kungl. Fysiografiska Sällskapet i Lund*" is also gratefully acknowledged.

The Physical Laboratory, University of Lund. April 1949.

REFERENCES. 1. **Arvidsson, G.,** Wellenlängenmessungen in den höheren Funkenspektren von Blei und Wismut im äussersten Ultraviolett. Diss. Uppsala 1932 (see also Ann. Phys., Lpz., *12*, 787, 1932). — 2. **Bethe, H. A.,** The electromagnetic shift of energy levels. Phys. Rev. *72*, 339, 1947 (see also **Fowles,** Phys. Rev. *74*, 219, 1948). — 3. **Bethe, H. A.,** and **Longmire, C.,** On the experimental value of the fine structure constant. Phys. Rev. *75*, 306, 1949. — 4. **Birge, R. T.,** A new table of values of the general physical constants. Rev. Mod. Phys. *13*, 233, 1941. — 5. **Bowen, I. S.,** Series spectra of boron, carbon, nitrogen, oxygen and fluorine. Phys. Rev. *29*, 231, 1927. — 6. **Boyce, J. C.,** Spectroscopy in the vacuum ultraviolet. Rev. Mod. Phys. *13*, 1, 1941. — 7. **de Bruin, T. L.,** and **Bakker, C. J.,** Struktur und Zeemaneffekt des Neonfunkenspektrums, Ne II. Z. Phys. *69*, 19, 1931. — 8. **Campbell, J. S.,** Hyperfeinstruktur im Bogenspektrum des Fluors. Z. Phys. *84*, 393, 1933. — 9. **Carragan, G. H.,** The Zeeman effect for the spectrum of fluorine. Astrophys. J. *63*, 145, 1926. — 10. **Dingle, H.,** The spectrum of fluorine (F I). Part I and II. Proc. Roy. Soc. A, *113*, 323, 1926 and *117*, 407, 1928. — 11. ——, The spectrum of ionised fluorine (F II). Proc. Roy. Soc. A, *128*, 600, 1930. — 12. **Eastman Kodak** Company, Photographic plates for use in spectroscopy and astronomy. New York, July 1946. — 13. **Edlén, B.,** Beitrag zu den Spektren F III, F II und F I. Z. Phys. *93*, 433, 1935. — 14. ——, Über die Bogenspektren von Fluor und Kalium. Z. Phys. *98*, 445, 1936. — 15. ——, Zur Kenntnis der Cl I-ähnlichen Spektren Cl I, A II, K III, Ca IV, Ti VI, V VII, Cr VIII, Mn IX, Fe X und Co XI. Z. Phys. *104*, 407, 1937. — 16. ——, Das Bogenspektrum des Sauerstoffs, O I. Kungl. Svenska Vet.-akad. Handl. *20*, n:r 10, 1943. — 17. ——, Unpublished material 1948 (Wave-lengths of some Ne I-lines). — 18. ——, Unpublished material 1948 (Pair coupling in the rare gases). — 19. **Edlén, B.,** and **Lidén, K.,** A note on the arc spectrum of lithium. Phys. Rev. *75*, 890, 1949. — 20. **Ferner, E.,** Die Spektren von hochionisiertem Aluminium, Silicium und Schwefel. Ark. Mat. Astr. Fys. *36 A*, n:r 1, 1948. — 21. **Gale, H. G.,** and **Monk, G. S.,** The spectrum of fluorine. Astrophys. J. *59*, 125, 1924. — 22. **Green, J. B.,** and **Lynn, J. T.,** The Zeeman effect in the spectrum of chlorine I. Phys. Rev. *69*, 165, 1946. — 23. **Harrison,**

**G. R.**, M. I. T. Wavelength Tables. John Wiley & Sons. New York 1939. — 24. **Hunter, A.**, The spectra of singly and doubly ionized sulphur in the region $\lambda\lambda$ 3300—4900 A. Philos. Trans. *233*, 303, 1934. — 25. **Kayser, H.**, Tabelle der Schwingungszahlen. Leipzig 1925. Revised Edition, Ann. Arbor, Mich., 1944. — 26. **Kiess, C. C.**, A new description and analysis of the arc spectrum of chlorine. J. Res. Nat. Bur. Stand., Wash. *10*, 827, 1933. — 27. **Kiess, C. C.**, and **de Bruin, T. L.**, The arc spectrum of chlorine and its structure. J. Res. Nat. Bur. Stand., Wash. *2*, 1117, 1929. — 28. ——, The arc spectrum of bromine and its structure. J. Res. Nat. Bur. Stand., Wash. *4*, 667, 1930. — 29. ——, Second spectrum of chlorine and its structure. J. Res. Nat. Bur. Stand., Wash. *23*, 443, 1939. — 30. **Lacroute, P.**, Effet Zeeman du brome et de l'iode. Ann. Phys. Paris *3*, 5, 1935. — 31. **Lamb Jr., W. E.**, and **Retherford, R. C.**, Fine structure of the hydrogen atom by a microwave method. Phys. Rev. *72*, 241, 1947. — 32. **Lidén, K.**, Stark effect in the spectrum of neutral fluorine, F I. Ark. Mat. Astr. Fys. *35 A*, n:r 23, 1948. — 33. ——, Wave-length measurements and new energy levels in the arc spectrum of fluorine, F I. Ark. Mat. Astr. Fys. *35 A*, n:r 24, 1948. — 34. **Meggers, W. F.**, Infrared spectra of noble gases (10500 to 13000 A). J. Res. Nat. Bur. Stand., Wash. *14*, 487, 1935. — 35. **Meggers, W. F.**, and **Humphreys, C. J.**, Interference measurements in the spectra of noble gases. J. Res. Nat. Bur. Stand., Wash. *13*, 293, 1934. — 36. **Meissner, K. W.**, Interference spectroscopy. Part I. J. Opt. Soc. Amer. *31*, 405, 1941. — 37. **Meissner, K. W.**, **Mundie, L. G.**, and **Stelson, P. H.**, Structure of the $^2D$ terms of the arc spectrum of lithium. Phys. Rev. *74*, 932, 1948. — 38. **Moisson, H.**, Sur la couleur et sur le spectre du fluor. C. R. Acad. Sci., Paris, *109*, 937, 1889. — 39. ——, Determination de quelques constantes physique du fluor. Ann. Chim. phys. *35*, 125, 1891. — 40. **Moore, C. E.**, Atomic energy levels. Nat. Bur. Stand. Wash., in press. (Circ. U. S. Bur. Stand. 467, 1948.) — 41. **More, K. R.**, and **Rieke, C. A.**, Wavelength standards in the extreme ultraviolet. Phys. Rev. *50*, 1054, 1936. — 42. **McNally Jr., J. R.**, **Harrison, G. R.**, and **Rowe, E.**, A hollow cathode source applicable to spectrographic analysis for the halogens and gases. J. Opt. Soc. Amer. *37*, 93, 1947. — 43. **Paschen, F.**, Das Spektrum des Neon. Ann. Phys. Lpz., *60*, 405, 1919. — 44. **Penney, W. G.**, Hydrogen and helium lines as standards of wave-length. Phil. Mag. *9*, 661, 1930. — 45. **Porlezza, C.**, Sugli spettri del silicio e del fluoro in tubo di Geissler. Gaz. chim. ital. *42*, II, 42, 1912. — 46. **Racah, G.**, On a new type of vector coupling in complex spectra. Phys. Rev. *61*, 537, 1942. — 47. **Ramanadham, R.**, and **Rao, K. R.**, Investigations on the spectrum of bromine. II. Structure of Br II. Indian J. Phys. *18*, 317, 1944. — 48. **Rasmussen, E.**, On the planeness of interferometer plates. K. Danske Videns. Selsk. Mat.-fys. Medd. *XXIII*, nr 3, 1945. — 49. **Rydberg, J. R.**, Sur une certaine asymetrie dans les réseaux concaves de M. Rowland. Bihang till Kungl. Svenska Vet.-akad. handl. *18*, I, nr 9, 1893. — 50. **Shenstone, A. G.**, Disagreements with the predictions of the Hund theory of series limits. Phys. Rev. *31*, 1124, 1928. — 51. ——, The first spark spectrum of copper. Philos. Trans. *235*, 195, 1936. — 52. ——, The first spectrum of copper (Cu I). Philos. Trans. *241*, 297, 1948. — 53. **Smythe, W. R.**, The spectrum of fluorine. Astrophys. J. *54*, 133, 1921. — 54. **Söderqvist, J.**, Vakuumfunkenspektren der Elemente Natrium, Magnesium, Aluminium und Silicium. Nova Acta Reg. Soc. Sci. Ups. *IV. 9*, n:r 7, 1934. — 55. **Tolansky, S.**, High resolution spectroscopy. Methuen & Co, Ltd. London 1947. — 56. **Tomboulian, D. H.**, New terms in the spectrum of Na III. Phys. Rev. *54*, 347, 1938. — 57. **White, H. E.**, Introduction to atomic spectra. Mc Graw-Hill, New York 1934.

## Description of Plates I—X

Plates I, VI b, VIII b, IX and X are obtained with an enlarger with a 25 watt concentrated arc lamp as light source and a Sonnar 1 : 2 with antireflection coatings as projection lens.

Spectrograms obtained with a hollow cathode and a 6.5 m grating spectrograph in Wadsworth mounting:

I. CN band $\lambda$ 4216, 2. order (disp. 3.7 A/mm); carbon arc, exposure 3 min on Ilford thin film half-tone plate; slit 0.008 mm. (× 35)

II. F I 11600—9900 A, 1. order; $SF_6$ + Li + He + Ne, 0.75 amp.; exposure 15 hours on Eastman I Z hypersens; slit 0.030 mm. (× 2.7)

III. F I 9900—9300 A, 1. order; exposure 10 hours on Eastman I M hypersens.

- a. $SF_6$ + Li + He + Ne, 0.7 amp.; slit 0.025 mm. (× 2.7)
- b. LiF + He (the last 20 min. Ne was used as filling-gas and the slit shortened); slit 0.030 mm. (× 2.7)

IV. F I 8350—7850 A, 1. order; Eastman I N hypersens.
  a. $SF_6$ + Li + He, 0.3 amp., 30 min; slit 0.020 mm. (×2.7)
  b. $SF_6$ + Li + Ne + He, 0.5 amp., 20 min; slit 0.023 mm. (×2.7)

V. F I 5750—5150 A, 1. order; Eastman 103a C; slit 0.020 mm.
  a. $SF_6$ + Li + He, 0.2 amp., exposure 3.5 hours. (×2.7)
  b. LiF + He, 0.3 amp., exposure 3 hours. (×2.7)

VI. a. F I 6500—5900 A, 1. order; $SF_6$ + Li + He, 0.2 amp., exposure 15 min on Eastman 103a C; slit 0.020 mm. (×2.7)
  b. F I 3750—3550 A, 1. order; $SF_6$ + Li + He, 0.13 amp., exposure 45 min on Eastman 103a O; slit 0.020 mm. (×5.9)

Spectrograms obtained with hollow cathode and 1.5 m grazing incidence vacuum spectrograph:

VII. a. F I 977—951 A, 1. order; LiF + He, 0.2 amp., exposure 5 min on Ilford Q 2; slit 0.003 mm. (×7.3)
  b. F I 977—951 A, 2. order; hollow cathode lined with copper foil, Ilford Q 1; slit 0.0035 mm.
    1. He, 0.6 amp., exposure 45 min.
    2. $SF_6$ + He, 0.3 amp., exposure 45 min. (×7.4)

VIII. a. F I 809—680 A, 1. order; LiF + He, 0.5 amp., exposure 1.5 hours on Ilford Q 2; slit 0.003 mm. (×5.3)
  b. F I $2p-3d$ from the previous plate, enlarged ×14.4.

Spectrograms obtained with a Fabry-Perot interferometer and a stigmatic 6.5 m grating spectrograph:

IX. a. F I 6773—6909 A, 1. order; 10 mm etalon. $SF_6$ + He, 0.09 amp., exposure 20 min on Eastman 103a F; Heliar f = 24 cm. (×3.6)
  b. F I 7398—7607 A, 1. order; 10 mm etalon. $SF_6$ + He, 0.2 amp., exposure 60 min on Eastman I N hypersens; Heliar f = 24 cm. (×3.6)

X. Selected F I lines from different spectrograms obtained with 10, 15 and 25 mm etalons. 15 and 25 mm etalons were combined with a Tessar, f = 60 cm and the 10 mm etalon with a Heliar, f = 24 cm. (×4.2)

Tryckt den 10 maj 1949

Uppsala 1949. Almqvist & Wiksells Boktryckeri AB

# The arc spectrum of fluorine

By KURT LIDÉN

(See volume *1*, pages 229–267, 1949)

## Errata

Page 230, line 3: for (26, 27), read (26, 27, 28).
» 234, line 2: for »by SHENSTONE», read »in the theory of the concave grating».
» 236, line 11: for Cu I/Cu II, read Cu II/Cu I.
» 238, »2. The vacuum region», line 8: for C I . . . Ne II, read O I . . . Ne I.
» 239, table 2, read:

| n | $\nu$ | $\lambda$ |
|---|---|---|
| — — — | — — — | — — — |
| 3 | 97492.553 | 1025.7223 |
| — — — | — — — | — — — |
| 6 | 106632.427 | 937.8035 |
| 7 | 107440.713 | 930.7483 |
| — — — | — — — | — — — |
| 9 | 108324.992 | 923.1504 |

» 241, $\lambda$ 10064.25: for $3p\ ^2S_{4/2}$, read $3p\ ^2S_{1/2}$.
» 253, table 8: last line, omit $^2S^0$.
» 255, table 9:

n $d\ ^4D_{7/2}$, for 3086.03, read 3085.96
n $d\ ^4D_{3/2}$, » 4434.66, » 4434.88
n $d\ ^2F_{5/2}$, » 3940.05, » 3940.19
» » 2583.06, » 2582.97

» 260, table 12. The values of the ground term should read:

$2s^2\ 2p^5\ ^2P^0_{1/2}$ 140120.4
*−404.1*
$^2P^0_{3/2}$ 140524.5

» 263, table 13, $\lambda$ 7898: for $3d\ ^2P_{3/2}$, read $3d\ ^2F_{5/2}$.
» » $\lambda$ 7800: » 0.090, » 0.098.
» 264, table 15, $3p\ ^4P_{1/2}$: for $+0.050$, read $-0.050$.
» »: » $3d\ ^2P_{3/2}$, $-0.016$, read $3d\ ^2F_{5/2}$, $-0.012$.

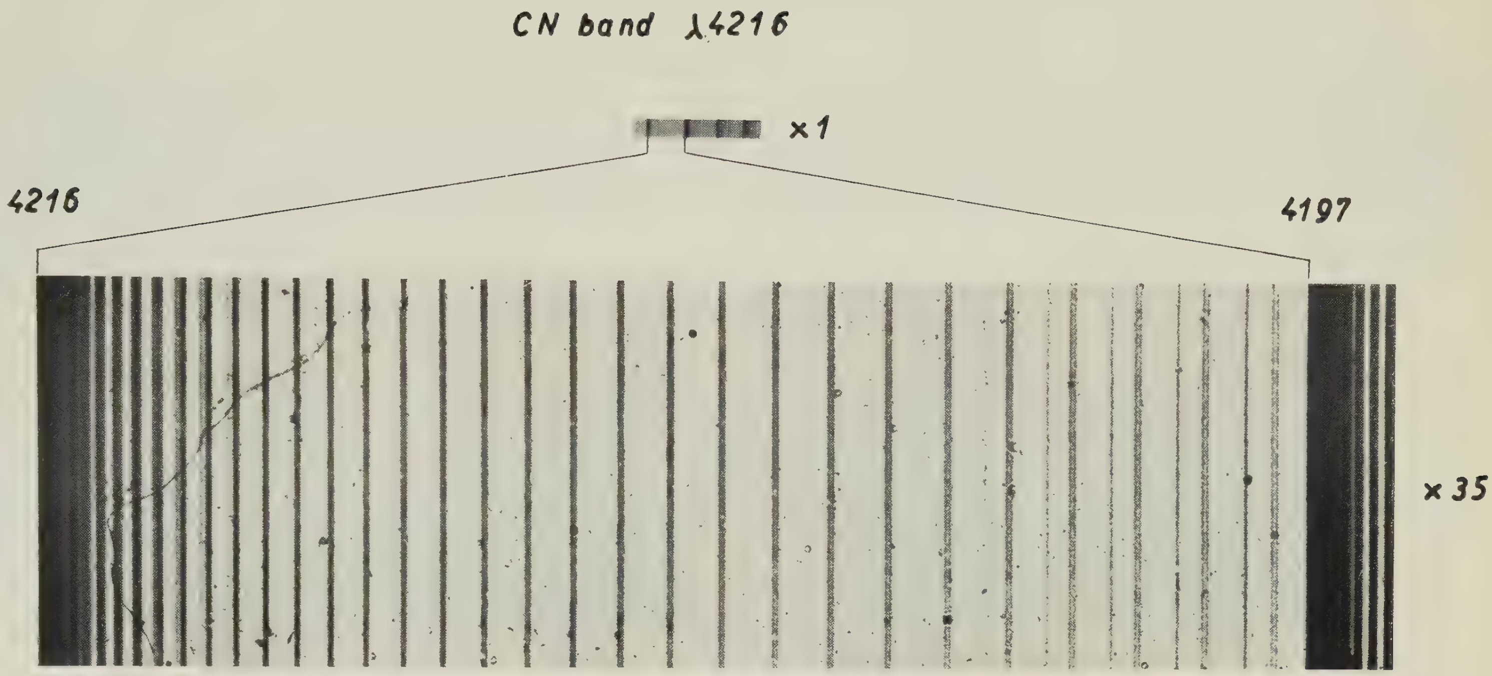
CN band λ4216
×1
4216
4197
×35

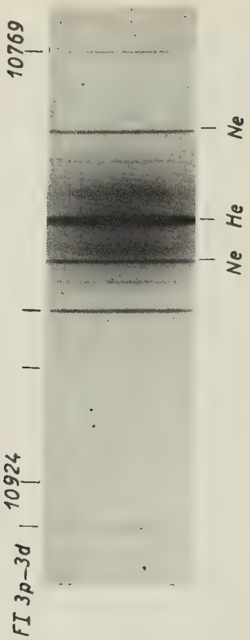
10769
Ne
He
Ne
10924
FI 3p–3d

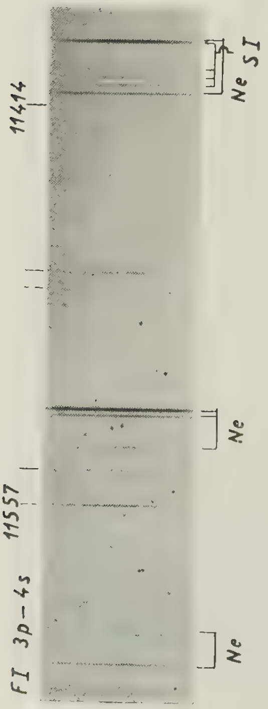
11414
SI
Ne
Ne
11557
FI 3p–4s
Ne

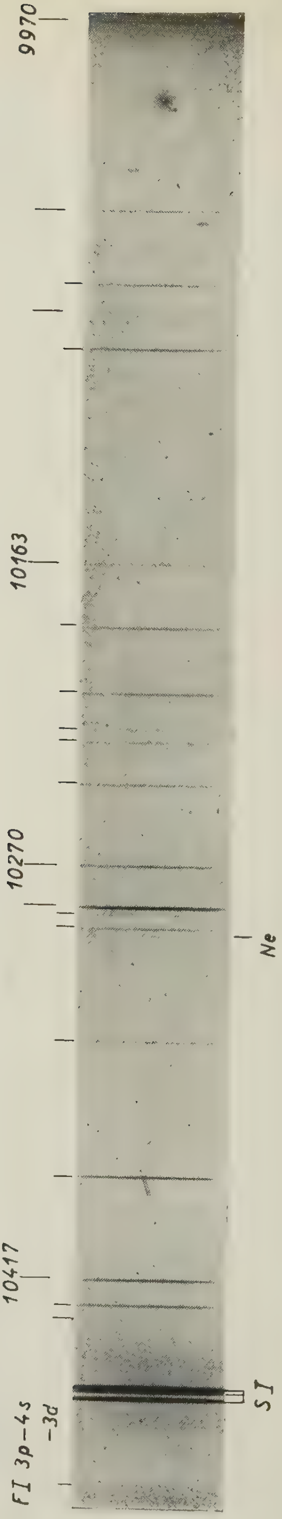
9970
10163
10270
Ne
10417
SI
FI 3p–4s
–3d

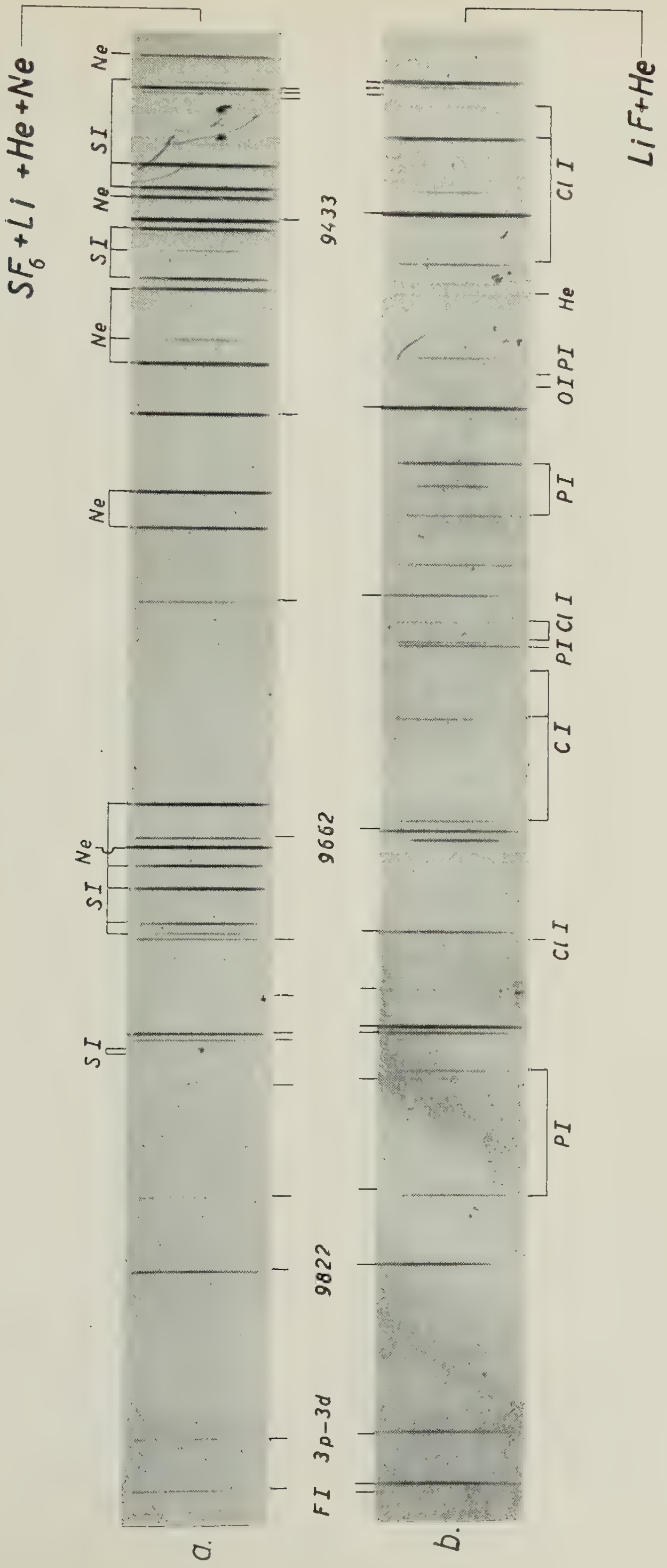
$SF_6$+Li +He+Ne
Ne
SI
Ne
SI
Ne
Ne
Ne
SI
SI
9433
9662
9822
FI 3p–3d
a.
b.
LiF+He
Cl I
He
OI PI
PI
PI Cl I
CI
Cl I
PI

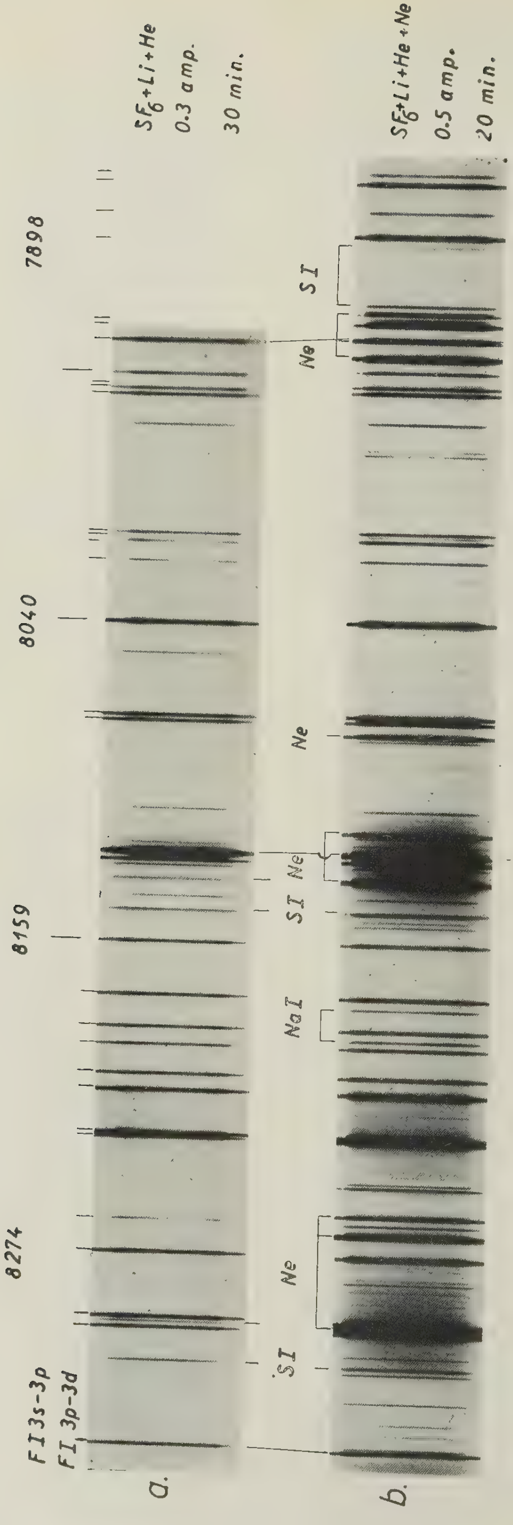

a.
b.
$SF_6$+Li+He
0.3 amp.
30 min.
$SF_6$+Li+He+Ne
0.5 amp.
20 min.
7898
8040
8159
8274
F I 3s-3p
F I 3p-3d
S I
Ne
Ne
S I
Ne
Li I
Na I
Ne
S I

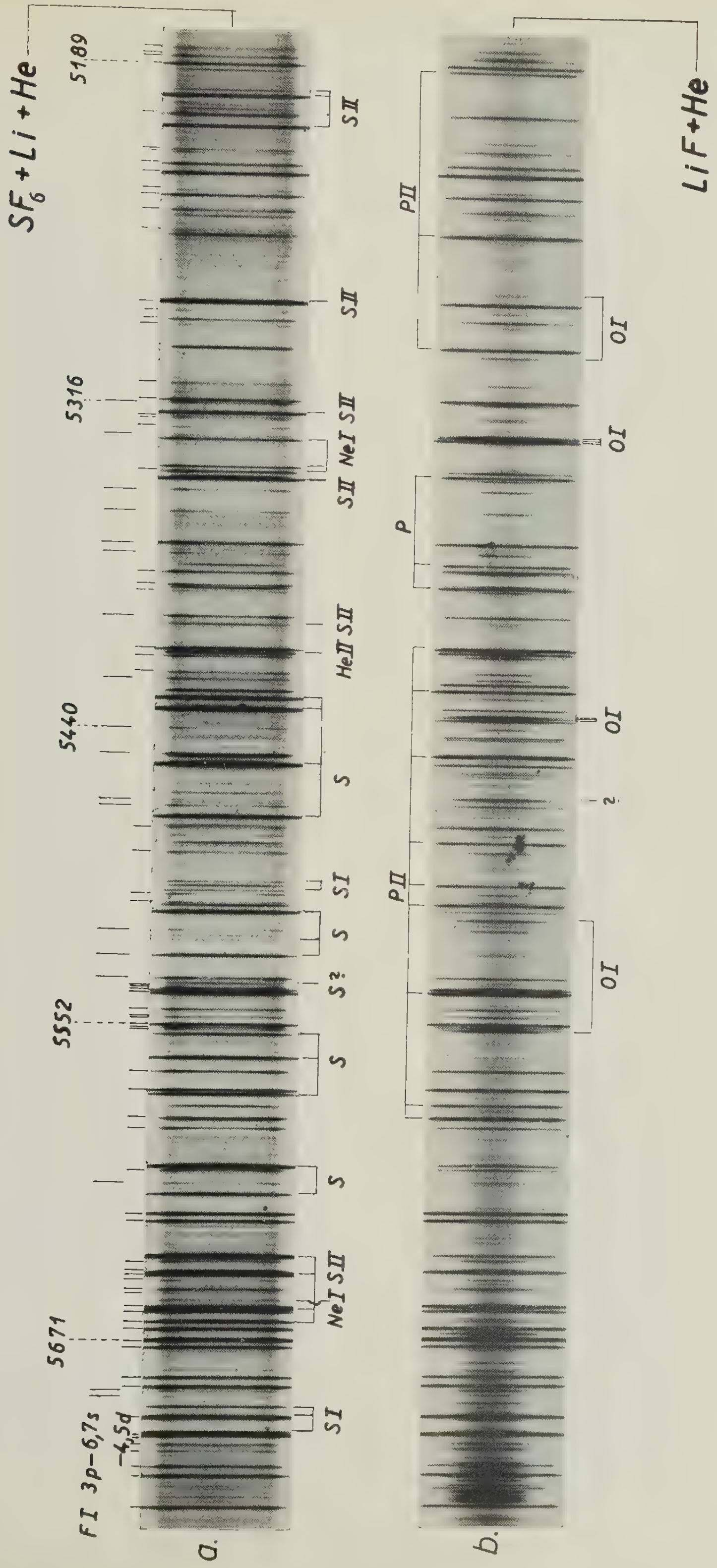
$SF_6 + Li + He$
5189
SII
SII
5316
NeI SII
SII
HeII SII
5440
S
SI
S
S?
5552
S
S
NeI SII
5671
SI
FI 3p–6,7s –4,5d
a.
LiF+He
PII
OI
OI
P
OI
?
PII
OI
b.

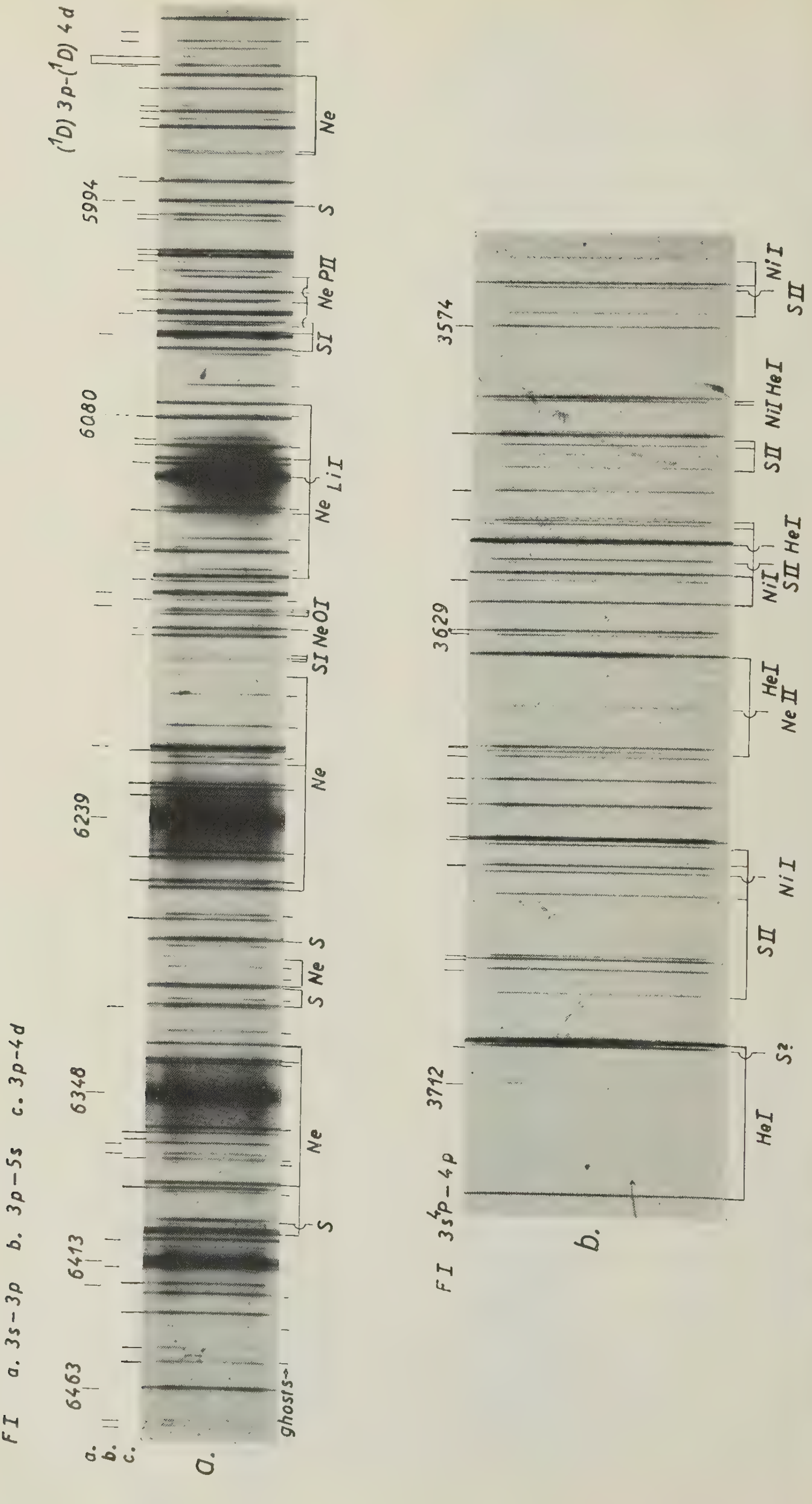
F I a. 3s−3p b. 3p−5s c. 3p−4d
(¹D) 3p−(¹D) 4d
5994
6080
6239
6348
6413
6463
a.
b.
c.
a.
ghosts→
Ne
S
Ne P II
S I
Ne Li I
S I Ne O I
Ne
S Ne S
Ne
S
F I 3s⁴P−4p
b.
3574
3629
3712
Ni I
S II
Ni I He I
S II
S II He I
Ni I
He I
Ne II
Ni I
S II
S?
He I

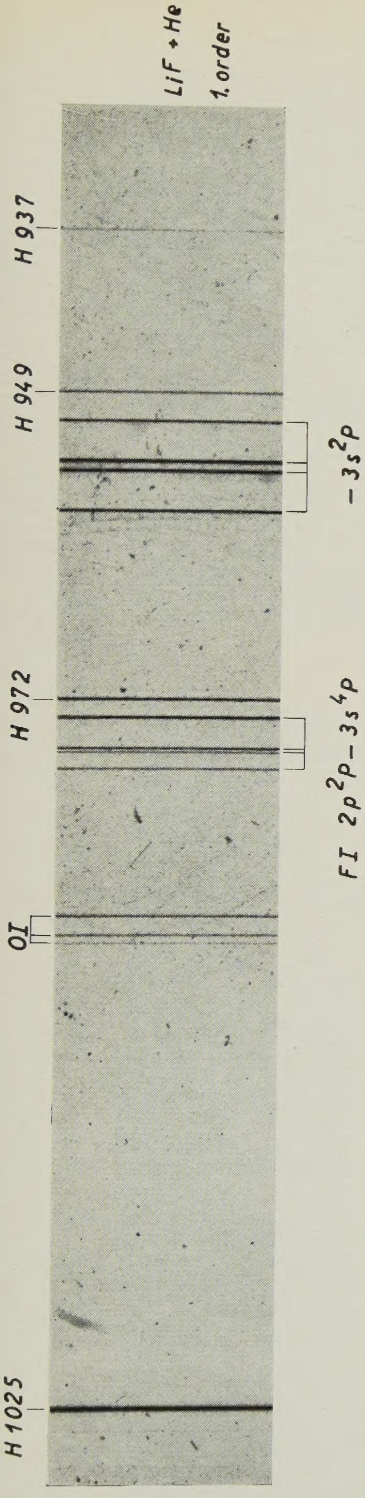
LiF + He
1. order
H 937
H 949
−3s²P
H 972
FI 2p²P−3s⁴P
OI
H 1025

a.

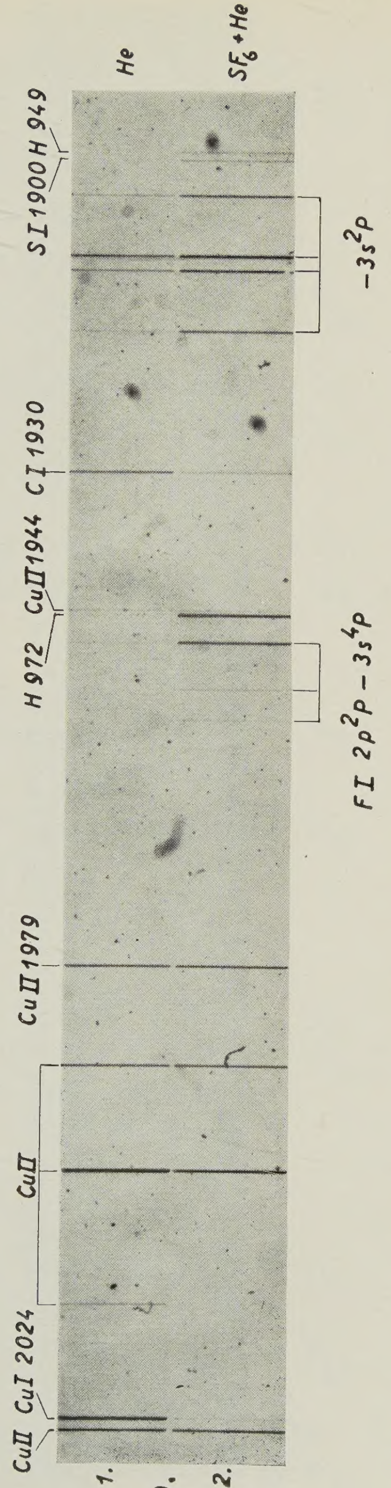
He
SF₆ + He
SI 1900 H 949
−3s²P
CI 1930
CuII 1944
H 972
FI 2p²P−3s⁴P
CuII 1979
CuII
CuI 2024
CuII
1.
2.

b.

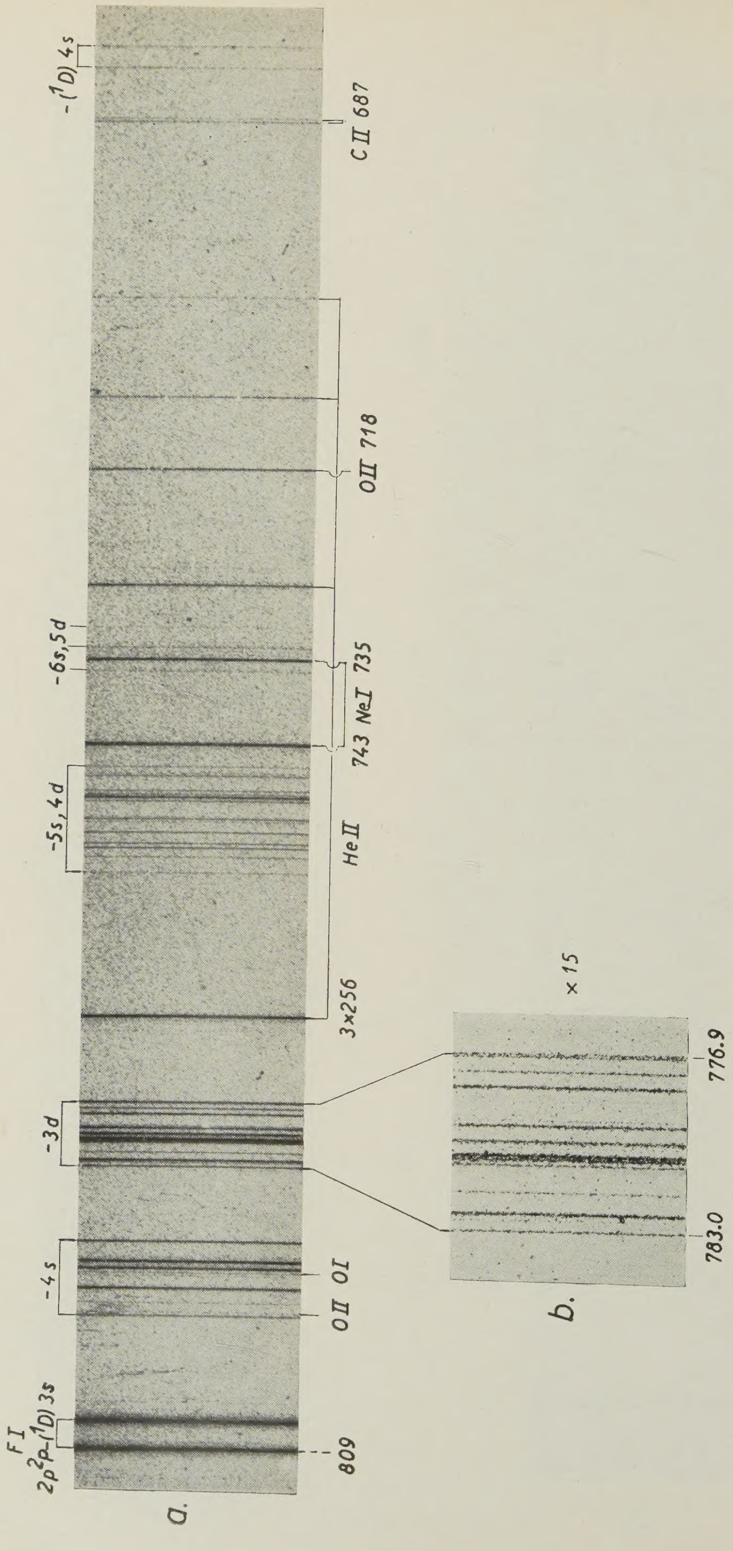
a.
F I
$2p^2P-(^1D)\,3s$
809
-4s
OII
OI
-3d
3×256
He II
-5s, 4d
743 NeI 735
-6s, 5d
OII 718
CII 687
$-(^1D)\,4s$
b.
783.0
776.9
×15

10 mm etalon

FI

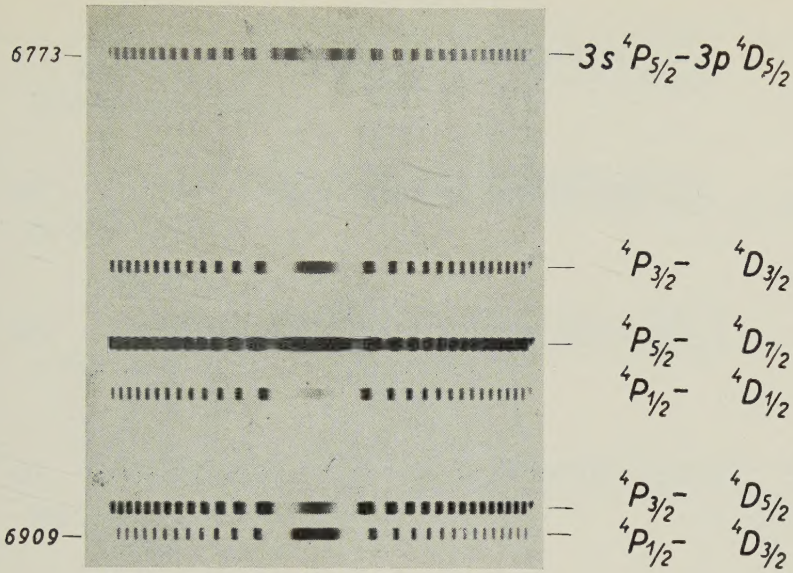
6773
$3s\,{}^4P_{5/2}-3p\,{}^4D_{5/2}$
${}^4P_{3/2}-\ {}^4D_{3/2}$
${}^4P_{5/2}-\ {}^4D_{7/2}$
${}^4P_{1/2}-\ {}^4D_{1/2}$
${}^4P_{3/2}-\ {}^4D_{5/2}$
6909
${}^4P_{1/2}-\ {}^4D_{3/2}$

a.

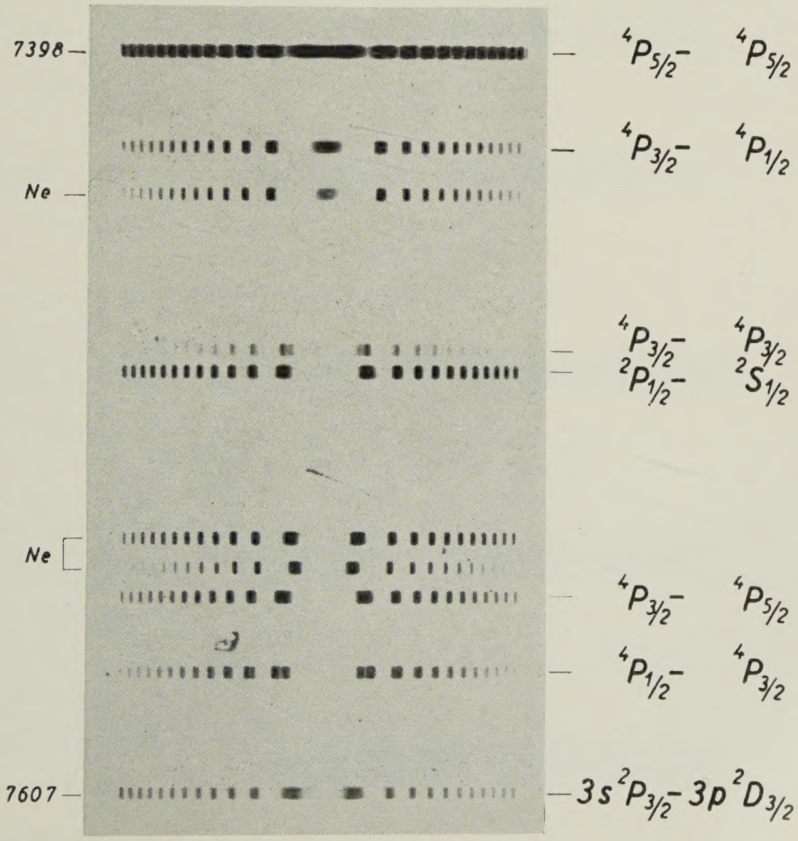
7398
${}^4P_{5/2}-\ {}^4P_{5/2}$
${}^4P_{3/2}-\ {}^4P_{1/2}$
Ne
${}^4P_{3/2}-\ {}^4P_{3/2}$
${}^2P_{1/2}-\ {}^2S_{1/2}$
Ne
${}^4P_{3/2}-\ {}^4P_{5/2}$
${}^4P_{1/2}-\ {}^4P_{3/2}$
7607
$3s\,{}^2P_{3/2}-3p\,{}^2D_{3/2}$

b.

Etalon

# F I

10 mm

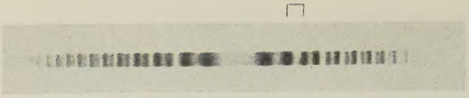

$3s\,^4P_{5/2} - 3p\,^4S_{3/2}$

λ6239

10 mm

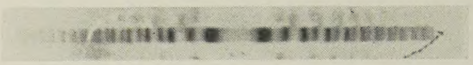

$-3p\,^4D_{3/2}$

λ6708

15 mm

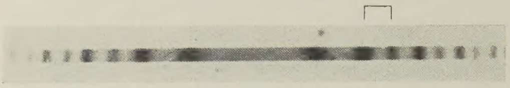

$-3p\,^4D_{5/2}$

λ6773

10 mm

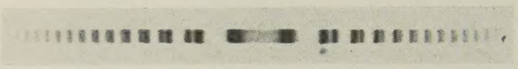

$-3p\,^4P_{5/2}$

λ7398

25mm

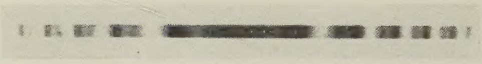

$3s\,^4P_{3/2} - 3p\,^4P_{5/2}$

λ7552

25 mm

$3s\,^4P_{1/2} - 3p\,^4P_{3/2}$

λ7573

25 mm

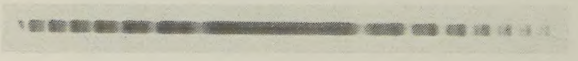

$3s\,^4P_{3/2} - 3p\,^4D_{5/2}$

λ6902

10 mm

$3s\,^2P_{3/2} - 3p\,^2P_{3/2}$

λ7037

10 mm

$(^1D) - (^1D)$

$3s\,^2D_{5/2} - 3p\,^2D_{5/2}$

$^2D_{3/2} - \quad ^2D_{3/2}$

λλ6767-62